LATE HOLOCENE ENVIRONMENTAL RECORD AND GEOLOGICAL HISTORY OF THE LAKE COLENSO AREA, NORTH-WESTERN RUAHINE RANGE, NEW ZEALAND

A thesis presented in partial fulfilment of the requirements for the degree of

Master of Science

in

Quaternary Science

Soil and Earth Sciences, Institute of Natural Resources,

Massey University, Palmerston North, New Zealand

Amanda Mallory MacDonald-Creevey

2011

Abstract

Sediment cores from a landslide-dammed lake, Lake Colenso (North Island, New Zealand), contain a decadal- to centennial-scale record of changing climate spanning the past 1800 years. A multi-proxy approach has been used to obtain a high-resolution record of variability from the Lake Colenso catchment, and tephra horizons combined with radiocarbon ages provide chronological constraints. Since the lake is located within a mountainous forested catchment of the northern Ruahine Range, it has remained pristine and isolated from human disturbance. Additionally, pollen analysis indicates minimal human influence in the lake catchment; hence the site offers a rare opportunity to investigate natural environmental change during a period in which anthropogenic impact has tended to obscure natural variability in many records from elsewhere in New Zealand (Wilmshurst *et al*., 1997).

Sedimentology and elemental geochemistry reflect periods of rapid sediment influx into the lake, here interpreted as storm events which are preserved at an average of 1 every 150 years. This record, supported by stable isotope records from ostracods, shows distinct periods of increased storminess, and is related to the interaction between regional atmospheric circulation systems, El Niño-Southern Oscillation, Southern Annular Mode and the Pacific Decadal Oscillation. Furthermore, the association with other regional records of climate over the late Holocene highlights the effect of regional climatic forcing. A combination of findings is characterised by broad changes that correlate to the regionally distinctive Medieval Warm Period and Little Ice Age periods, providing further evidence for a climatically variable Holocene (Mayewski *et al*., 2004). The multi-proxy record presented here is a valuable contribution to existing paleoenvironmental knowledge of the late Holocene in New Zealand.

The geology of the study area is characterised by alternating periods of subsidence and uplift throughout the Plio-Pleistocene which resulted in the deposition of Wanganui Basin sediments in the region. Historic earthquake records from nearby major faults are commensurate with ages obtained for landslides at Lake Colenso, which allow a further understanding into landscape evolution and the development of present-day Lake Colenso.

Acknowledgements

Huge thanks to my supervisors, Prof. Vince Neall, whose idea this project stemmed from, and also Dr. Kat Holt and Dr. Marcus Vandergoes (GNS Science), for their help and encouragement throughout the project. Without their support, this project would not have been possible.

For field and technical assistance at Massey, thanks to David Feek, Anja Moebis, Ian Furket, and Glenys Wallace. Andrew Mercer (Department of Conservation) and Stephen Carey are thanked for their assistance in the field. Margaret Morley (Geomarine Research), Bruce Hayward (Geomarine Research), Alan Beu (GNS Science), and Bruce Marshall (Te Papa Museum) are thanked for assistance in identifying ostracod and mollusc species. Marco Brenna is thanked for performing the analysis on the electron microprobe. Thanks to Tony Gates (Palmerston North Tramping and Mountaineering Club) for the use of his photos of the Ruahine Range, and for discussions about the area.

Huge thanks to fellow MSc students, Emma Phillips and Simon Vale, for their support during the duration of the Masters degree. Also, thanks to Rob Tinkler for his helpful suggestions, ideas and reading through the final drafts.

Lastly, the support from my friends and family has been fantastic. My mum, grandma, sister and the rest of the family have been encouraging all the way through university life and I am hugely grateful for everything.

Table of contents

List of figures

List of tables

Chapter 1: Introduction

1.1 Introduction

The area of focus in this study (Lake Colenso) is in the northern Ruahine Range in the central North Island of New Zealand. Within this region there has been a wide scope of research into environmental conditions including: anthropogenic drivers of vegetation change (Colenso, 1884; James, 1973; Cunningham, 1979); natural changes in vegetation inferred from palynology (Moar, 1956, 1961, 1967; Lees, 1981, 1986; Rogers, 1987; Rogers and McGlone, 1989); geology (Smale *et al.*, 1978; Marden, 1984); fault history (Hanson, 1998); and erosion (Grant 1985, 1989; Hubbard and Neall, 1980). While these studies provide information useful for the interpretation of past environments over Quaternary or longer timescales, none of them provide in-depth detail for the late Holocene. More specifically, there is a lack of knowledge in the decadal- to centennial-scale environmental variability over this period in the Ruahine Range.

This study presents a high-resolution record of environmental change from Lake Colenso in an attempt to increase the understanding of environmental change and the impact of regional climate-forcing spanning the late Holocene. While other key studies are reviewed and provide a basis for this study, environmental variability is explored using a multi-proxy approach from landslide-dammed lake, Lake Colenso. New Zealand, because of its latitudinal range (34 to 46°S), is highly responsive to long-term global climatic variation (Newnham *et al*., 1999) as well as the effects of regional forcing patterns (Shulmeister *et al.*, 2006; Schaefer *et al.*, 2009). The interaction between mid-latitude climate systems and New Zealand's mountainous physiography produces spatially variable climatic patterns (Lorrey *et al.*, 2007) that are generally responsive to small synoptic changes (Sturman, 1999). Hence, New Zealand is an ideal location for the investigation of environmental change and key driving processes.

1.2 Aims of the study

This study comprises two parts. The first part of the project determines the timing and formation of Lake Colenso with comparison to paleoseismic records of the nearby major faults. Finally, this is used to construct a geomorphological model of landscape evolution and lake formation. In addition, a 1:30000 geological map of the study area is then produced, involving: (1) the mapping of major lithotypes; (2) the correlation of units with other geological studies and determination of age; and, (3) the mapping of faults and geological structures.

The second part of the project involves analysis of sediment cores collected from Lake Colenso, using a multi-proxy approach: 1) tephra horizons combined with radiocarbon ages provide a chronological framework; 2) sedimentological analyses allow an evaluation of changes in sedimentation styles; 3) biogeochemical proxies such as organic matter content and stable isotope records are used to evaluate alterations in watershed conditions; 4) fossil pollen is used to assess changes in vegetation composition occurring in response to climate variability or other forcing mechanisms; and 5) ostracod and mollusc assemblages are used to provide evidence of ecological variability from within the lake.

Finally, findings from both parts are combined to provide a high-resolution record of late Holocene environmental change from the northern Ruahine Range; and identification of geological and geomorphological characteristics of the area. Both of which are put into a wider regional context.

1.3 Rationale

Cunningham and Stribling (1978) were the first to suggest the landslide-dammed origin of Lake Colenso, though they could not identify timing of the landslide or lake formation. Other examples from New Zealand show that a landslide-dammed lake in a seismically active area is likely to be the result of an earthquake (Perrin and Hancox, 1992). Thus, this investigation into the age of Lake Colenso provides an opportunity to correlate findings with paleoseismic records of the nearby faults.

Smale *et al*. (1978) point out that the Lake Colenso area is misunderstood in terms of geology, as had been originally mapped by Kingma (1962). An examination into the geology allows a further understanding of the landscape and how it has evolved to its present-day setting.

Additionally, lakes tend to be an ideal place for paleoenvironmental reconstruction for a number of reasons. First, the fossil records of flora and fauna present evidence of ecological variability, which occurs in response to climate change, or other influences such as human activity and volcanism. Second, the sediments provide an opportunity to look at past environmental conditions, particularly where lake levels and sedimentation may fluctuate in response to climate (Lowe and Walker, 1997). In a lake environment, sediments are derived from within the lake or from the catchment, and the various components can provide a great deal of information about the lake and its catchment environment. Third, the use of biogeochemistry can offer insights into changes in watershed conditions. An approach using a combination of these proxies gives an opportunity to provide a comprehensive overview into local and regional environmental change throughout the lifetime of Lake Colenso.

1.4 Thesis structure

Given that this study has a two-fold approach, most chapters have been split into two sections; the first part typically covering the geology and geomorphology, and the second part covering the environmental history as inferred from the lake sediments.

- Chapter 2 reviews literature on the nature of landslide-dammed lakes and their occurrence in New Zealand, as well as paleovegetation studies in the Ruahine Range and New Zealand over the late Holocene.

- Chapter 3 provides a synopsis of the study area, including vegetation, climate, and geology.

- Chapter 4 outlines the methods used, both in the field and in the laboratory.

- Chapter 5 presents results of the geological and geomorphological characteristics of the study area based on field observations. The chapter also outlines the results used for the construction of an environmental history.

- Chapter 6 provides a discussion into the evolution of the landscape with respect to the geology, geomorphology and formation of the lake, and then offers an interpretation of the environmental history of the lake within a regional context.

- Chapter 7 provides a summary of the main findings in the study and concludes by considering avenues for future research.

Chapter 2: Literature review

The main aims of this study are; 1) to further understand the evolution of the landscape with respect to lake formation and paleoseismic records, and 2) to provide an environmental history of the Lake Colenso region. This literature review has been split into two sections in an attempt to cover the necessary and relevant work for each topic. The first section will discuss landslide-dammed lakes, their nature, typical setting and past studies in New Zealand. The second section will look at previous studies that have been done in the Ruahine Range with a focus on paleovegetation records. Relevant palynological studies will be discussed and then evidence from the Ruahine Range will be put into a regional context. Tectonic, geological and storm/erosion studies in the Ruahine Range are discussed in context later in the study so are not referenced here to avoid repetition.

2.1 Landslide-dammed lakes and earthquakes

2.1.1 Background

Landslide-dams are characteristically complex geomorphic features and are common in mountainous terrain (Costa and Schuster, 1988). Areas of high relief usually have tectonic and climate controls which are known to be the causal factors for 90% of lake formation, with the remainder caused by glacial, volcanic, and anthropogenic activity (Costa and Schuster, 1988). The mountainous nature of New Zealand as a result of its position astride a plate boundary, and the oceanic-driven climate causing relatively high precipitation means that landslide-damming is a common occurrence (e.g. Lake Waikaremoana, Lake Tutira, and Green Lake). Lake volumes range from $<0.1 \times 10^8$ m^3 to 6.2×10^8 m^3 and are predominantly situated in eastern/central North Island, northwest Nelson, North Westland, western Canterbury and Fiordland (Korup, 2002).

Landslide-dams often occur in groups and have a relatively short life span (Korup, 2002); their permanence principally depends on the size and the lithology of the landslide (Adams, 1981). While much of the landslide surface is a jumble of large blocks, the landslide debris is commonly fine-grained and often contains remains of vegetation that

once grew on the pre-landslide slope (Adams, 1981). The deposition of the debris against the far valley wall will usually cause the lake to lie between the landslide scar and debris mound, and lake drainage is usually underground (Adams, 1981).

Mass movement can either cause an entire blockage of the stream/river system, channel constriction, diversion or avulsion, all of which can result in a significant change in stream flow and bed morphology (Korup, 2002). In some cases, the landslide impedes valley drainage rather than actual stream blockage (Adams, 1981). However, there is a lack of understanding in the processes at any given locality because studies tend to be purely descriptive (Korup, 2002).

2.1.2 Past studies in New Zealand

Adams (1981) published the first account of earthquake-dammed lakes with a list of 38 temporary and permanent lakes, and also presented the potential for the reconstruction of paleoseismicity citing the strong relationship between the distribution of lakes and isoseismic ellipses of earthquake intensity. It has been found that the formation of earthquake triggered landslide-dammed lakes are the result of earthquakes larger than magnitude 6 (Adams, 1981), so these lakes can provide an estimate of the paleoseismicity of an area. The magnitude 7.6 Murchison Earthquake (1929) caused numerous landslides over an area of ~5000 km^2 (Adams, 1981). This resulted in damming of the Buller, Mokihinui, Karamea, Matakitaki, and Maruia Rivers which formed 11 landslide-dammed lakes, though most of these landslides have since been eroded naturally (Adams, 1981).

Recognition of a paleoseismic event ideally should not be based on the dating of a single landslide-dammed lake as it is possible that due to New Zealand's variable climate that the lake may have formed as a result of a storm or other non-seismic event (Adams, 1981). However, historic examples from New Zealand show that a landslide-dammed lake in a region of active tectonism is almost always formed by an earthquake (Perrin and Hancox, 1992).

Less than a decade later, Livingston *et al*. (1986) published an inventory of New Zealand lakes which was followed up by a compilation of the origin and the development of New Zealand lakes (Lowe and Green, 1987; 1992). Hancox and Perrin (1994) highlight the value of geomorphologic mapping of landslide-dammed lakes (i.e., in the case of Green Lake) in the construction of landscape evolution models. The majority of geomorphic mapping of New Zealand landslide-dammed lakes has been carried out through the analysis of aerial photography, with little ground truth work. An example that has been extensively studied with respect to mapping is Lake Waikaremoana (Rijkse, 1979; Read *et al*., 1992). This lake is the largest landslide-dammed lake in New Zealand and has an area of 54 km^2 (Adams, 1981). The lake was formed by a two-phase landslide which caused blockage of the Waikaretaheke River, as a result of a major earthquake (Read *et al*., 1992). The landslide (~2200 cal yr BP) was dated from standing trees exposed at low lake level (Newnham *et al*., 1998).

A later review of landslide-dammed lakes by Perrin and Hancox (1992) identified 82 landslide-dammed lakes, and showed that the majority of these New Zealand lakes are formed by rock slumps, rock block slides in Tertiary sediment, or a combination of rock block slides, debris flows, and debris avalanches. At present, a focus of landslide research is the association between specific earthquake and landslide events (Hancox *et al*., 1997). To identify a seismic cause for the origin of a landslide-dammed lake, there are several factors that must be considered; event synchronicity, distribution of lakes in relation to fault lines, and the stability of the landscape (Hancox *et al*., 1997). However, areas in which landslides are frequent also tend to experience a high precipitation rate, which potentially masks the seismic signal (Crozier, 1997).

A review by Korup (2002) explores the developments in New Zealand with regards to research on landslide-dams. One finding shows that the majority of work has been descriptive, with a lack of research particularly into the evolution of the landscape, quantification of sediment budget and paleoenvironmental reconstruction (Korup, 2002). Because landslide-dammed lakes are a common occurrence in highly active tectonic areas, there is an opportunity to use these lakes (pending on the longevity of the lake) for a record

of environmental variability (i.e., erosion, and climate) within the lake catchment. Lake Waikaremoana (Newnham *et al*., 1998) and Lake Tutira (Page *et al*., 1994a, b; Page and Trustrum, 1997; Eden and Page, 1998; Trustrum *et al*., 1999; Orpin *et al*., 2010; Page *et al*., 2010) are examples where this potential has been utilised. Lake Waikaremoana provides evidence for pre-European forest clearance in New Zealand from a palynological record (Newnham *et al*., 1998). Lake Tutira, formed by a landslide ~6500 cal yr BP, presents a decadal-scale sediment record of natural and anthropogenic environmental change, as a result of climate, tectonism, and volcanism (Page *et al*., 2010).

2.1.3 Conclusion

It is apparent that there is a need for more detailed geomorphological maps on landslide-dammed lakes to gain a full understanding of the processes that formed them. Dating of landslide-dammed lakes will improve knowledge of the size and recurrence interval of past earthquakes in New Zealand (Adams, 1981). The combination of known paleoseismic records and an understanding of landslide geomorphology present an ideal opportunity to constrain stages of landscape evolution.

While paleoenvironmental records from landslide-dammed lakes have been shown to be a useful tool (e.g., Lake Tutira), there is potential for further research into this field with a wider use of proxies to provide more understanding into the dynamics of such lakes and their environment.

2.2 The Ruahine Range and wider environmental changes from 2000 years to present

2.2.1 Past vegetation change in the Ruahine Range

The first studies using fossil pollen in the Ruahine Range were carried out by Moar (1956; 1961; 1967) on the Mokai Patea Ridge, Whanahuia Range and No Man's Land bog respectively (Fig. 2.1). These studies all covered the mid-late Holocene period (Fig. 2.2). Lees (1981; 1986) then expanded the paleoenvironmental knowledge to the southern Ruahine Range region from sites at Delaware Ridge, West Tamaki River, Manawatu Gorge and Ballantrae (Fig. 2.1). These individual sites present discontinuous records, though when combined provide complete coverage of the post-glacial period. Rogers (1987) and Rogers and McGlone (1989) investigated areas in the northern Ruahine and southern Kaweka Ranges, on Three Kings Range and Reporoa Bog (Fig. 2.1), also covering the Holocene period.

All studies used a combination of tephrostratigraphy and radiocarbon dates for chronological constraints. The Taupo Tephra, dated at 1717 cal yr BP (Lowe *et al*., 2008), in each of the late Holocene sites allows a reasonably accurate means of correlation.

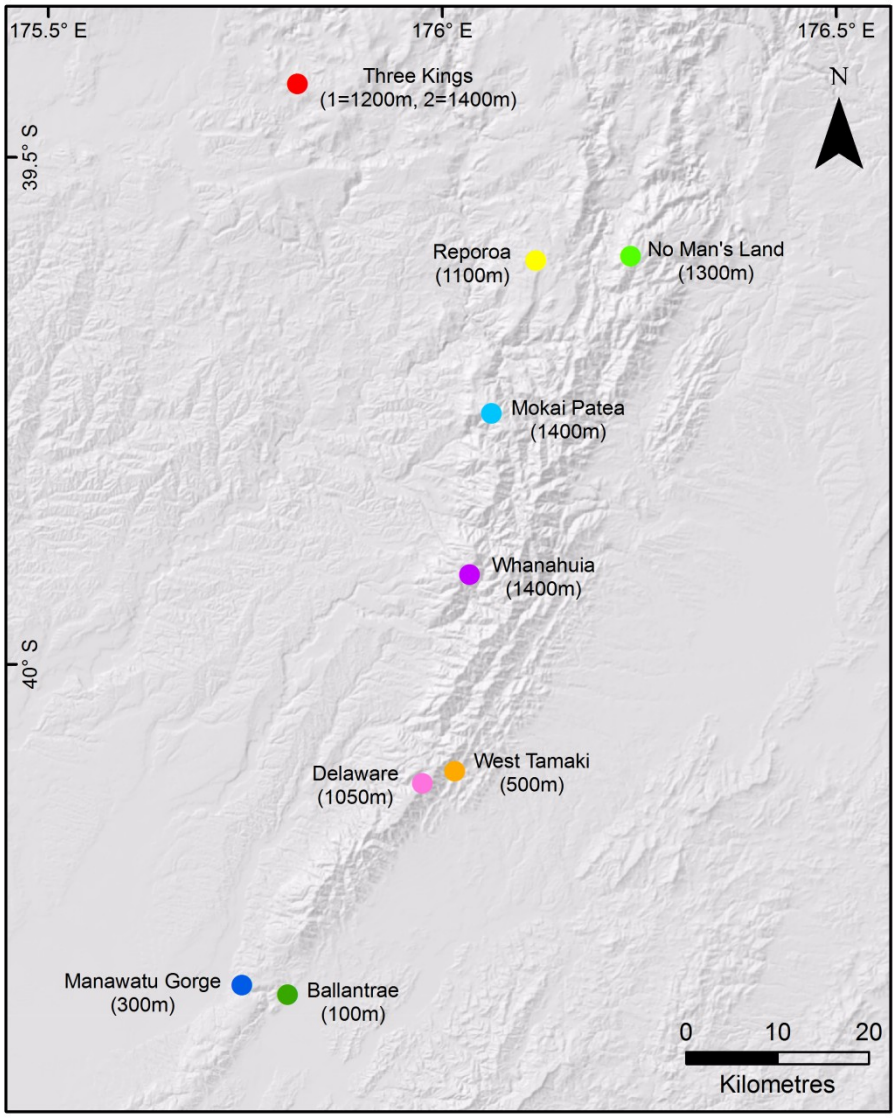

Figure 2.1. Map showing the palynological study sites mentioned in the text. Three Kings 1 and 2, refer to the separate Three Kings Range study sites (Rogers, 1987).

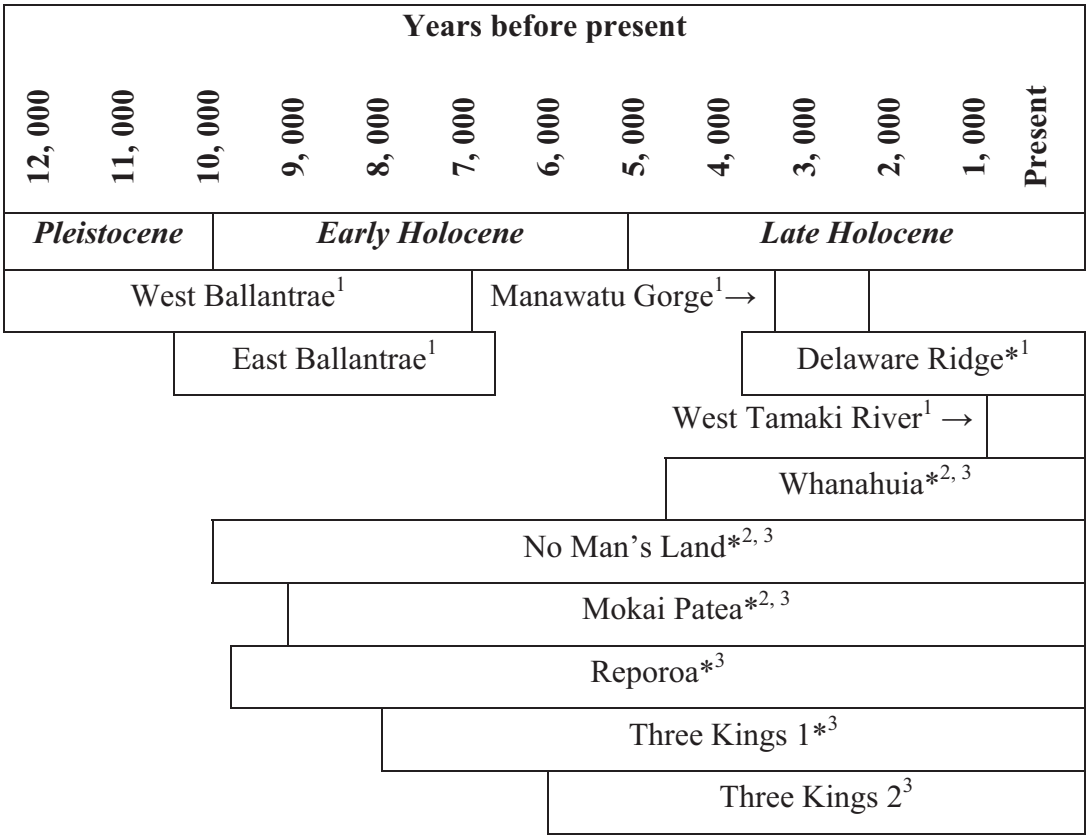

Figure 2.2. Diagram showing period of time represented from each study site. [1]Lees (1981; 1986), [2]Moar (1959; 1961; 1967), [3]Rogers and McGlone (1989) and *ombrogenous peat bogs (Froggatt and Rogers, 1990).

Summary of the pollen data over the past 2000 years

In the Mokai Patea (Moar, 1956) and Whanahuia pollen profiles (Moar, 1961), a dominance of tree pollen is obvious throughout the past 2000 years, with a marked increase in fern species in the last ~500 years. From 2000 cal yr BP there is a distinct increase in Fuscapora to the expense of Podocarpaceae, as well as a slight rise in *Coprosma*, Poaceae and *Cyathea*, while levels of *Dacrycarpus dacrydioides*, *Phyllocladus* and *Cyperaceae* are constant throughout. Pollen records from No Man's Land Bog (Moar, 1967) complement records obtained from Whanahuia and Mokai Patea with an increase in herbs and ferns (Moar, 1956; 1961).

Only two sites described by Lees (1981; 1986) cover the last 2000 years (Fig. 2.2), Delaware Ridge and West Tamaki River. The record at Delaware Ridge shows a gradual rise in Fuscaspora and *Olearia* with an associated decline in Podocarp varieties, *Quintinia*

and *Ascarina*. Levels of *Dacrycarpus* and *Dacrydium cupressinum* are relatively consistent throughout the pollen record at this site. The pollen diagram from West Tamaki River shows a discernible increase in *Weinmannia*, as levels of Fuscaspora, *D. cupressinum*, Podocarpus and *Fuschia* decline (Lees, 1981, 1986).

Both Three Kings sites show comparable pollen records for the late Holocene, (with the exception of the dominance of herbs and ferns at Three Kings 2). They show a distinct increase in *Poaceae*, *Halocarpus*, *Cyperaceae*, *Gleichenia*, *Pteridium*, and exotic species, while Fuscaspora and Podocarpus decline (Rogers and McGlone, 1989). Reporoa Bog shows similarities to the Three Kings site with a decrease in Fuscaspora, *D. cupressinum* and Podocarpus to the advantage of *Poaceae*, *Empodisma*, *Gleichenia*, *Pteridium* and exotic species (Rogers and McGlone, 1989). Pollen sums from the Three Kings and Reporoa are analogous to those produced by Moar (1956; 1967) with a dominance of tall tree taxa and an increase in Fuscaspora, Poaceae and *Pteridium* to the expense of Podocarpus and *D. cupressinum*.

Interpretation of vegetation history in the Ruahine Range

In general, palynological evidence from the Ruahine Range is suggestive of a shift towards wetter, colder conditions in the late Holocene. Moar (1967) shows evidence for a rise in Fuscaspora, grasses and sedges to the detriment of podocarps in the last 800 years, which backs up ideas put forward by Elder (1963) that an expansion in *Nothofagus solandri var. cliffortioides* is indicative of an increasingly wetter and cooler climate. The absence of *Quintinia* at Delaware Ridge and decline at West Tamaki, coupled with the decrease in *Ascarina* at both locations indicates that climatic extremes (i.e. frosts and droughts) are much more frequent during the late Holocene (Lees, 1986). However, the decrease in Ascarina may also be due to the shade intolerance of this taxon. The increase of *Olearia* at Delaware Ridge is thought to be a result of wetter climate (Lees, 1986).

Based on vegetation evidence, Elder (1965) put forward that the tree-line in the Ruahine Range was lowered by ~200 m in the late Holocene, as cloud cover increased at higher altitudes. The inception of ombrogenous peat bogs in the Ruahine Range during the late

Holocene (Fig. 2.2) is also suggestive of increasingly wetter conditions (Froggatt and Rogers, 1990), and provides evidence for climatic variability in the Ruahine Range region (Rogers and McGlone, 1989).

A persistent rise in *Pteridium* (a colonizing fern) in the last 500 years and a further rise in *Pteridium* and the appearance of exotic species (*Pinus*) after 150 years, suggests an anthropogenic influence in all sites (McGlone and Wilmshurst, 1999). Exotic species are not recorded at No Man's Land, Mokai Patea, and Whanahuia, but all 3 sites show a considerable amount of *Pteridium*. Typically, *Pteridium* has increased in response to volcanism (Wilmshurst, 1997). However, an increase in *Pteridium* spores does not accompany tephra layers from volcanic events (e.g. Taupo) at these Ruahine Range sites, so it can be assumed that the appearance and rise in *Pteridium* is associated with deforestation by humans.

There is a distinct variance in vegetation response to climate over the past 2000 years, particularly in Fuscaspora (indicative of a cooler, harsher climate; McGlone and Topping, 1983), which does not appear to correlate to latitude or altitude. Decreases in the Fuscaspora trend appear at Three Kings, Reporoa and West Tamaki sites, while increases occur at Delaware Ridge, Mokai Patea, No Man's Land, and Whanahuia. This response suggests that the Ruahine Range experiences local variability in the climatic regime that is not necessarily related to regional forcing. It is also possible that this concurrent rise and fall of Fuscaspora may be due to anthropogenic influence as suggested by Elder (1963).

Severe storms are also likely to have an influence on forest composition (McKelvey and Murton, 1992). It may only be when other factors predispose trees to wind damage that harmful damage will severely affect the tree (Wardle, 1970). This was found with Cyclone Bernie in 1982, which affected the east coast of the North Island, where a harsh drought occurred immediately after the storm and enhanced mortality rates in affected forests (Shaw, 1983). The close proximity to Tongariro and Taupo Volcanic Centres increases the probability that vegetation would have been influenced by volcanic activity. For example, the eruption of the Taupo Pumice, 1717 cal yr BP (Lowe *et al*., 2008) has been shown to

have caused major disturbance to forests, particularly in the central North Island (Wilmshurst and McGlone, 1996). The different regeneration pattern in different forest types in parts of the Ruahine Range is likely a combination of all these factors. Community patterns often reflect the influence of climate, altitude, slope instability, volcanism, fires, humans, and introduced animals (Rogers, 1987).

2.2.2 Vegetation and environmental changes in a regional context

There have been a wide range of paleovegetation records covering the past 2000 years in New Zealand (Newnham *et al*., 1999). A review of palynological evidence shows a general decline in drought and frost sensitive taxa such as *Ascarina lucida* (McGlone and Moar, 1977) and an increase in *Prumnopitys taxifolia* (McGlone and Topping, 1977) and *Nothofagus* sp. (Newnham *et al*., 1999) suggesting a response to a cooling climate during the late Holocene.

A marked increase in *Libocedrus* (Horrocks and Ogden, 1998) in the central North Island at the time of the Taupo eruption indicates a response to volcanism, though Horrocks and Ogden (1998) note that the expansion of *Libocedrus* was already in progress as climate changed to stormier and cooler conditions. The change in Holocene climate has also been favourable for the initiation and continuation of wetlands (Rogers and McGlone, 1989) especially in the drier, eastern areas (McGlone, 2009) as the strengthened southerlies have augmented precipitation (McGlone, 2002). These regional changes are synchronous with vegetation changes recorded from the Ruahine Range (Moar, 1967; Lees, 1981; Rogers and McGlone, 1989)

The use of different proxies from varying environments has given more insight into the climatically variable late Holocene in New Zealand, mostly pointing to a progressively cooler, wetter climate in the last 2000 years (Lorrey *et al*., 2008). The records available are from palynological studies (e.g. Wilmshurst *et al.*, 1997; Augustinus *et al.*, 2006), tree-ring datasets (e.g. Palmer *et al*, 2004; Cook *et al*, 2006), speleothems (e.g. Wilson, 1979; Williams *et al*., 2004; Lorrey *et al.*, 2008), glacier advances and retreat (e.g. Gellatly *et al.*, 1988; Schaefer *et al*., 2009), and lake sediments (e.g. Page *et al*., 2010). It is thought that

the strengthening in the Southern Hemisphere westerlies is thought to have been a main factor for climate variability (Shulmeister *et al.*, 2004).

Globally distinct periods of rapid climate change throughout the Holocene are characterised by major atmospheric circulation changes (Mayewski *et al*., 2004). The period from 1150 – 750 cal yr BP. is globally recognised as a period of warming (Broecker, 2001), and termed the Medieval Warm Period (MWP); in New Zealand this has been recorded in speleothem records (Williams *et al*., 2004) and tree-ring derived temperatures (Cook *et al.*, 2002). The period 600 – 150 cal yr BP is recognised as a period of cooling, and has been identified from glacial advances in the Southern Alps (Schaefer *et al*., 2009), and isotope records (Lorrey *et al*., 2008). This cool phase is recognised in many locations around the globe (Hendy *et al*., 2002), is termed the Little Ice Age (LIA). These periods of rapid climate change (Mayewski *et al*., 2004) presents a basis for the reconstruction of paleoclimate during this time.

The majority of New Zealand palynological records of environmental change occurring after ~600 cal yr BP are obscured by the arrival of humans at approximately this time in New Zealand (Wilmshurst *et al.*, 1997; Eden and Page, 1998). However, the date for arrival of people in New Zealand is still debated. This has led to some uncertainty for the causal factors of environmental change over this time period (Newnham *et al*., 1998), whether changes can be attributed to changing climate, or are a result of anthropogenic activity (Mayewski *et al*., 2004).

2.2.3 Conclusion

Compared to some other mountain ranges in New Zealand, there has been a wealth of information gleaned from the sites in the Ruahine Range which cover the last 2000 years. In addition to vegetation, further work has been carried out on tectonics (Hanson, 1998) and erosion (Grant, 1985), though the separate research areas have not been assimilated in any way to present a complete record of environmental history.

In order to identify processes and gain a higher understanding of the variability and regional climatic within the late Holocene, a multi-proxy study would be useful. While there is a wealth of information available, high-resolution records of environmental change spanning the late Holocene are relatively sparse in New Zealand (Schaefer *et al*., 2009).

Chapter 3: Study area

3.1 Site location

Lake Colenso lies at an altitude of 720 m in the north-western Ruahine Range (Fig. 3.1A). The lake is a closed system with no significant inlets or outlets, has a mean depth of 5 m and covers an area of 0.03 km^2. The lake was initially identified as a landslide-dammed lake by Cunningham and Stribling (1978), where landslide scarps are evident to the NW and SSW (Fig. 3.1B). It is likely that these landslides were caused by an earthquake on a nearby major fault, which explains the significant displacement of material. Lowe and Green (1987) recognized that the date of formation for Lake Colenso was prehistoric, though no other published work has so far been conducted on the origins of the lake.

The Ruahine Range, trending NNE-SSW, spans over 100 km length, from the Ngaruroro-Taruarau River confluence in the north, to the Manawatu Gorge in the south (Hanson, 1998). The landscape of the southern part of the North Island is a direct result of the North Island Dextral Shear Belt (Beanland *et al*., 1998) and this tectonically active zone marks the innermost deforming part of a 200 km-wide active boundary (Wang and Grapes, 2008). Here, dextral strike-slip faults have formed in response to the Pacific Plate subducting obliquely beneath the east coast of the North Island (Lamb and Vella, 1987; Langridge *et al*., 2005). Major features include the axial ranges (Tararua and Ruahine Range), and also the Kaimanawa Mountains, which are predominantly formed along the major faults. Summit heights range from 450 – 1730 m, and the average rate of uplift in the Ruahine Range is approximately 2 – 3 mm/yr (Marden, 1984).

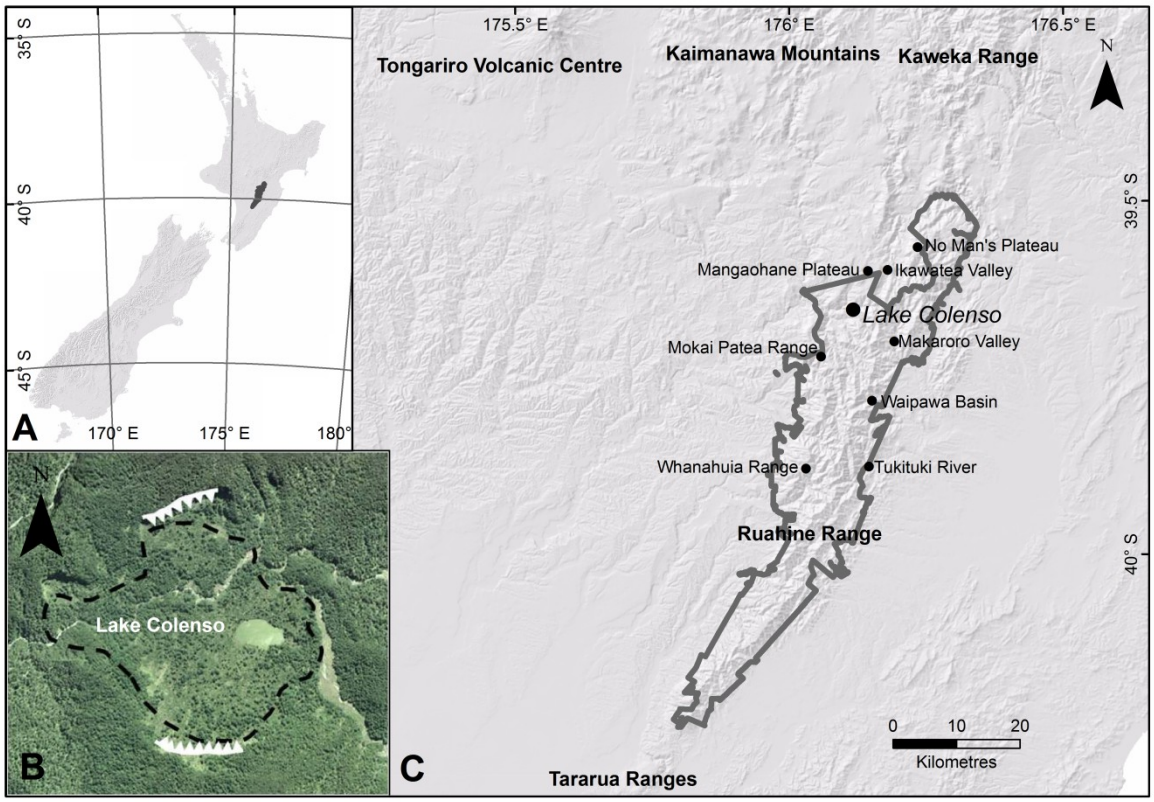

Figure 3.1. A. Map showing the Ruahine Range in central-southern North Island. **B**. Aerial photo showing forested environment of Lake Colenso area, dashed line represents the podocarp-broadleaf forest boundary discussed in section 3.2.1, while the toothed white lines mark the dominant landslide scarps (aerial photo from Land Information New Zealand, 2010). **C**. Regional map of Ruahine Range (grey line showing the boundary of the Ruahine Forest Park), showing proximity to Tongariro Volcanic Centre, and locations named in-text.

3.2 Vegetation

3.2.1 Present vegetation

Nothofagus solandri var. *cliffortioides* is dominant above 610 m in the northern Ruahine Range, except in areas of poor drainage where *Dacrydium biforme* and *Chionochloa rubra* are dominant (Wardle, 1970). The average tree line of the northern Ruahine Range is 1400 m; *C. rubra* is present on the wider crests and gentler slopes while *Nothofagus* forest dominates the steeper slopes and narrower ridges, with some isolated vestiges in the tussock areas (Grant, 1996).

Nothofagus fusca is also present along major waterways and eastern forest margins (Elder, 1965), and stands are frequent in the upper Ikawatea Valley, Makaroro Valley and in the eastern margins southwards to the Tukituki River (Grant, 1996). Isolated stands of podocarp-broadleaf forest remain in several areas, mainly around the forest margins at lower altitudes and within sheltered basins, such as Pohokura Basin, and Wild Sheep Spur (Fig. 3.1; Grant, 1996). *Prumnopitys taxifolia*, *Podocarpus totara*, *Dacrycarpus dacrydioides*, *Weinmannia racemosa*, *Nestegis cunninghamii* and *Nestegis lanceolata* are the dominant species in podocarp-broadleaf stands, with lesser amounts of *Dacrydium cupressinum* and *Prumnopitys ferruginea* (Grant, 1996). *Libocedrus bidwillii* is common on the Mangaohane Plateau, which is largely made up of limestone (Rogers, 1987). In this area, *N. fusca* is invasive at lower levels and *N. solandri* var. *cliffortioides* at higher levels (Rogers, 1987).

The Lake Colenso basin is particularly sheltered due to the landslide scarps which stand at approximately 40 m height (Fig. 3.1B) resulting in a distinctive pocket of podocarp-broadleaf forest within the surrounding *Nothofagus* forest (Fig. 3.1B).

3.2.2 Change in the last 150 years

Colenso (1884), who first documented the Ruahine Range vegetation, noted that the flora appeared to be flourishing in isolated parts of the Range (particularly near the main drainage divide), and attributed this to the fact that human impact was relatively minimal in the upper altitudes of the Ruahine Range. Aston (1914) later noticed an absence of *Nothofagus menziesii* in the Ruahine Range, in comparison with the Tararua Range and Kaimanawa Mountains.

One-off events such as fire, drought or human activity have had an impact on forest composition; particularly small fires associated with early Maori are thought to partly explain sporadic patterns in vegetation regeneration (Elder, 1963; 1965). Rogers (1989) found that beech expansion in the Ruahine Range, originally noted by Elder (1965), was also a factor in spatial forest variability. Indeed, present spatial forest variability depends primarily on slope and the favourable conditions for growth as determined by local climate (Elder, 1965). Though overall, vegetation on steeper slopes is most susceptible to collapse, regardless of composition (Rogers and Leathwick, 1997).

Although climatic changes during the late Holocene have affected the vegetation of the Ruahine Range, the impact of introduced animals such as deer (*Cervus elaphus*), goats (*Capra hircus*) and possums (*Trichosurus vulpecula*) on the vegetation largely obscures natural change after 1920 (Cunningham, 1979). Possums were found to be the main cause of forest deterioration (Rogers and Leathwick, 1997), with red deer and goats being responsible for inhibiting canopy replacement.

The establishment of *Pinus radiata* forests was relatively widespread throughout the region in the 1950s (Page *et al*., 1994a), though the gazetting of the Ruahine Forest Park in 1976 (Department of Conservation, 2008) meant that exotic plantations were kept out of the Ruahine Forest Park area (Fig. 3.2).

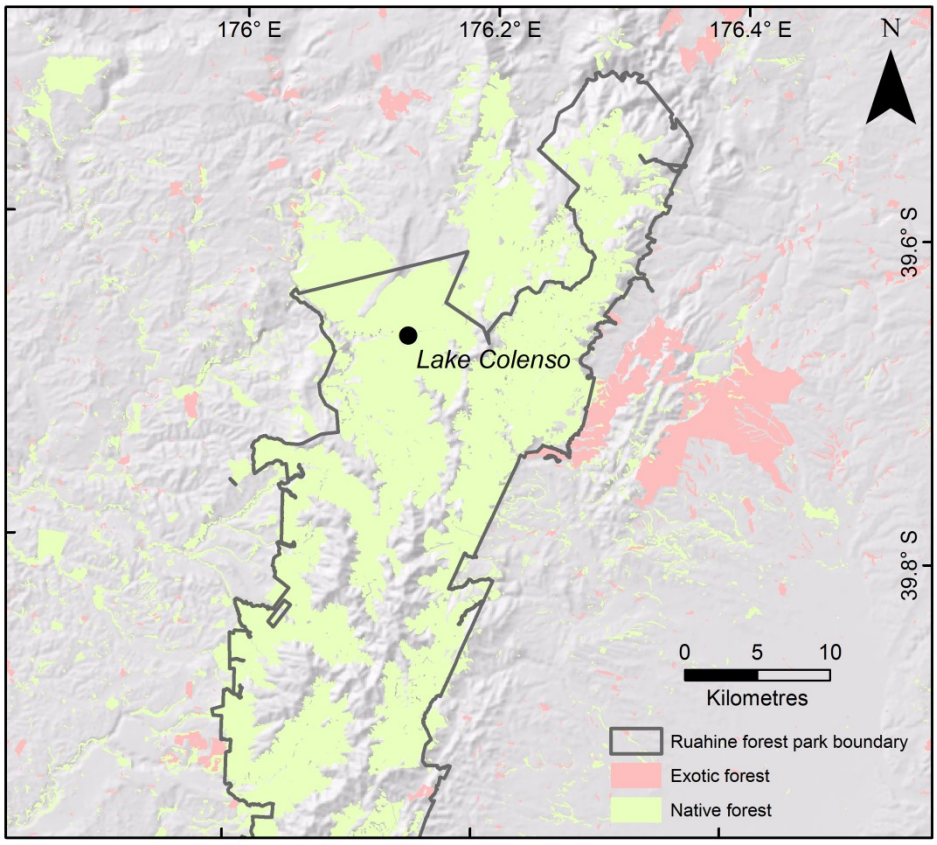

Figure 3.2. Present vegetation distribution in the northern Ruahine Range.

3.2.3 History of fire and burning

Evidence of pre-European fire is obvious on the No Man's Plateau, Mokai Patea Range, Whanahuia Range and the Mangaohane Plateau (Elder, 1965), where *Chionochloa rubra* now dominates. It was likely caused by early Maori burning (Elder, 1965) rather than as a result from the Taupo eruption (1717 cal yr BP, Lowe *et al*., 2008), where vegetation recovery was rapid in the Kaimanawa Mountains and Ruahine Range (Elder, 1962). From radiocarbon evidence (NZ 6682: 550 ± 76 cal yr BP and NZ 6917: 534 ± 22 cal yr BP) and age of *Libocedrus* stands, Rogers (1987) puts forward a period of major deforestation by fire from 530 to 550 cal yr BP.

Colenso (1884) and Elder (1965) present evidence of smaller fires around 1847, and during the 1880s, respectively. It is likely that these fires were to make travel through the Range easier and also farming, where it was common practice for shepherds to burn tussock at the close of the spring muster (Rogers, 1987).

3.3 Climate

The climate in the Ruahine Range is described as being cloudy, with rainfall ranging from 1150 mm near the north-eastern foothills, to 5000 mm near the main drainage divide (Marden, 1984). Rain records for the northern Ruahine Range (Fig. 3.3), started in 1926 and shows correspondence to ENSO variability (Fig. 3.4). Prevailing south-westerly winds cause an orographic effect, resulting in a dry eastern district and relatively wetter western district in the Ruahine Range (Rogers and McGlone, 1994). Easterly climate systems also have a significant effect in the area (Rogers, 1987). Cloudbursts frequently occur, causing high amounts of rain to fall in a relatively short time (Elder, 1965), while snow is frequent above 1300 m in winter months (Grant, 1985). Average daily temperatures range from 4.5°C to 10.5°C, with a minimum of 0°C and a maximum of 15°C (Elder, 1965).

Rogers (1987) suggests that in the northern-most Ruahine Range, summers are warm and dry while winters tend to be cold and wet. Because there is very little information on climate for the Lake Colenso basin, information has been drawn from nearby climate stations (Table 3.1). From an average of the data from the district (Fig. 3.3), the climate in the montane-subalpine Lake Colenso area has an average of 1460 mm rainfall and an average of 168 rain days.

Table 3.1. Summary of data from climate stations closest to Lake Colenso, north-western Ruahine Range (National Institute of Water and Atmospheric research, 2011)

Site	Altitude (m)	Distance (km)[a]	Years[b]	Annual rainfall (mm)[c]	Years[b]	Rain days[d]
Lake Colenso	720	0	-	1460	-	168
Pukeokahu, Kowhai Hills	549	11.7	1958-1989	968	1959-1971	143
Mangaohane Station	777	14.6	1922-1964	1011	1922-1952	137
Pukeokahu, Koitiata	520	15.1	1992-2010	954	2005-2010	178
Upper Kawhatau Valley	625	15.4	1975-1997	1421	1975-1997	217
Pohokura Outstation	488	18.7	1960-1964	1277	-	-

[a] Distance from Lake Colenso
[b] Years that records are available
[c] Taken as an average over the number of years that records are available
[d] Number of days per year with 0.1 mm or more rain and taken as an average over the number of years that records are available

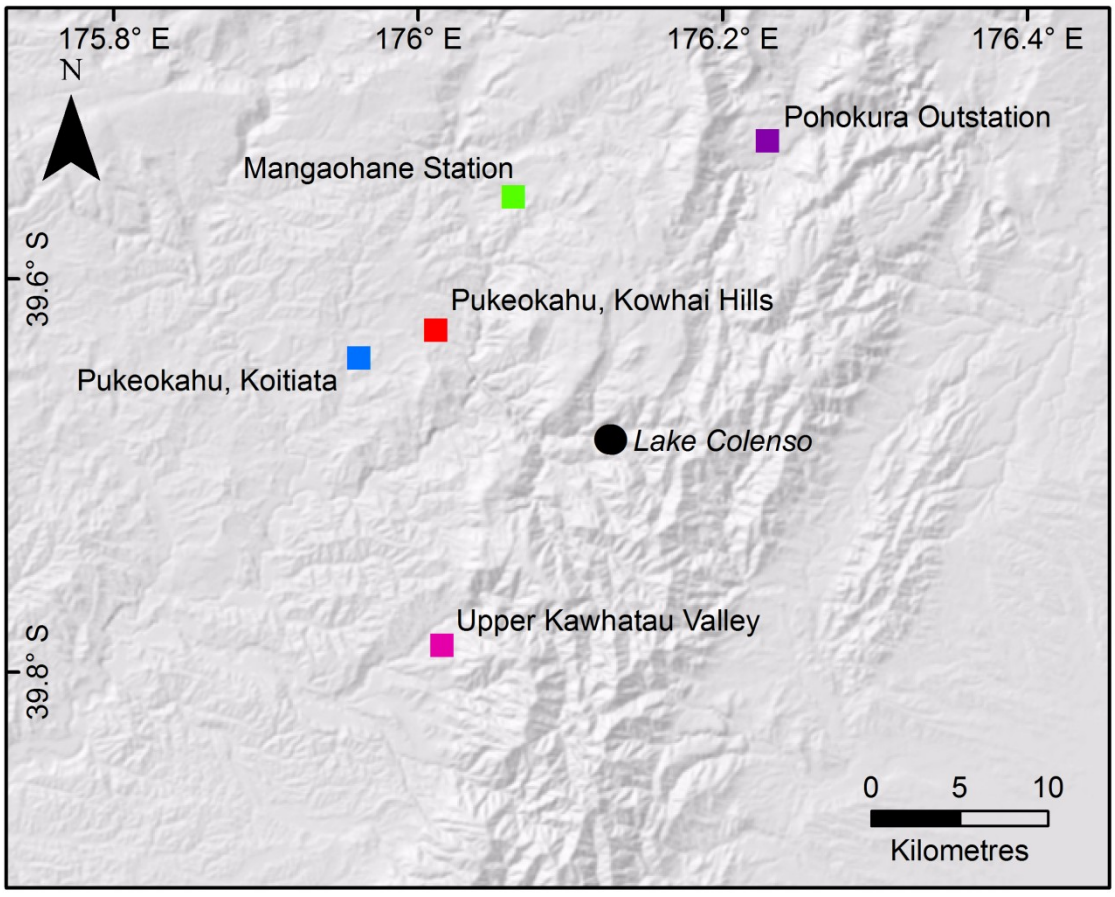

Figure 3.3. Selected climate stations marked with squares in the north-western Ruahine Range with respect to Lake Colenso.

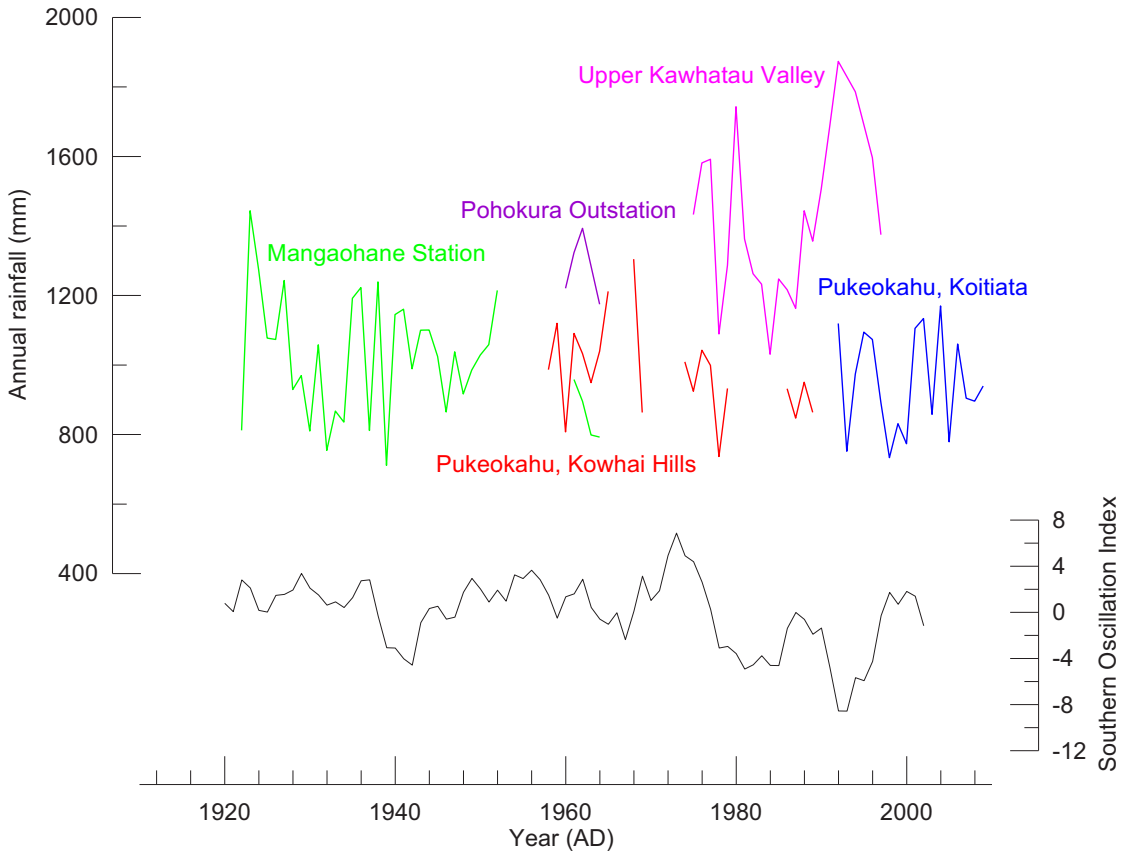

Figure 3.4. Annual rainfall from selected locations within the north-western Ruahine Range (National Institute of Water and Atmospheric research, 2011), and SOI (Bureau of Meteorology, 2011).

3.4 Geology

3.4.1 Geological history

The main lithology of the Ruahine Range is undifferentiated greywacke of the Torlesse Supergroup (Suggate *et al*., 1978), which dominates the geology of the majority of the axial ranges of New Zealand (Williams, 1991). These sediments were deposited between the Carboniferous and the Cretaceous in an offshore marine basin setting and were subsequently compressed and uplifted during the Rangitata Orogeny (early Cretaceous) (Kingma, 1959). The Rangitata Orogeny was followed by a period of tectonic quiescence in the late Cretaceous, in which some of the Torlesse rocks were gradually eroded resulting in the formation of an extensive peneplain (Williams, 1991). This was followed by a repeated marine transgression in Pliocene times (Rogers, 1987), where shallow and deep marine sediments were deposited in the Wanganui Basin (Katz, 1979). Uplift associated with the Kaikoura Orogeny began again in the Pleistocene (Thornton, 2009), as a result of convergence between the Pacific and Australian Plates at the Hikurangi Trench (Lamb and Vella, 1987), causing a marine regression and further deformation of the Torlesse Supergroup, and the newly deposited Plio-Pleistocene sediments (Browne, 1978). Increased erosion from the current orogenic phase has resulted in the vast deposition of alluvial gravels derived from the Ruahine Range onto the adjacent alluvial plains (Hubbard and Neall, 1980).

The geology of the Ruahine Range was initially mapped by Firth and Feldmeyer (1943) with more localized studies produced by Lillie (1953) and Fleming (1953), and on a regional scale by Kingma (1962). It has since been synthesized into a New Zealand-wide map (Geological and Nuclear Sciences, 2010), which is presented with the geology of the study area in Fig. 3.5. The geology of the immediate Lake Colenso area is poorly understood and misrepresented (Smale *et al.*, 1978) by the regional geological map published by Kingma (1962). A study of the Mangaohane Plateau (10 km north of Lake Colenso) by Browne (1978) is the most detailed geological work that has been conducted on the broader northwest Ruahine Range area, where the focus was on the sedimentology and faunal relationships of the Plio-Pleistocene strata.

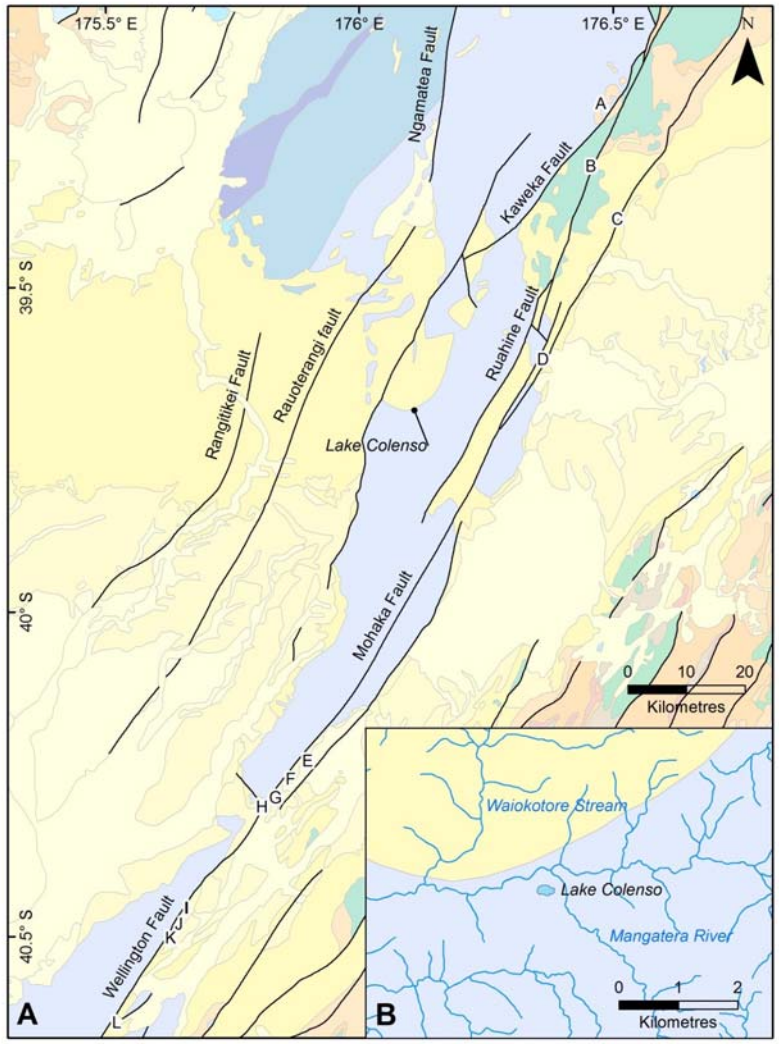

Age	Lithology
Upper Quaternary	Alluvium
	Laharic colluvium
	Dune sand
	Aggradation (in part glacial) gravel
	Marine sand, silt of coastal beaches, mostly covered by alluvium
	Andesite of volcanoes and flows; agglomerate and breccia
	Pumiceous pyroclastics
	Rhyolite of domes and flows
Lower Quaternary	Marine gravel, sand, silt, in part tuffaceous; coquina limestone
	Aggradation gravel
	Marine gravel, sand, and silt mostly covered by alluvium
	Ignimbrite and associated ash-flow tuff, rhyolitic to dacitic
Pliocene	Marine sandstone, siltstone, pumiceous tuff, coquina limestone, conglomerate
Upper Miocene	Calcareous sandstone and siltstone (partly alternating with graded sandstone), pumiceous and andesitic tuff, limestone
Lower Miocene	Calcareous sandstone and siltstone (partly alternating with graded sandstone), pumiceous and andesitic tuff, limestone
Oligocene	Calcareous sandstone and siltstone (partly alternating with graded sandstone), limestone, greensand, conglomerate
Eocene	Bentonitic mudstone, greensand, siliceous claystone and limestone, flint beds; coal measures, sandstone
Upper Cretaceous	Sandstone and siltstone (partly alternating with graded sandstone), greensand, siliceous shale, conglomerate
Jurassic-Lower Cretaceous	Greywacke and argillite (partly alternating with graded greywacke), minor spilitic tuff and lava, chert, limestone, manganese-bearing rocks
Jurassic	Greywacke and argillite (partly alternating with graded greywacke), minor spilitic tuff and lava, chert, limestone, manganese-bearing rocks
Triassic-Jurassic	Greywacke and argillite (partly alternating with graded greywacke), minor spilitic tuff and lava, chert, limestone, manganese-bearing rocks
Permian-Triassic	Greywacke and argillite (partly alternating with graded greywacke), minor spilitic tuff and lava, chert, limestone, manganese-bearing rocks
?Upper Paleozoic	Chlorite Subzone II pelitic schist, phyllite, deformed conglomerate, with steeply-plunging lineation

Figure 3.5. A. Geological map showing of central/southern North Island (adapted from Geological and Nuclear Science, 2010). Letters represent trench locations mentioned in Table 3.2 (Hanson, 1998; Langridge *et al*., 2007), A. Wedd; B. Davis; C. Syme; D. McCool; E. Trotter; F. Paper Road; G. Beagley; H. Inglis; I. Army Depot; J. Ebbett; K. Hughes; and L. Death. **B**. Local geology of the immediate Lake Colenso area by Kingma (1962).

3.4.2 Fault and tectonic history

The Wellington Fault was first recognised by McKay (1892), and further analysed by later workers (e.g., Cotton, 1916; Adkin, 1949; Wellman, 1953) who identified traces and evidence of historic fault movement. At the Manawatu Gorge the Wellington Fault bifurcates to become the Ruahine and Mohaka Faults (Hull, 1983). These have been studied in further detail by Marden (1984), and Hanson (1998). Because of the relatively late arrival of humans to New Zealand, there is a lack of accurate dates for seismic activity on these faults, so palaeoseismic studies offer a way in which past earthquake and fault behaviour can be assessed (Hanson, 1998). Interpretations of palaeoseismic records rely on the premise that seismic events cause catastrophic change of the landscape either during or immediately after a strong earthquake (Hanson, 1998).

Radiocarbon dates are obtained from depositional units that are interpreted as having a co-seismic origin, such as peat bogs in sag ponds, or organic matter associated with units that have poor sorting and are identified as deposits from destabilised slopes (Van Dissen *et al*., 1992). These dates are used to build records of palaeoseimicity and such records (Table 3.2) have been constructed for the Wellington (Berryman, 1990; Beanland and Berryman, 1991; Van Dissen *et al.*, 1992; Van Dissen and Berryman, 1996; and Langridge *et al*., 2005, 2007), Ruahine, Kaweka, and Mohaka Faults (Hanson, 1998). Periods of major earthquake activity from the Pahiatua region of the Wellington Fault are 2350 - 1890 cal yr BP, 1260 - 790 cal yr BP, and 280 - 150 cal yr BP (Langridge *et al*., 2007).

Table 3.2. Table showing reconstructed earthquake events from the Wellington (northern section), Ruahine, Mohaka and Kaweka faults over the late Holocene.

Fault	Site	Lab number or tephra	Mid-point 2σ range (cal yr BP) [c]
Wellington	Army depot[a]	NZ 7574	385
	Death-1[a]	Wk 1796	1280
		WK 10066	1460
		NZS 7552	147.5
	Death-2[a]	Wk 1798	810
		Wk 1797	1105
		Wk 1799	1220
	Ebbett-1[a]	Wk 1800	930
		Wk 1802	4160
		Wk 1803	4210
		Wk 1801	4300
	Ebbett-2[a]	Wk 1804	330
		Wk 1806	1115
	Hughes-1[a]	NZ 8054	140
		Wk 10068	980
		Wk 10071	2090
		NZ 8052	2225
		Wk 10070	2625
		NZA 3604	3710
		Wk 10069	3890
		NZ 8049	3900
		NZ 8051	3935
		NZ 8053	3960
	Hughes-2[a]	NZ 8055	2005
Ruahine	Davis-1[b]	NZ 8230	>1137
		Tephra (Taupo)	>1717
		Tephra (Waimihia)	<3410
		NZ 8232	>3885
	Davis-2[b]	Tephra (Taupo)	>1717
Mohaka	Inglis-3[b]	NZA 3698	<156
		NZA 8007	>4790
	Inglis-4[b]	NZA 3070	>983
	Paper Road-1[b]	NZA 5365	1611
	Syme-1[b]	Tephra (Taupo)	>1717
	Beagley Farm[b]	Wk 3151	305.5
	Trotter-1[b]	Wk 3143	<2005
		Wk 3144	<5740
		NZA 8228	219.5
	Trotter-2[b]	Wk 3140	829.5
		Wk 3148	>3236
		NZ 8291	5760
	McCool-1[b]	NZ 8293	>678
		Tephra (Taupo)	>1717
		Tephra (Waimihia)	<3410
		Tephra (Taupo)	>1717
Kaweka	Wedd-1[b]	Tephra (Taupo)	>1717

[a] Langridge *et al*. (2007)
[b] Hanson (1998)
[c] Ages calibrated from original dates using OxCal 4.1 (Bronk Ramsey, 2001) and ShCal04 database (McCormac *et al*., 2004)

3.5. Summary

While the Ruahine Range has been well studied, the history of Lake Colenso remains poorly understood. Hence, research of the area could provide not only information about the lake but also details about the paleoseismicity of the area, if indeed the landslide was triggered by an earthquake on a nearby fault. The geology, as mentioned, is not well understood and research into this would offer more insight into landscape evolution, from both a geological and geomorphological perspective. An environmental record from Lake Colenso would provide more insight into the present and past climate of the area.

Chapter 4: Methods

This chapter outlines methods used in the two-part study; the first part explains methods used in the field for geological mapping and for the investigation of landslide ages. The second part summarises the laboratory procedures and techniques used for the different proxies in the construction of the environmental history of the lake.

4.1 Geology

4.1.1 Geological mapping

The forested setting of the Ruahine Range means geological outcrops are scarce, so Department of Conservation tracks and streams were traversed to attain structural and lithological information. Photos and samples were taken where possible and the geology of the localities that were not visited during fieldwork was inferred from aerial photographs. The lithologies were matched to those of Browne, (1978; 2004a), Erdman and Kelsey, (1992), and McIntyre and Kamp (1998). The resulting map was produced using ESRI ArcMap, and a number of informal names have been introduced to avoid ambiguity.

4.2 Geomorphology

4.2.1 Determination of ages

Determination of landslides and age of the lake

At Colenso Hut section (~720 m altitude) in the Mangatera River (Fig. 4.1), a piece of carbonized wood lay stratigraphically 1 m below the landslide debris (Fig. 4.2) on which Lake Colenso is situated. When extracted, sediment was cleaned off and the wood dried in perforated foil for 2 weeks, and then sent to The University of Waikato Radiocarbon Dating Laboratory for standard radiometric dating (Wk 29531). This provides a maximum age for landslide timing.

A second landslide is interpreted to have occurred sometime after the first. To determine the age of the landslide upon which Lake Colenso is situated, the sediment was radiocarbon dated (NZA 34331) at the peat/basal silt boundary and is interpreted to be the point at which peat formation was initiated almost immediately or soon after a landslide event.

It is thought that a third landslide event ultimately blocked valley drainage, causing lake formation. This point in time is identifiable in the sediment core as the boundary between the peat and the organic lake sediment (Fig. 4.6) and is dated using the age model (discussed in section 6.2.1).

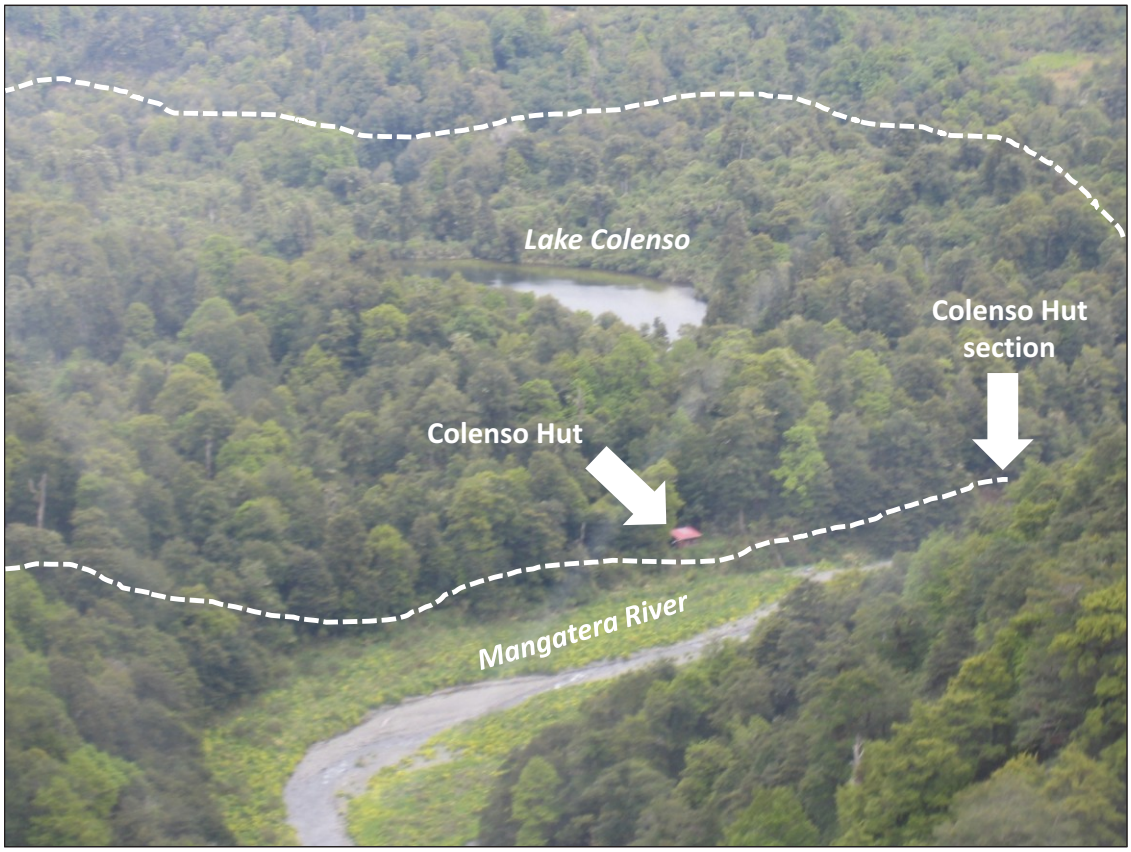

Figure 4.1. Location of Colenso Hut section relative to Lake Colenso and Colenso hut. The dashed line represents the outer limit of landslide material mapped from field mapping and aerial photography.

Figure 4.2. Top. Colenso Hut section. Lines are drawn to distinguish the main lithostratigraphic changes. 'X' shows the positioning of the wood sampled for radiocarbon dating (person for scale). **Bottom.** Diagram showing different lithological units.

4.3 Lake Colenso

This section outlines the laboratory procedures and methods used for the different proxies in the construction of the environmental history of the lake.

4.3.1 Core extraction, analysis and stratigraphy

This section explains the processes and techniques involved in the retrieval of sediment cores from Lake Colenso, and stratigraphic analyses.

Core extraction

Sediment cores were extracted from Lake Colenso in December 2009, from a specialized coring platform (Fig. 4.3) which was transported in via helicopter. Transects of the lake (Fig. 4.4.) were made using a depth sounder to decide appropriate places for coring. Cores were collected from the deeper parts of the lake using a modified Livingstone corer where lake sediment was extracted in one metre lengths (cores 1 and 2). A piston corer was then used so that continuous sediment could be retrieved (cores 3, 4 and 5); these were then cut into one metre lengths for transportation from the field to Massey University where cores were refrigerated at 4°C until processing.

Core analysis

Initially the cores were x-rayed which allowed layers of different density to be identified without destruction of the core material. This was done using the digital x-ray machine in the Institute of Veterinary, Animal and Biomedical Sciences (IVABS). Images were taken with 70 kv (kilovolts) at an exposure of 20 mAs (milliamps/second), and x-ray images were then studied and layers of interest identified.

Figure 4.3. Specialized platform used for coring.

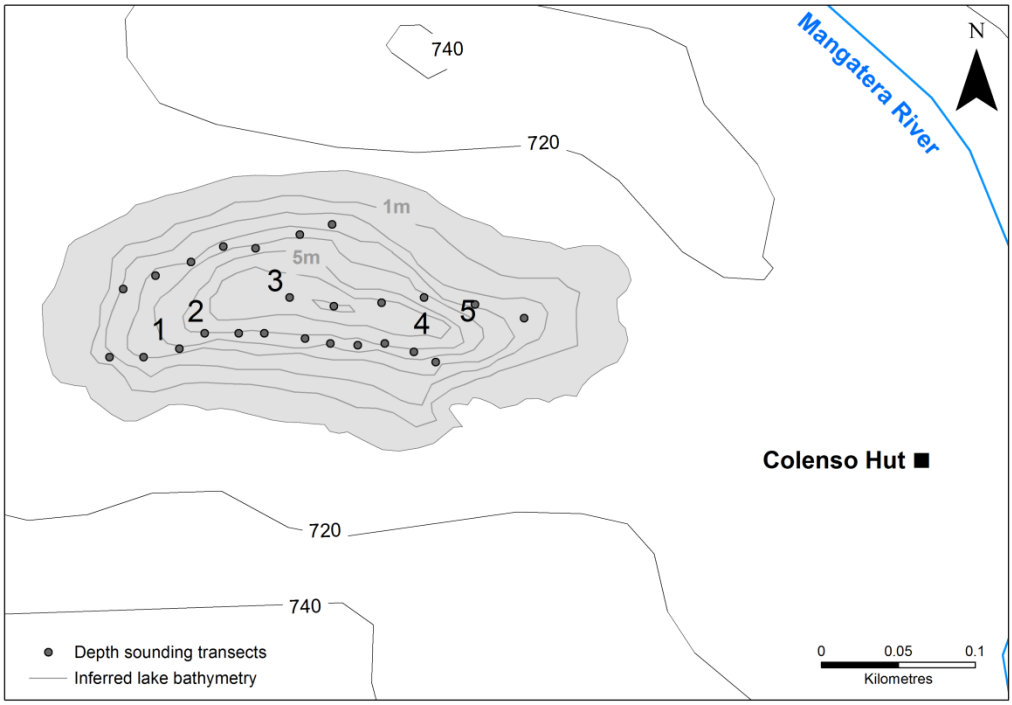

Figure 4.4. Topographic map of Lake Colenso area, showing transects where depth was measured using a depth sounder, interpolated isobaths and locations where sediment cores were extracted (numbers represent the different locations).

Core stratigraphy

Cores were split lengthways, surfaces cleaned and a stratigraphic log prepared. Stratigraphic changes were recorded (Appendix 1) and stratigraphic logs were matched with x-rays so that any layers indistinguishable by eye could be identified.

Stratigraphy between separate cores was analysed (Fig. 4.5) and it was decided to use cores 2, 3 and 4 for analysis as these contained the most comparable stratigraphy. Samples for sedimentology, molluscs, ostracods, and biogeochemical analyses were taken from overlapping cores 3, and 4, termed as the composite core (Fig. 4.6). As there was a limited amount of material from the composite core, core 2 was used for palynological and tephra analyses.

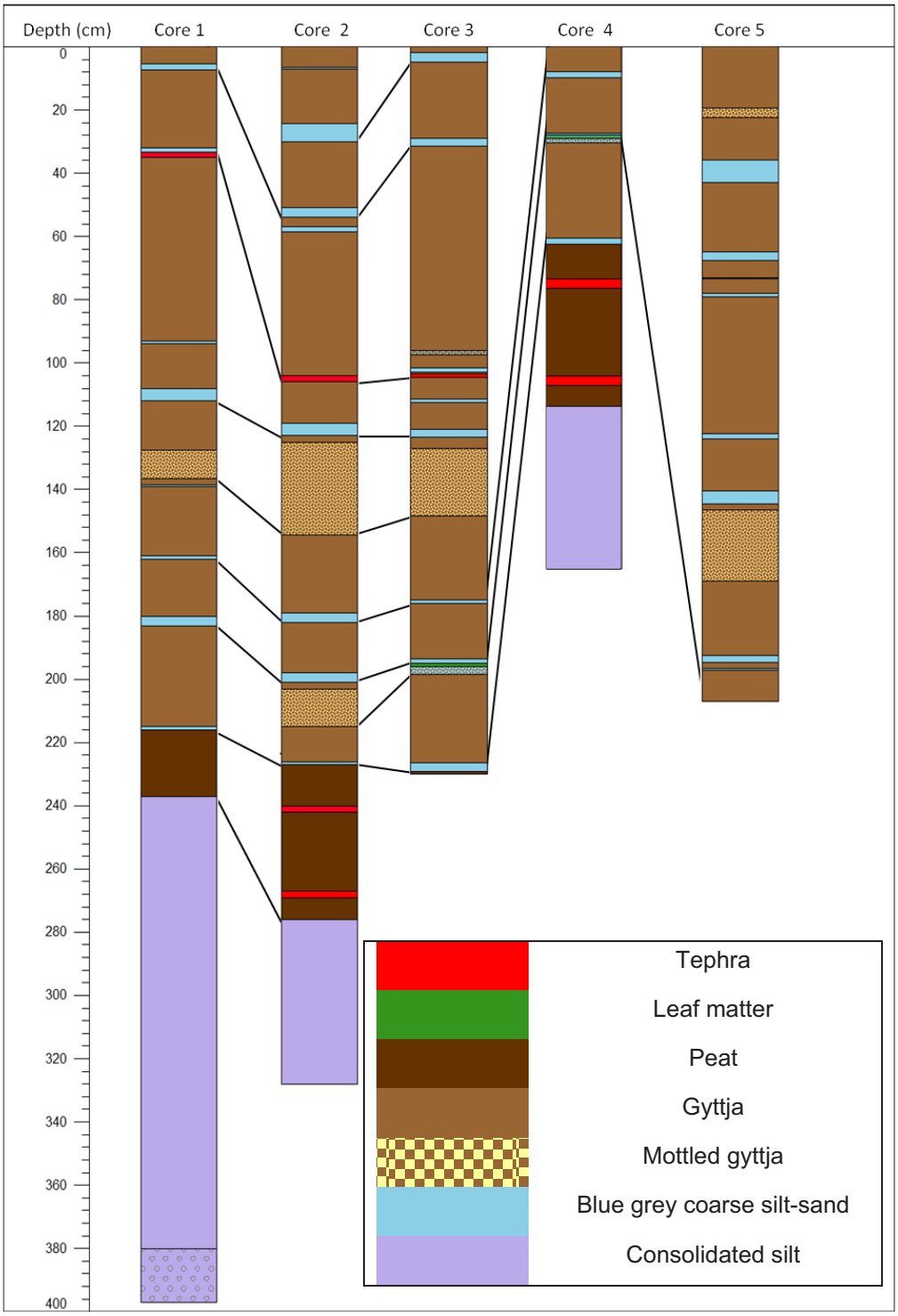

Figure 4.5. Correlation columns showing the relationship of strata between extracted sediment cores.

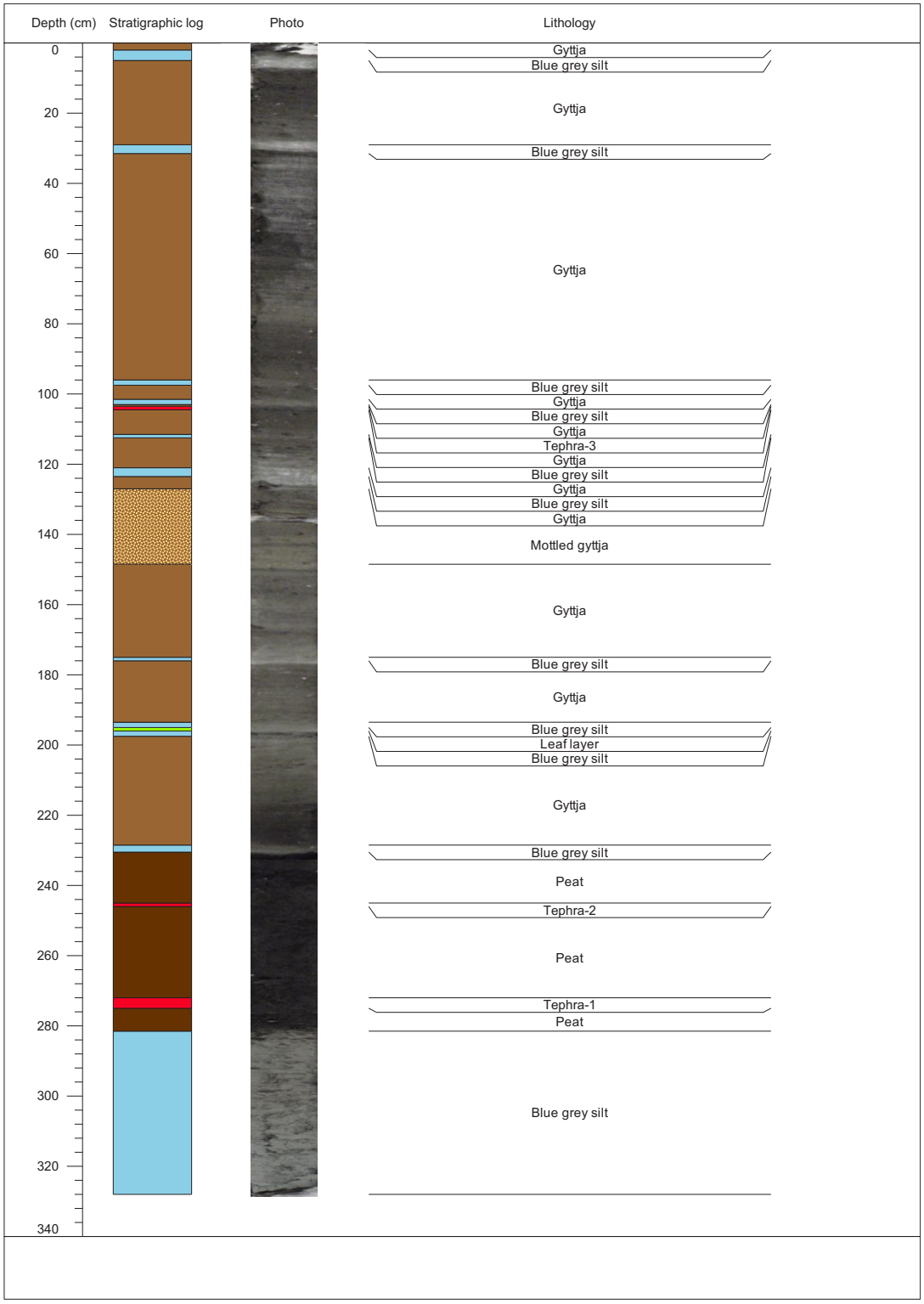

Figure 4.6. Stratigraphic column showing a photo and lithotypes of the composite core (cores 3 and 4). Key same as Fig. 4.5.

4.3.2 Sedimentology and dry bulk density

To quantify sedimentological changes, grain-size analysis was carried out at 1 cm intervals of a selected section (274 to 100 cm) of the composite core. This section was selected as it was decided that it represented the most active part of the lake system. Changes within the sediment, such as silt, tephra layers and the main lithological changes, were characterised and importance placed on changes vertically within individual layers.

Sedimentology

Pre-treatments similar to those outlined in Augustinus *et al*. (2008), Vaasma (2008), and Page *et al*. (2010) were carried out before laser diffraction analysis. The HORIBA Partica LA-950 Laser Diffraction Particle Size Distribution Analyzer (PSDA) in Soil and Earth Sciences at Massey University has an analytical range of 0.01 to 3000 μm with ± 0.6% accuracy, and uses a 5 mW 650 ηm red-laser diode and 3 mW 405 ηm blue-light emitting diode (LED) laser source.

The refractive index of minerals must be determined before analysis in the PSDA. Determining the refractive index of natural sediments is made difficult by the fact that most sediment is a mixture of different minerals (Sperazza *et al*., 2004), though variations of the refractive indices of common minerals (e.g. quartz [1.554], calcite [1.658], and mica [1.561]) are small enough to use a single refractive index (Loizeau *et al*., 1994), usually between 1.54 - 1.56 for quartzofeldspathic sediment (Loizeau *et al*., 1994; Murray, 2002; Sperazza *et al*., 2004).

Method: 5 - 10 grams of sediment was used for each sample and calcium carbonate ($CaCO_3$) material removed by adding 15 ml of 10% hydrochloric (HCl) acid to the wet sample and stirred. Samples were then washed with distilled reverse osmosis (RO) water by centrifugation at 3500 rpm for 4 minutes, and the solution carefully decanted so not to lose any material. To remove organic matter, samples were placed in a water bath at 80ºC and 35% hydrogen peroxide (H_2O_2) was added periodically until the effervescent reaction fully ceased, and the sample was bleached. Where the effervescent reaction became too violent Capryl ($C_8H_{18}O$) alcohol was added. Samples were again washed with distilled RO

water to neutralise the sample and centrifuged at 3500 rpm for 4 minutes before the solution was decanted.

Biogenic silica (diatom valves, phytoliths, and their fragments) was abundant in samples and was removed by treating samples with 10% potassium hydroxide (KOH) (Vaasma, 2008) in a water bath at 80ºC for 30 minutes. Samples were then washed with distilled RO water by centrifugation at 3500 rpm for 4 minutes and the solution decanted. Samples were then dried in an oven at 40ºC overnight, and subsequently sieved through a 2000 μm mesh sieve for use in the PSDA.

A refractive index of 1.55 was used for analyses of lake sediment, which is the same as that used in the Lake Tutira study (Alan Orpin *pers. comm.*), whereas tephra layers were assigned varying refractive index values dependent on tephra properties. Methods used in this study for the PSDA were similar to standard procedures outlined in the associated software. Distilled RO water was used in all analyses, and subsequently de-bubbled so that air bubbles did not affect grain-size measurement. Lasers were re-aligned and transmittance reset before ~0.2 g of sample was added. Samples were sonified for one minute and measurements were taken at least three times for each sample with a two minute interval between, or until measurements showed comparable results.

For a measure of clastic material in the sediments, samples were weighed before and after the removal of calcium carbonate, organic matter and biogenic silica.

Dry bulk density

To quantify the degree of compaction, measurements were made using 4 cm intervals from the composite core.

Method: Approximately 2 - 5 grams of sediment was weighed and dried for two days at 40°C. Samples were weighed again and dry bulk density calculated using the equation;

$$\rho = M_s / V_t$$

where ρ is the dry bulk density (g/cm^3), M_s is the dry weight (g) and V_t is the volume of the portion of the core sampled (4.618 cm^3).

4.3.3 Chronology

Two methods were used to develop an age model for the sediment cores: (1) tephrochronology; and (2) AMS radiocarbon dating.

Tephrochronology

Tephrochronology involves the use of volcanic ash and lapilli layers, collectively termed tephra, which have been characterised by mineralogical and geochemical properties and independently-dated using other methods, as chronostratigraphic layers, or isochrons to correlate sequences in different places (Alloway *et al*., 2007). A review by Lowe *et al*. (2008) outlines details of the stratigraphy, distribution and chemical composition of New Zealand tephra spanning the past 30,000 years.

Three layers of tephra were identified within the Lake Colenso cores. 'Tephra-1', a rhyolitic pumice lapilli, was identified at 275 cm; 'Tephra-2', an andesitic scoriaceous lapilli, was identified at 245 cm; and 'Tephra-3', a distinctly black (10YR 4/1) andesitic tephra layer, was identified at 103 cm. Samples were prepared so that the major elemental glass chemistry could be analysed and tephra source identified using geochemical values obtained from the Electron Microprobe (EMP) at the University of Auckland. Preparation methods, such as cleaning and sieving, were similar to those outlined in Steen-McIntyre (1977) and Rose (1996).

Method: Once sampled (10 - 20 grams), organic matter was removed by adding 50 ml of 35% hydrogen peroxide (H_2O_2) and heated at 60°C for 2 hours. A further 50 ml of H_2O_2 was then added until the reaction had ceased and the material was bleached. Where the effervescent reaction became too violent Capryl alcohol ($C_8H_{18}O$) was added. After removal of organic matter, the samples were washed with distilled reverse osmosis (RO) water, sieved through a 32 μm mesh and oven dried. Once dry, samples were separated by sieves into whole phi size fractions.

Lapilli from Tephra-1 and Tephra-2 was picked out from the 1000 μm size fraction and subsequently crushed to the 125 – 63 μm size fraction for EMP analyses. Tephra-3 had a high amount of calcium carbonate ($CaCO_3$), so was treated with 10% hydrochloric (HCl) acid. Heavy mineral separation using sodium polytungstate (SPT; specific gravity 2.45), was then carried out on the 250 – 125 μm size fraction of Tephra-3, to separate off the volcanic glasses for geochemical analyses following processes outlined in Steen-McIntyre (1977). Lastly, an epoxy plug was prepared for analysis using EMP following methods outlined in Froggatt and Gosson (1982).

Electron microprobe analysis (EMP) was performed on individual glass shards using an energy dispersive (EDS) Jeol JXA-840A electron microprobe at the School of Environment, University of Auckland. Assays were collected using a Princeton GammaTech Prism 2000 Si (Li) EDS X-ray detector using a 20 μm defocused beam to minimise loss of sodium and potassium, an accelerating voltage of 12.5 kV, a beam current of 600 pA, and 100 seconds live count time. An Astimex albite standard was analysed regularly (under a 2 μm focussed beam) during the course of analysis of the glass samples to ensure a consistent level of performance by the microprobe.

Radiocarbon analysis

To obtain a chronology of the lake cores, sediments were sampled at stratigraphic boundaries and at layers of interest for AMS radiocarbon dating.

Method: When extracted, samples were dried in perforated foil for 3 days and sent to the Rafter Radiocarbon Laboratory, Geological and Nuclear Science (GNS Science), Lower Hutt. Material was treated with an acid/alkali/acid process, and dried in a vacuum oven before radiocarbon dating using an Accelerator Mass Spectrometer (AMS). Three different materials were submitted for AMS dating; pollen (16 cm - NZA 35748, 16 cm - NZA 35749 and 91 cm - NZA 35692), bulk sediment (104 cm - NZA 34645) and plant macrofossils (196 cm NZA 35497 and 280 cm - NZA 34331).

4.3.4 Biogeochemistry

This section outlines the methods used for determining organic matter content from sediment, and stable isotope analyses using ostracods.

Bulk organic geochemistry

There are a variety of methods used to measure and analyse the amount of organic matter within sediment; the loss on ignition (LOI) method outlined by Heiri *et al*. (2001) is the most common. Other approaches include using a high induction furnace or wet oxidation. Organic matter tends to be over-estimated in analyses by the LOI method, where heating above 150°C tends to eliminate inter-crystalline H_2O in crystalline clays and allophane (Goldin, 1987). Analyses for this study were carried out using the high frequency induction furnace method outlined by Goldin (1987).

The electronically-operated resistance furnace (Leco FP-2000) located at Landcare Research, Palmerston North, measures both carbon and nitrogen content of the samples. Internal precision of measurements for the Leco furnace are 0.01% for carbon and 0.005% for nitrogen. Approximately 0.1000 g ± 10% of sediment was used per sample and a drifting correction was applied to samples where necessary. The total organic matter content per sample was calculated using: Organic matter = organic carbon × 1.724 (Waksman and Stevens, 1930).

Method: A sample resolution of 4 cm was used for the composite core. Samples were weighed while wet (so that water content could be measured) and subsequently dried in an oven at 40ºC and weighed again. The sample was then ground with a mortar pestle until grains were <2000 μm. As dried material adsorbs water readily it was briefly re-dried for one hour at 105ºC for an accurate determination of carbon and nitrogen.

Typically, calcium carbonate ($CaCO_3$) is removed prior to analysis for carbon content (Augustinus *et al*., 2008), though an investigation by Daly (2000) suggests that the presence of $CaCO_3$ has no significant effect on results from the Leco furnace.

Stable isotope analysis

Ostracods have long been recognised as a useful proxy for the reconstruction of lake temperature and chemistry, as specific characteristics from the host water are incorporated into the well-preserved carapace (Lowe and Walker, 1997; Keatings 2007). It is assumed that stable isotope equilibrium is reached during shell formation and is principally controlled by the $\delta^{18}O$ of the host water (Escobar *et al*., 2010). Stable isotope measurements of carbon and oxygen from ostracod carapaces have been extensively used in paleoenvironmental reconstructions in marine (e.g., Reeves *et al*., 2007), and freshwater (e.g., Li *et al*., 1997; Belis *et al*., 2008; Escobar *et al*., 2010; Mischke *et al*., 2010) settings.

Method: 5 - 10 grams of wet sediment was sampled every 7 cm from the composite core and soaked in distilled reverse osmosis (RO) water to disaggregate grains. The wet slurry was then put through a 32 μm sieve, fines discarded, and sediment >32 μm oven dried at 40°C. Once dry, 10 ostracod carapaces were hand-picked from each sample and were sent to the National Institute for Water and Atmospheric Research (NIWA) for stable isotope determination. Samples were reacted with three drops of H_3PO_4 at 75°C in an automated individual carbonate reaction (Kiel) device coupled with a Finnigan MAT252 mass spectrometer. Internal precision of measurements is 0.02 – 0.08‰ for $\delta^{13}C$ and 0.01 – 0.03‰ for $\delta^{18}O$, while external precision is 0.03‰ for $\delta^{13}C$ and 0.02‰ for $\delta^{18}O$.

4.3.5 Pollen, ostracods and molluscs

Pollen

Pollen analysis is the most versatile technique used in the reconstruction of Quaternary environments, as pollen and spore types are distinctive and can be identified to families, genera and down to the species level (Lowe and Walker, 1997). Pollen is typically well preserved because of the resistant outer exine layer.

Method: Samples were extracted at 5 cm intervals from core 2 and prepared following procedures adapted from Faegri and Iversen (1989). 10% hydrochloric (HCl) acid was added to remove calcium carbonate ($CaCO_3$), followed by an equal mixture of potassium hydroxide (KOH) and sodium pyrophosphate ($Na_4P_2O_7$) to neutralise humic acids and to deflocculate the clay material. To dissolve the siliceous material 30% hydrofluoric (HF) acid was used, and then acetolysis (using a ratio of 9:1 acetic anhydride to sulphuric acid) was used to remove cellulose. Samples were dehydrated using progressive strengths of ethanol, dried, then were mounted in silicon oil and sealed with paraffin wax.

Each sample was analysed at 400x magnification until a minimum count of 250 dryland pollen grains was reached. Pollen was identified with the aid of Moar (1993), *Podocarpus* and *Prumnopitys*-type pollen was differentiated using Pocknall (1981), and fern spores identified using Large and Braggins (1991). The resulting pollen diagram and CONISS cluster analysis was conducted using Tilia software (Grimm, 1987).

The pollen sum includes all dry land pollen and excludes ferns and wetland species. The Fuscaspora and *Dacrydium cupressinum* ratios are also presented, similar to those in McGlone and Topping (1977). The first ratio is between Fuscaspora and all other tree taxa, this ratio is a measure of the Fuscaspora trend which can be used as an indicator of cool, harsh conditions (McGlone and Topping, 1977). The second ratio is between *D. cupressinum* and other *Podocarpus-Prumnopitys* species (*Prumnopitys taxifolia*, *Prumnopitys ferruginea*, *Podocarpus totara*, *Podocarpus hallii*, *Podocarpus nivalis* and *Podocarpus acutifolious*). This is a measure of the frequency and intensity of precipitation

as *D. cupressinum* is tolerable to some water-logging but intolerant to drought, so a dominance of *D. cupressinum* over other *Podocarpaceae* is indicative of a wet climate (McGlone and Topping, 1977).

Ostracods

Ostracod species have different ecological requirements, in particular with respect to the host water chemistry as well as water depth, temperature, food type and availability, oxygen concentration, water turbidity and predation (Mischke and Holmes, 2008). An evaluation of the ecology and biology of paleoenvironmental proxies such as ostracod assemblages provide valuable and unique information for the field of paleoclimatology (Holmes, 2001). Increasingly, ostracods have been studied for use in paleoenvironmental reconstructions because of their sensitivity to ecological factors (e.g., Hayward *et al*., 2010).

Method: Approximately 5 - 10 grams of wet sediment was sampled from the composite core at 7 cm intervals, and samples were soaked in distilled reverse osmosis (RO) water overnight to disaggregate. Following disaggregation, the slurry was sieved through 63 μm and 5 μm sieves (with material <5 μm being discarded) to leave the size fraction containing most adult and later juvenile instars (Holmes, 2001). The remainder of the material was oven dried at 40°C, weighed and samples picked using a binocular microscope. Disaggregation methods used were similar to Holmes (2001), and Reeves *et al*. (2007).

Picking 300 – 500 ostracods valves is generally accepted as a representative amount (Belis *et al.*, 2008; Hayward *et al*., 2010) and in this study, at least 300 valves were counted per sample where possible. The dry weight of the sediment and the picked proportion of each sieve fraction picked was recorded which allowed a calculation of concentration (Holmes, 1998). The absolute abundance of valves is expressed as valves per cubic centimetre of sediment (Belis *et al*., 2008). Carapaces, where present, have been counted as two valves, and broken valves were generally excluded from counts to prevent counting errors and also reworked carapaces are likely not representative of the actual sample (Boomer, 2002).

Ostracods were identified (Appendix 2) using Hornibrook (1955), Chapman (1963), Barclay (1968), Eager (1971), and Rossetti *et al*. (1998, and with the aid of Margaret Morley *pers. comm.* (Geomarine Research, Auckland) with the resulting diagram made using Tilia software.

Freshwater molluscs

Molluscs tend to be an indicator of conditions within the water body, and an assessment of the mollusc assemblage provides valuable insight for use in paleoenvironmental reconstruction (e.g., Hayward *et al*., 2010).

Method: Molluscs were picked at the same time as ostracods though are split into a separate topic because of their different paleoenvironmental significance. Adult molluscs were picked from the >63 μm size fraction previously sieved in preparation for ostracods. A minimum of 300 molluscs (juvenile and adult) were counted where possible and molluscs were identified (Appendix 2) using Armon (1970), Beu and Maxwell (1990), and with the aid of Alan Beu (GNS Science, Lower Hutt), Bruce Marshall *pers. comm.* (Te Papa Museum, Wellington) and Margaret Morley *pers. comm.* (Geomarine Research, Auckland). The resulting diagram was made using Tilia software.

Chapter 5: Results

This chapter presents the results of geological and geomorphological investigations in the Lake Colenso area, and also outlines the results of the paleoenvironmental reconstruction from the Lake Colenso sediments.

5.1 Geology

This section presents geological findings and correlation with established units in the northern Ruahine Range (Browne, 1978, 2004a, b; Erdman and Kelsey, 1992; McIntyre and Kamp, 1998). Furthermore, a 1:30000 geological map of the study area is presented showing faults and a stratigraphic column displaying the stratal relationships.

5.1.1 Background

There are two dominant lithological units in the study area, distinguished by their different physiographic appearance and fossil content.

1) Mesozoic basement rock
2) Cenozoic marine sedimentary rocks

Mesozoic basement rock

The Mesozoic basement rock, part of the Torlesse Greywacke complex, is the dominant lithology in the Ruahine Range. The present Kaikoura Orogeny has uplifted the rocks which are bounded by various faults. The Torlesse complex has a dominant NE-SW trend in this region as shown by the rose diagram in Fig. 5.1.

Cenozoic marine sedimentary rocks

Late Tertiary sedimentary rocks form distinctive landforms in the Ruahine Range and in this region have dip angles up to 70° (Fig. 5.1). These rocks unconformably overlie the Mesozoic basement and were deposited during marine transgressions in the Plio-Pleistocene (Beu *et al*., 1981). The Mangatoro Formation (Browne, 1978) is conformably overlain by the Kaumatua Formation (Erdman and Kelsey, 1992) and these units are extensive in the Wanganui, and Hawkes Bay regions (Fleming, 1953; Lillie, 1953). Faunal and sedimentologic relationships of these Cenozoic units indicate high-energy sedimentation adjacent to an emerging greywacke fault block during early Wanganui times (Browne, 1978). The Plio-Pleistocene sedimentary rocks tend to be displaced by north and north-east trending faults, which have formed blocks providing repetitive sequences of strata (Browne, 1978).

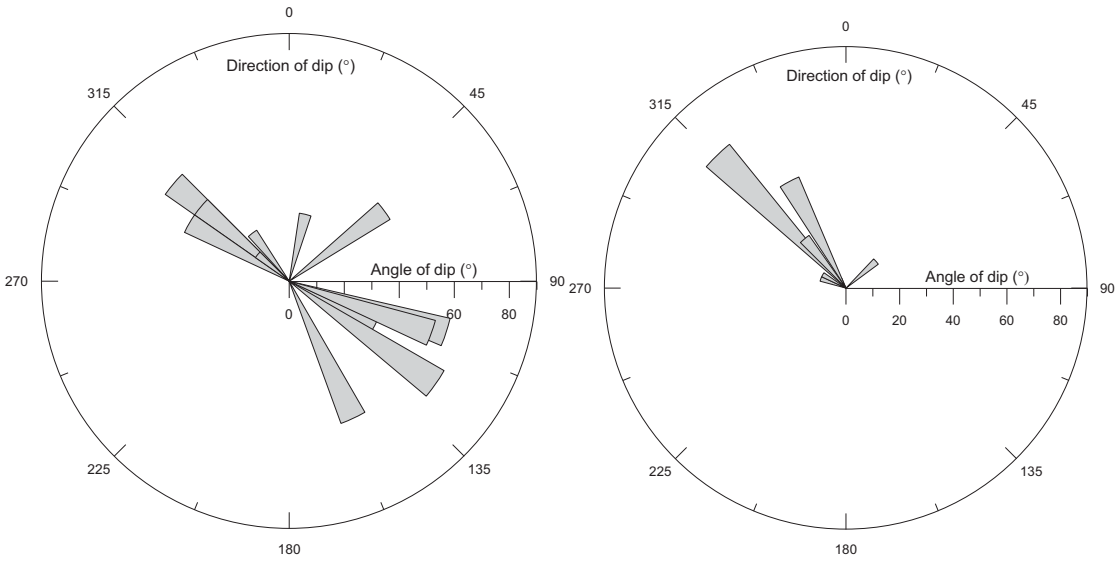

Figure 5.1. Rose diagrams showing the dip angle and dip direction of different lithological units. **Left**. Mesozoic basement rock. **Right**. Cenozoic marine sedimentary rock. Data presented is from Browne (1978), Smale *et al*. (1978) and from field mapping in this study (Fig. 5.10).

5.1.2 Local geological sequence

Torlesse Greywacke

Rocks are typically composed of fine- to coarse-grained sandstone interbedded with argillite (Browne, 1978). Due to deformation during two orogenies, the structure of Mesozoic rocks tends to be highly fractured (Fig. 5.2).

Figure 5.2. Folded greywacke of the Mesozoic basement rock, Maropea Stream.

Basal conglomerate

This poorly bedded greywacke conglomerate unit (Fig. 5.3) unconformably overlies the Mesozoic greywacke, and in this area is thought to be 80 m in thickness (Browne, 1978). The poorly sorted nature of this unit with sub-rounded to sub-angular clasts indicates rapid sedimentation; it was likely deposited during the upheaval of the Ruahine Range in a shallow basin environment (Browne, 1978).

Figure 5.3. A, **B**. Float of the Basal conglomerate**,** Mangatera River (Photos: Vince Neall). **C**. Basal conglomerate, Unknown Stream (Photo: Stephen Carey).

Mangatoro Formation (Browne, 1978)

A blue grey, massive fossiliferous siltstone layer found in the study area is correlative to the Mangatoro Formation (Browne, 1978) also found on the Mangaohane Plateau. This unit is thought to be 20 m in total thickness (Browne, 1978), and the presence of *Chlamys gemmulata* (Reeve, 1853) indicates Opoitian age. The molluscs, *Purpurocardia purpurata* (Deshayes, 1854) (Fig. 5.4A) and *C. gemmulata*, and echinoderm, *Fellaster zelandiae* (Gray, 1843), indicate a littoral-near shore depositional environment (Beu and Maxwell, 1990). Shells are concentrated in layers (Fig. 5.4B), and also articulated and imbricated (convex up), which is suggestive of a current-dominated environment during time of deposition, while good fossil preservation indicates proximity to the source area (Browne, 1978).

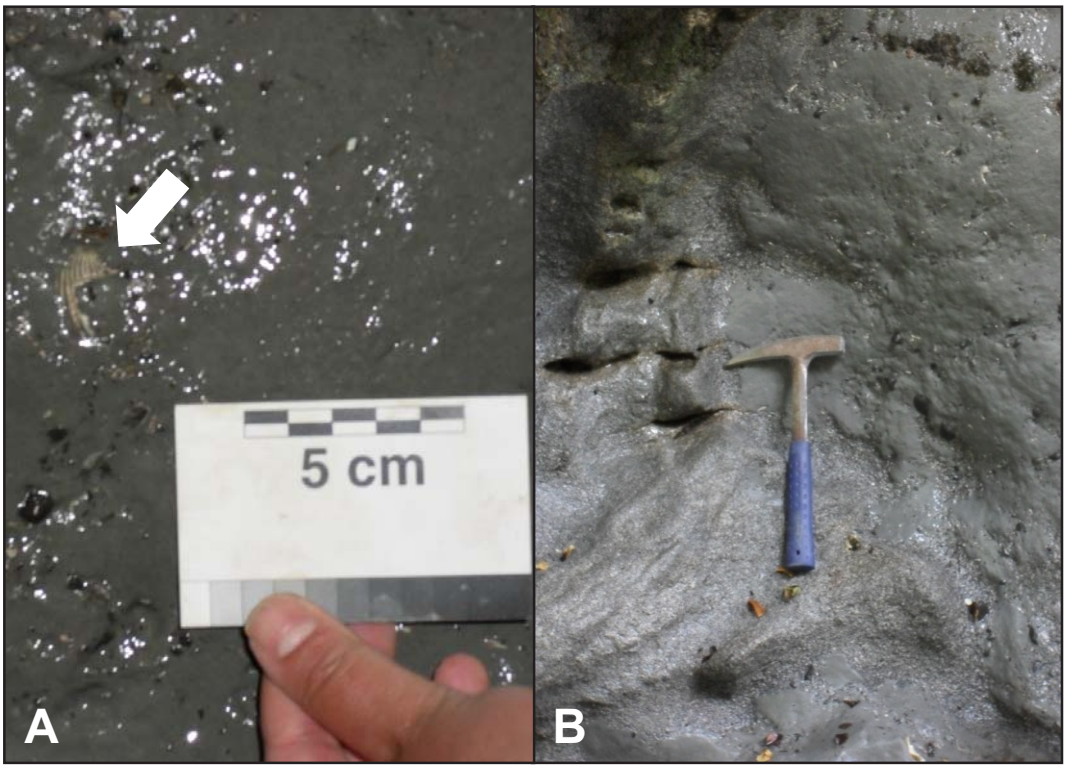

Figure 5.4. A. Broken *Purpurocardia purpurata,* Mangatoro Formation, Unknown Stream. **B**. Mangatoro Formation, Unknown Stream.

Kaumatua Formation (Erdman and Kelsey, 1992)

A sandstone and limestone in the study area are correlated with the Kaumatua Formation, which is part of the Te Aute sediment group (Beu, 1995). This is based on the similarities in lithological descriptions by Browne (1978, 2004b), and the presence of Plio-Pleistocene fossils such as *Crassostrea ingens* (Zittel, 1864), the trace fossil *Ophiomorpha*, and sandstone inter-bedded with siltstone. The Kaumatua Formation comprises two lithofacies, massive sandstone (Fig. 5.5) and an overlying limestone (Fig. 5.6). The formation is Mangapanian in age and thought to have a total thickness of 170 m (Browne, 2004a).

Sandstone: This unit is a well sorted, graded, massive sandstone unit and generally lacks fossils in the basal section with an increase to centimetre-decimetre thick fossil beds towards the upper part (Fig. 5.5A, B). The fine- to medium-grained sandstone has occasional siltstone bands and occurrence of ichnofossils (Fig. 5.5C). The concentration of fossils suggests a considerable energy regime at the time of deposition (Browne, 1978).

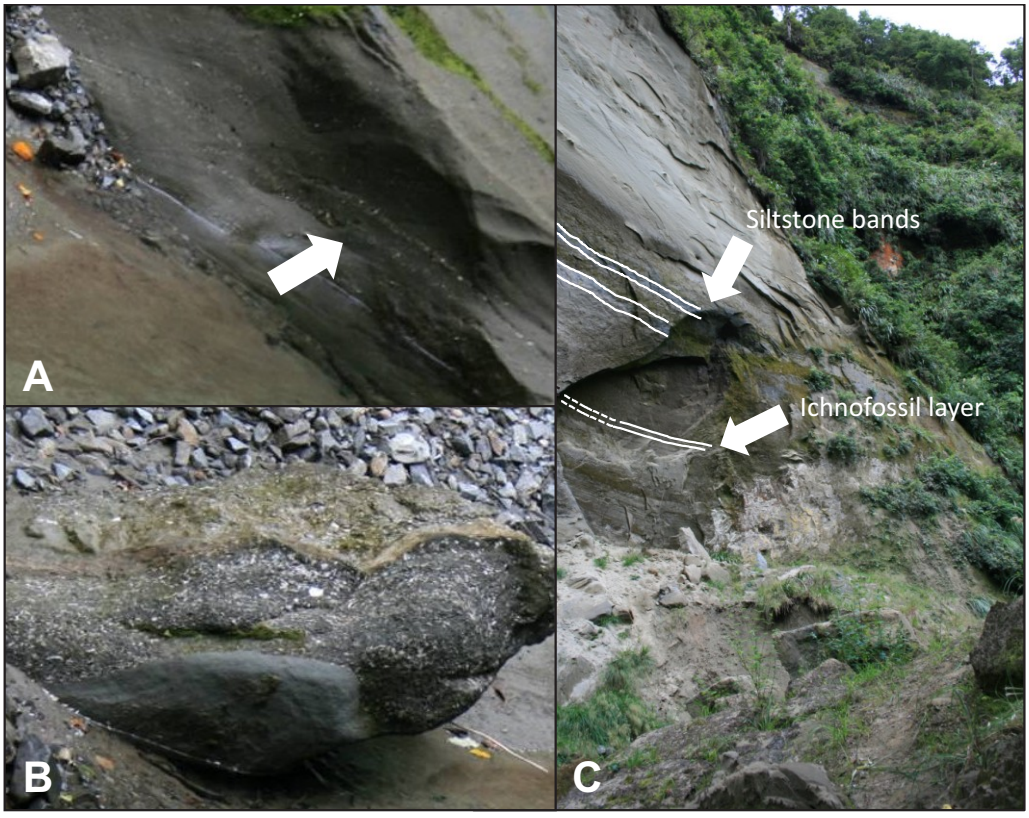

Figure 5.5. A, **B**. Float material showing concentration of fossils beds, sandstone unit of the Kaumatua Formation, Potae stream (This is not an approved New Zealand Geographic name; it has been introduced here to avoid ambiguity). **C**. Siltstone bands and ichnofossil layer, Potae stream.

Limestone: This unit is crystalline (Fig. 5.6A) with decimetre-sized flags in the basal section, grading into impure, shell-rich limestone that marks the upper boundary of the Te Aute Formation in this region. The sharp contact between the massive sandstone and overlying limestone unit (Fig. 5.6B) implies a rapid facies change, typical during the Plio-Pleistocene period. The presence of greywacke clasts in the upper part of the limestone (Fig. 5.6C, D) are likely sourced from the Torlesse group of the uplifting Ruahine Range (Erdman and Kelsey, 1992).

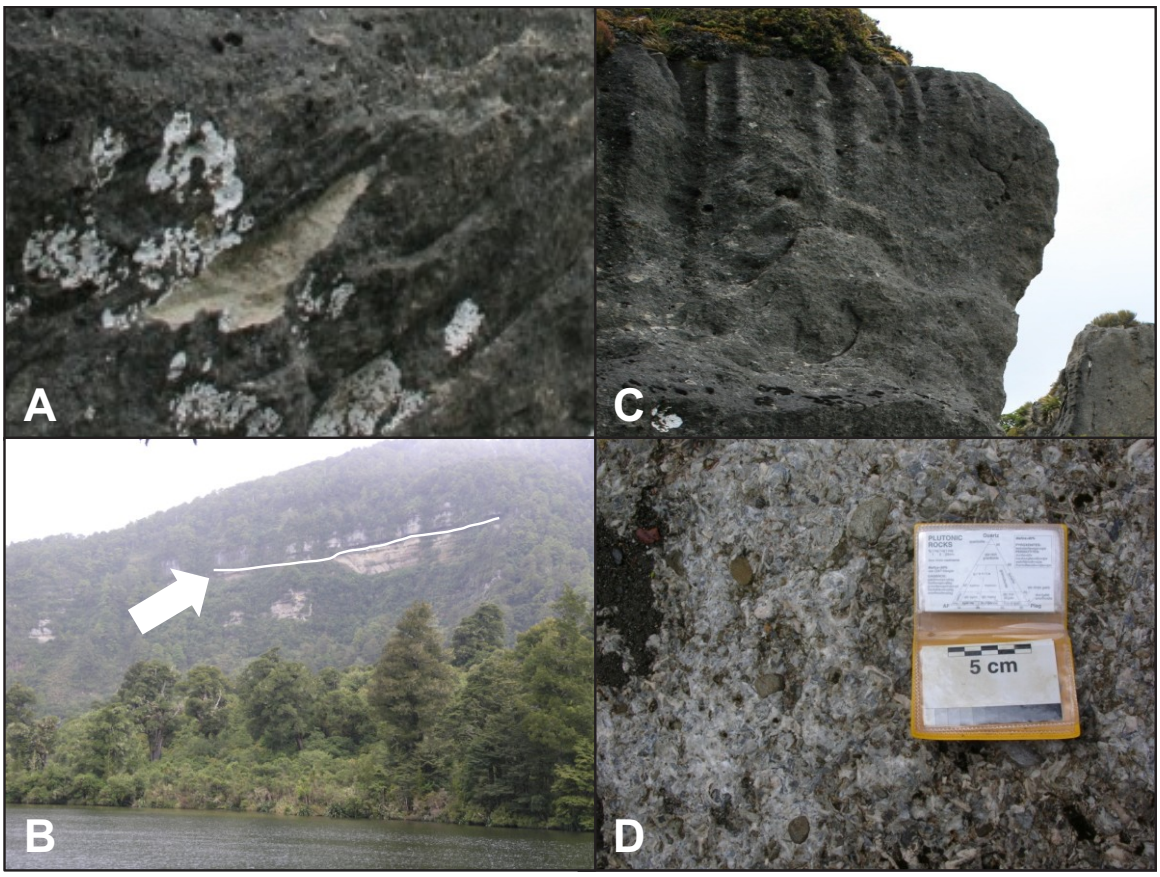

Figure 5.6. A. Freshly exposed surface showing crystalline structure of unit. **B.** Northern scarp, Lake Colenso, line showing sharp contact between sandstone and limestone. **C.** Limestone flags (weathered) (Photo: Andrew Mercer). **D.** Shell-hash limestone, Unknown Stream-Colenso saddle.

Whariki Formation (McIntyre and Kamp, 1998)

The presence of *Chlamys delicatula* in this clastic limestone unit indicates it is a likely correlative to the lower part of the Hautawa shellbed (Feldmeyer and Jones, 1943) of the Whariki Formation (McIntyre and Kamp, 1998). This formation comprises a clastic limestone with decimetre-sized flags and cross-bedding, and is thought to be ~20 m thick. The presence of *C. delicatula* (Hutton, 1873) in the limestone capping Te Rakaunuiakura (Fig. 5.7A, B, C) and Aorangi (Fig. 5.7D) found by Beu *et al*. (1981) indicates Nukumaruan age for this formation.

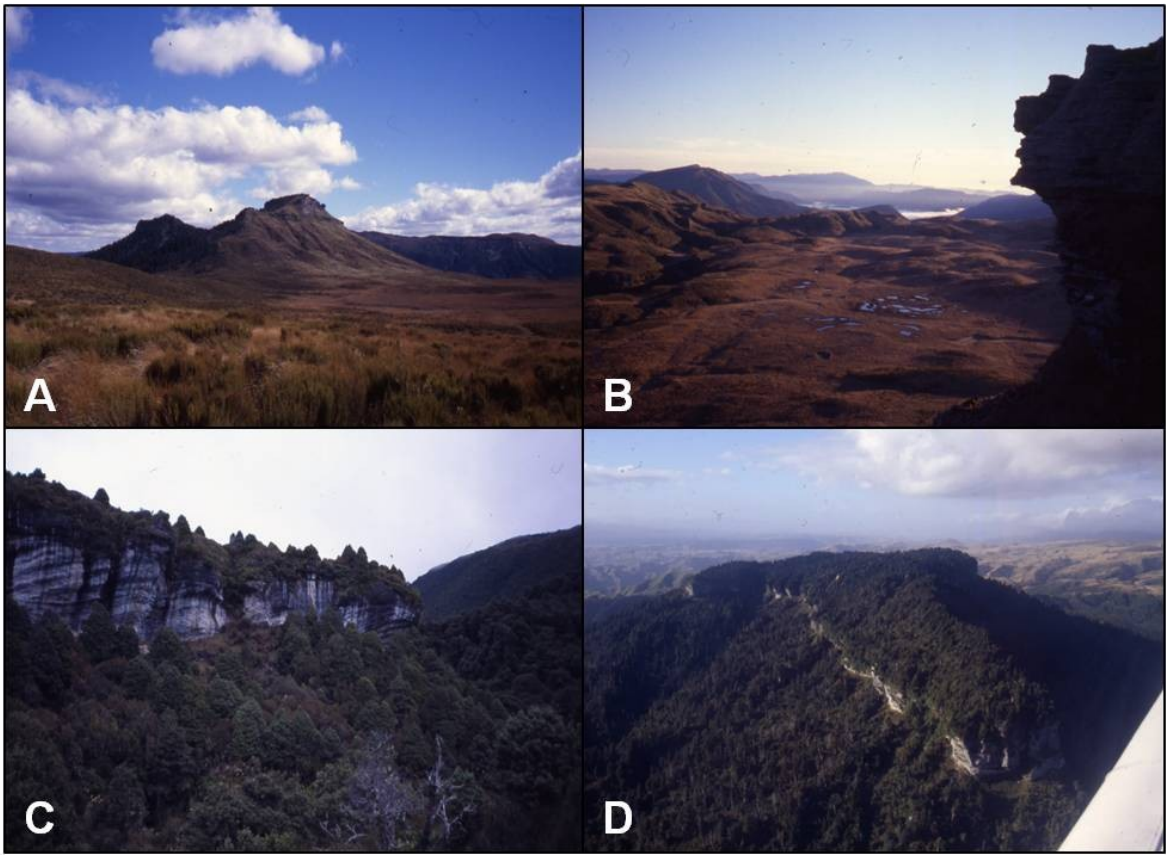

Figure 5.7. A. Te Rakaunuiakura from Makirikiri Tarns (Photo: Tony Gates). **B**. Makirikiri Tarns from Te Rakaunuiakura looking north-east (Photo: Tony Gates). **C**. Te Rakaunuiakura. **D**. Aorangi from an oblique aerial view (Photo: Tony Gates).

Faults

Ohutu and Potae faults (Fig. 5.8 and 5.9; informal names have been introduced to avoid ambiguity) were originally identified by Browne (1978) in the area of the Mangaohane Plateau; here they have been extended southwards (with the aid of photos and field mapping) to the area investigated in this study.

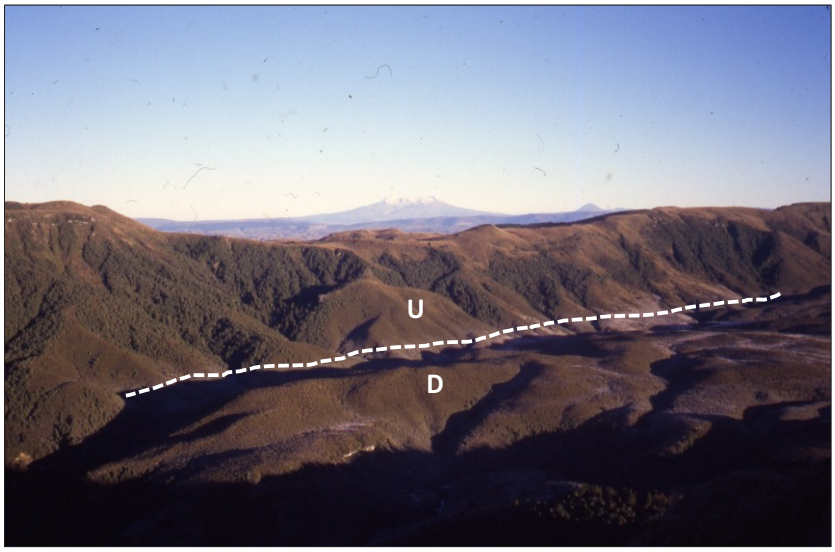

Figure 5.8. Oblique view of Ohutu fault showing vertical displacement, Mt Ruapehu is visible in the background. Taken from Te Rakaunuiakura looking towards Ohutu Ridge, note the relatively flat surface of the limestone on the downthrown side (Photo: Tony Gates).

Figure 5. 9. Oblique view of Potae fault showing vertical displacement. Taken from Potae looking north-east. Note the relatively flat surface of the limestone on the downthrown side that has since been tilted to form cuesta landforms along the fault (arrows).

5.1.3 Geological map

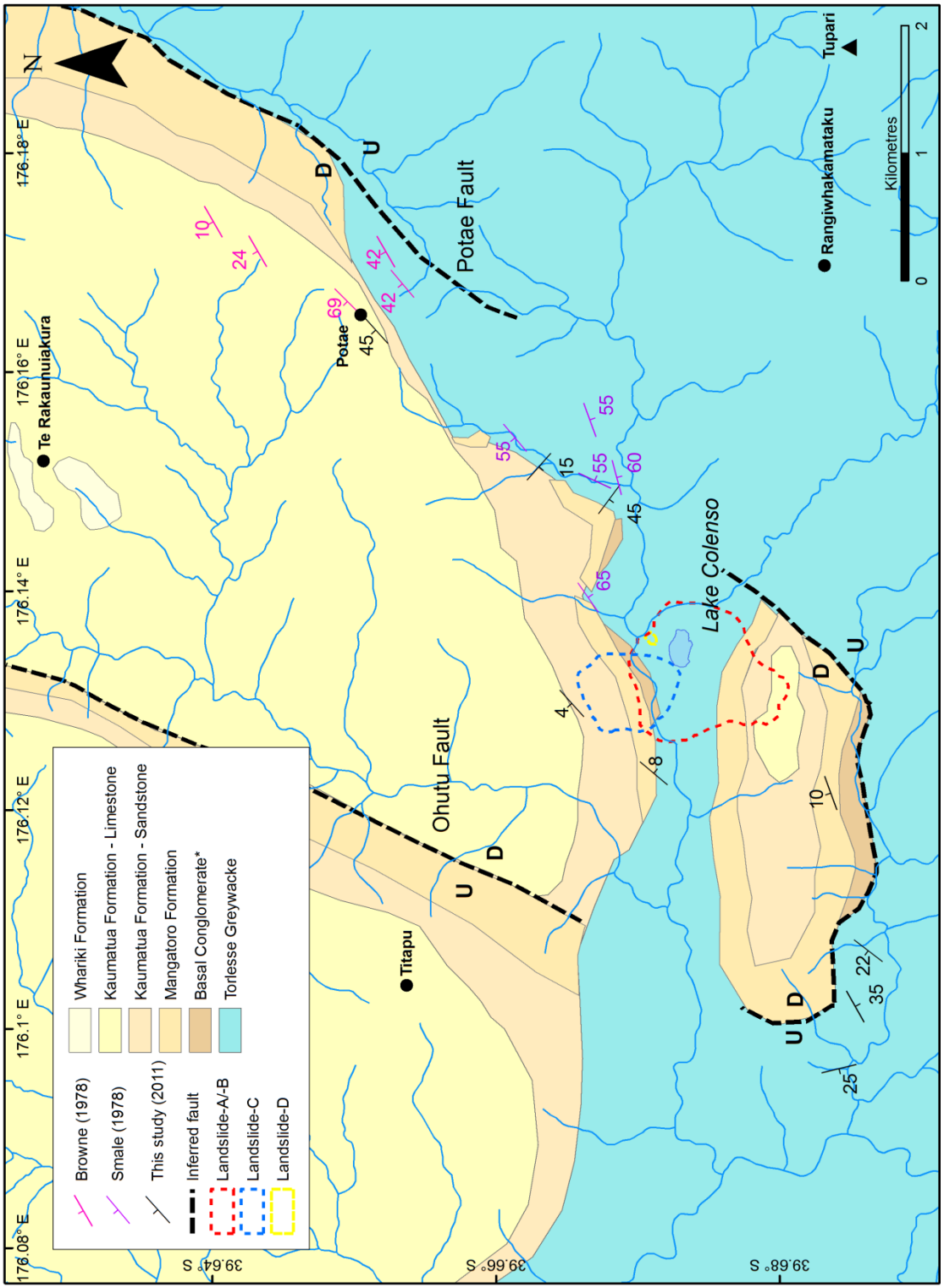

Figure 5.10. Geological map of the Lake Colenso region.

5.1.4 Stratigraphic column

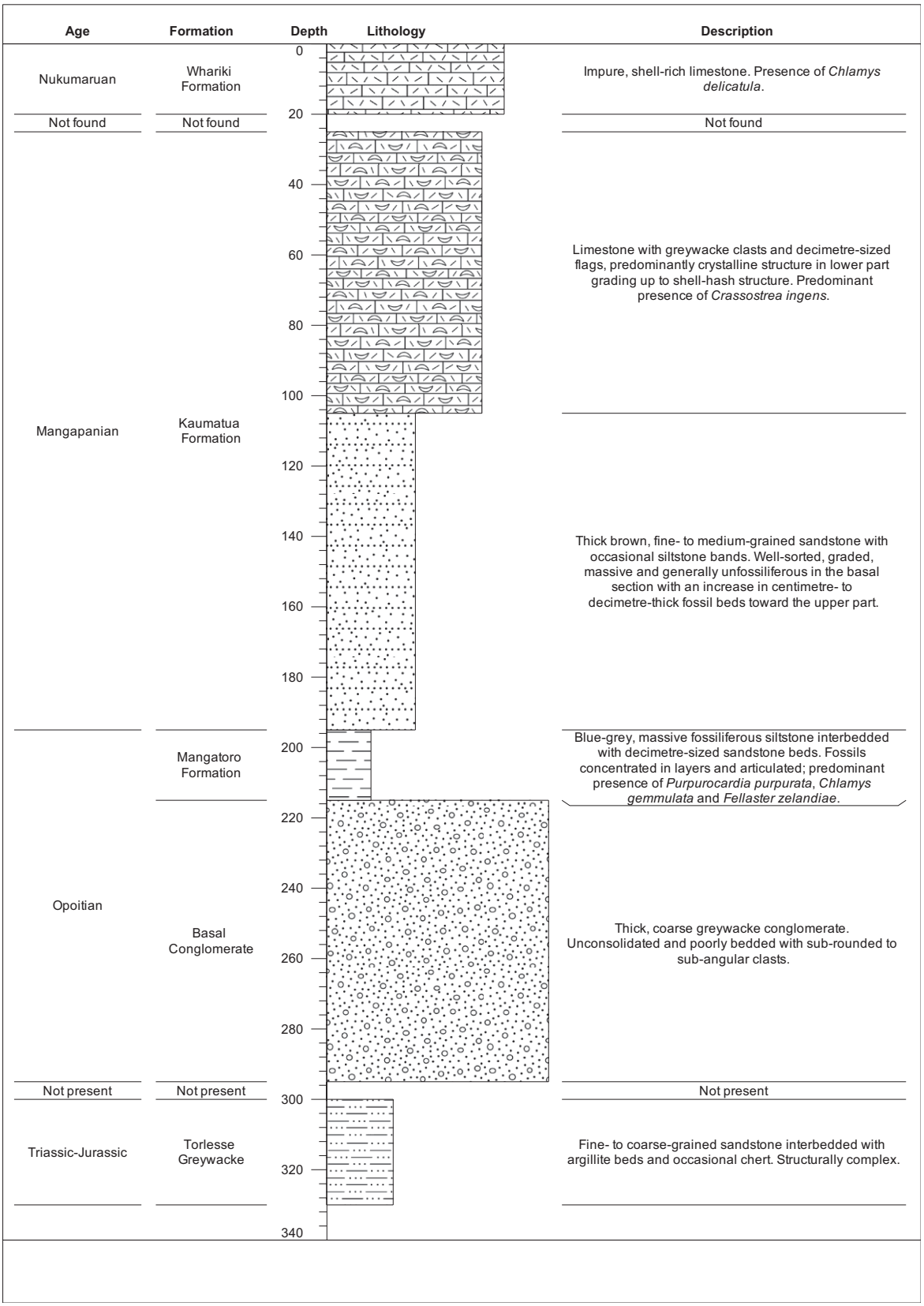

Figure 5.11. Stratigraphic column for Lake Colenso region.

5.2 Geomorphology

This section presents the reconstruction of the Lake Colenso basin.

Lake Colenso is one of the many landslide-dammed lakes in New Zealand (Adams, 1981; Lowe and Green, 1987; 1992; Korup, 2002), and this has been supported by examination of aerial photographs and field mapping. Landslide-dammed lakes commonly occur in groups (Korup, 2002), though it is apparent that Lake Colenso is isolated within the immediate region of the northern Ruahine Ranges and reasons for this remain unclear. The Lake Colenso landslide complex consists of three major landslide events (landslide-A, -B and –C) which have caused considerable geomorphic change, and also a minor event (landslide-D; Fig. 5.12). It is thought that at the time of the landslide-A and -B, that the flow of the Mangatera River would have been diverted. Evidence for the longevity of the present Mangatera River channel, is seen at the Mangatera River-Potae stream confluence where a greywacke spur (Fig. 5.12) has been incised by fluvial processes.

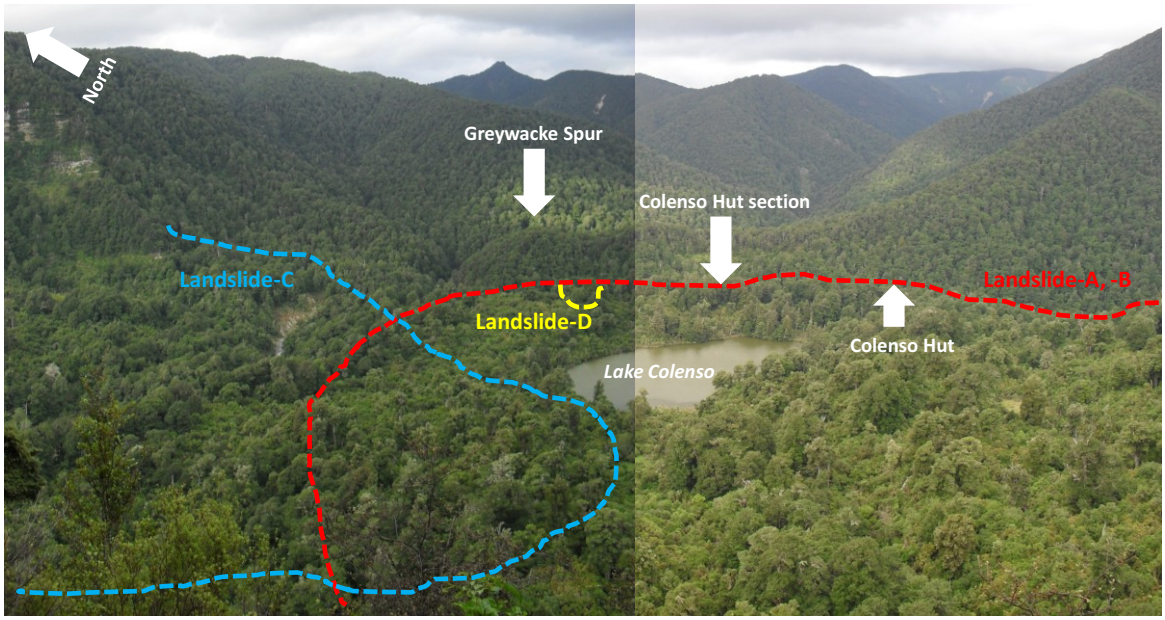

Figure 5.12. Oblique view of landslide and locations discussed in text

The base of landslide-A is apparent in Colenso Hut section (described earlier in section 4.2.1), where a silt deposit is truncated by unsorted, irregular material of landslide origin. A carbonized wood sample (Wk 29531) retrieved from this silt yields an age of 45172 ± 1261 yr BP (uncalibrated) providing a maximum age for landslide-A. The result here has

not been calibrated as it is at the upper limit of radiocarbon dating and calibration will likely result in an unreliable date (Alan Hogg, *pers. comm.*).

Table 5.1. Radiocarbon age data from geomorphological investigation, Lake Colenso.

Sample id	Lab code	$\delta^{13}C$ (‰)	^{14}C yr BP (1σ) [a]	Cal yr BP (mid-point 2σ)	Material dated
Colenso Hut section	Wk 29531	-27.6 ‰	45,172 ± 1261	NA [b]	Wood
Lake Colenso-280 cm	NZA 34331 [c]	-28.7 ‰	1923 ± 20	1799 ± 74 [d]	Leaves

[a] Based on the half-life of 5730 years (Stuiver and Polach, 1977)
[b] At the upper limit of radiocarbon dating, too inaccurate to calibrate
[c] From dates retrieved from Lake Colenso sediment cores (Table 5.5)
[d] AMS ^{14}C ages calibrated using OxCal 4.1 (Bronk Ramsey, 2001) and ShCal04 database (McCormac *et al*., 2004)

The age of landslide-B is based on the date (1799 ± 74 cal yr BP; Table 5.1) obtained from the base of the composite sediment core, interpreted as the start of peat accumulation on the landslide deposit, retrieved from Lake Colenso, i.e. 1799 ± 74 cal yr BP (NZA 34331) (table 5.1). It is thought that this landslide followed the same route as landslide-A, and a resulted in the hummocky topography seen today. It is hard to distinguish the deposits of this landslide from the deposits of landslide-A; indeed the occurrence of landslide-B can only be inferred from the ages available.

The accumulation of peat persisted for ~429 years (as inferred from the age model; Fig. 6.2) until landslide-C occurred which ultimately blocked the valley drainage and initiated the formation of the present Lake Colenso. It is apparent from field mapping the landslide debris remains unstable, Landslide-D was identified at the toe of landslide-A/-B as evidence. It is likely that this landslide occurred in recent times, due to the presence of early stage succession vegetation on the landform (Fig. 5.13).

Figure 5.13. Landslide-D extent (dashed line) with Mangatera River in the foreground (photo: Vince Neall).

Table 5.2. Summary of the characteristics of the landslides in Lake Colenso catchment shown in Fig. 5.14)

Landslide	Area[a]	Direction of flow[b]	yr BP (1σ)
A*	0.93 km^2	NNE	< 45,172 ± 1261
B*	0.93 km^2	NNE	>1799 ± 13 [c]
C	0.26 km^2	SSE	~1370 [c, d]
D	0.01 km^2	NNE	Unknown

[a] Estimated from mapped aerial extent of landslide deposits (Fig. 5.14)
[b] Direction at which the landslide travelled
[c] AMS ^{14}C ages calibrated using OxCal 4.1 (Bronk Ramsey, 2001) and ShCal04 database (McCormac *et al*., 2004)
[d] From age model (discussed in section 5.3.1)
* Difficult to differentiate deposits

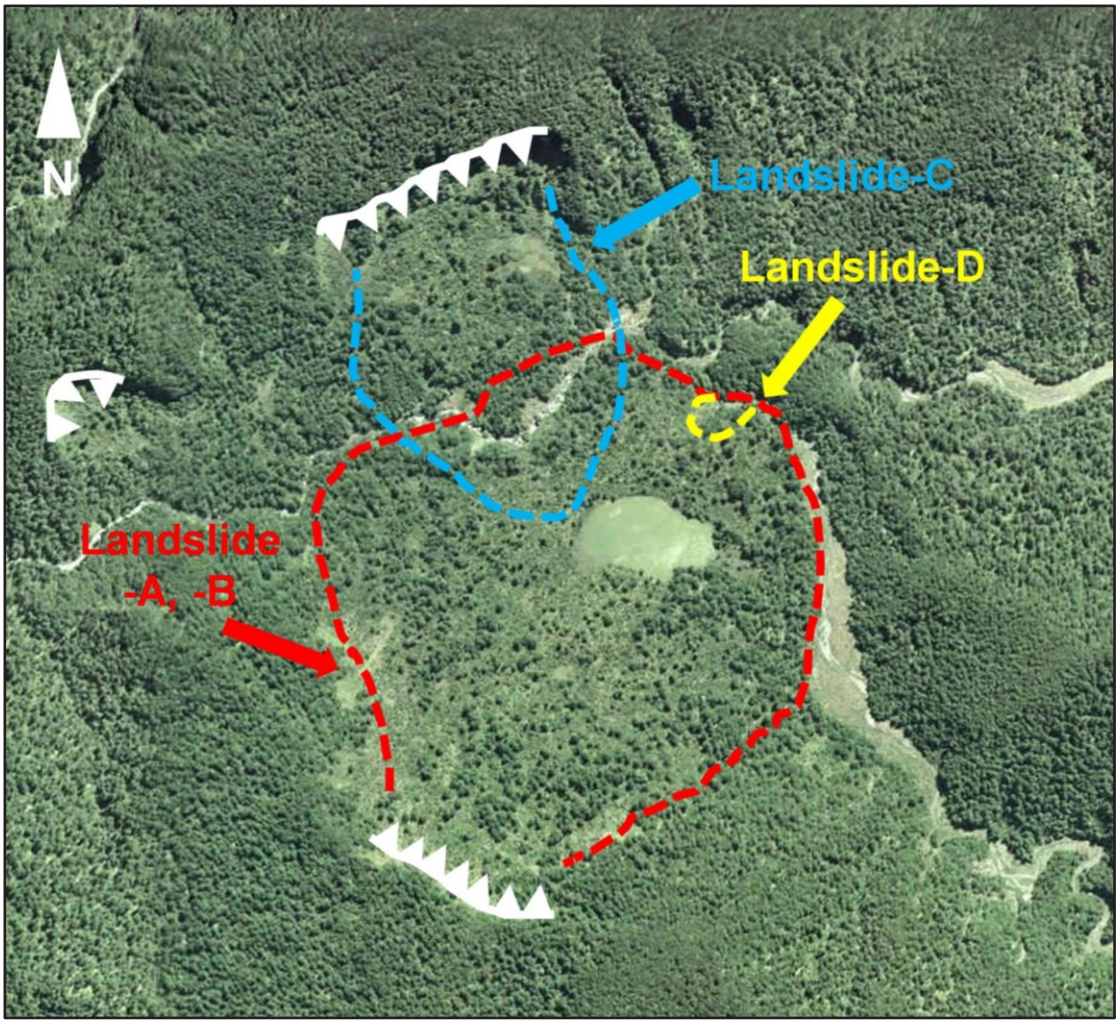

Figure 5.14. Aerial photograph of landslides in the Lake Colenso basin.

5.3 Lake Colenso

This section presents results from the different proxies used in the paleoenvironmental reconstruction of Lake Colenso.

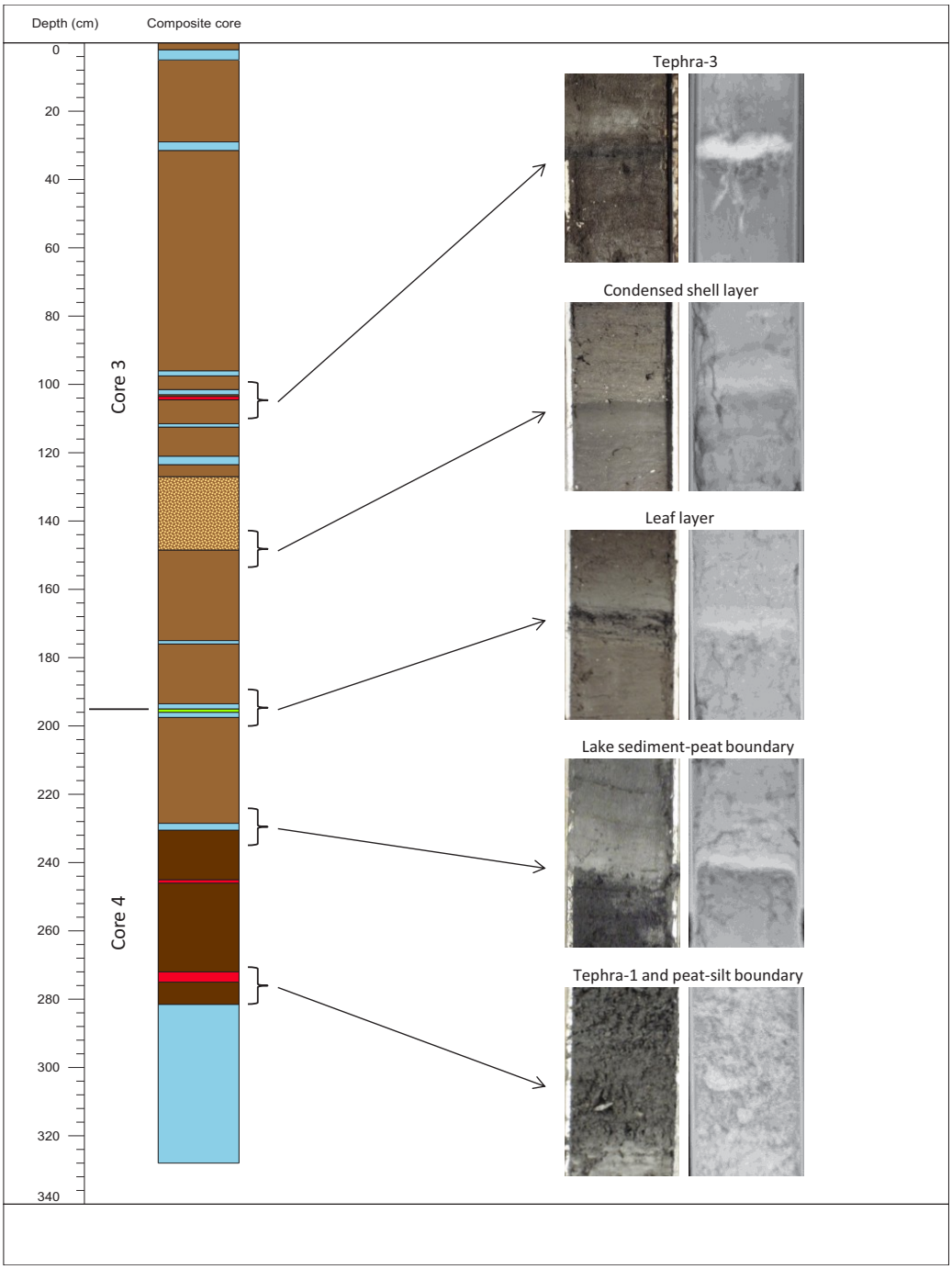

Figure 5.15. Composite core constructed from cores 3 and 4, as well as photos and x-ray images from the main stratigraphic boundaries and layers of interest (n.b. Tephra-2 is not shown here as it is difficult to identify in photos and x-ray images). Key same as in Fig. 4.5.

The base of the core until 280 cm (Fig. 5.15) consists of hard semi-consolidated silt, interpreted as part of the landslide debris, most likely reworked Tertiary sediment. This sediment is overlain by organic-rich peat with abundant plant material until 230 cm, where fine-grained organic lake sediment, also known as gyttja, then dominates the uppermost part of the core. Occurring at irregular intervals within the gyttja are silt layers which have sharp basal contacts and gradational upper contacts, and tephra layers are also interspersed throughout the sediment core.

5.3.1 Chronology

The results from tephrochronology and radiocarbon analyses are presented separately to avoid confusion.

Tephrochronology

Physical characteristics

Grain-size analysis was conducted on the individual tephras (Fig. 5.16) to help understand provenance. The bimodal distribution is likely representative of the mixed sediment source (McLaren, 1981). In this case the peak dominant at 10 µm is likely representative of the lake sediment in the sample, while the remainder is dominated by the volcanic glass size fraction (63 - 125 µm).

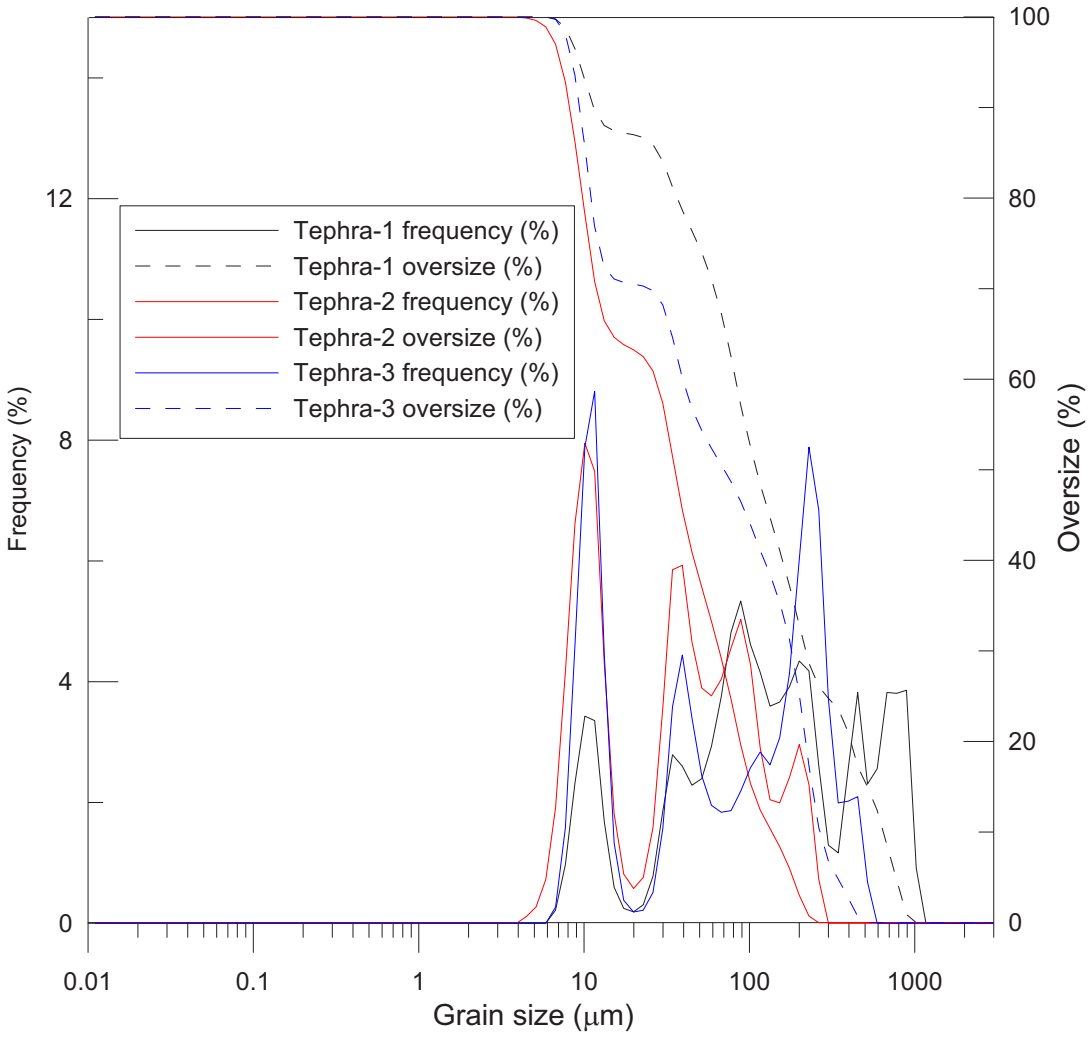

Figure 5.16. Grain size distribution for tephra-1, -2 and -3.

Glass chemistry

Glass fingerprinting in conjunction with stratigraphy and chronology is essential in developing an age model in which tephras are used. The technique, first developed in New Zealand by Froggatt (1983), has been widely used to characterise tephra beds in a range of environments (Lowe *et al*., 2008). Tephras of different composition are distinguishable following the compositional scheme of Le Maitre (1984) in a bi-plot of SiO_2 and $Na_2O + K_2O$ (Fig. 5.17).

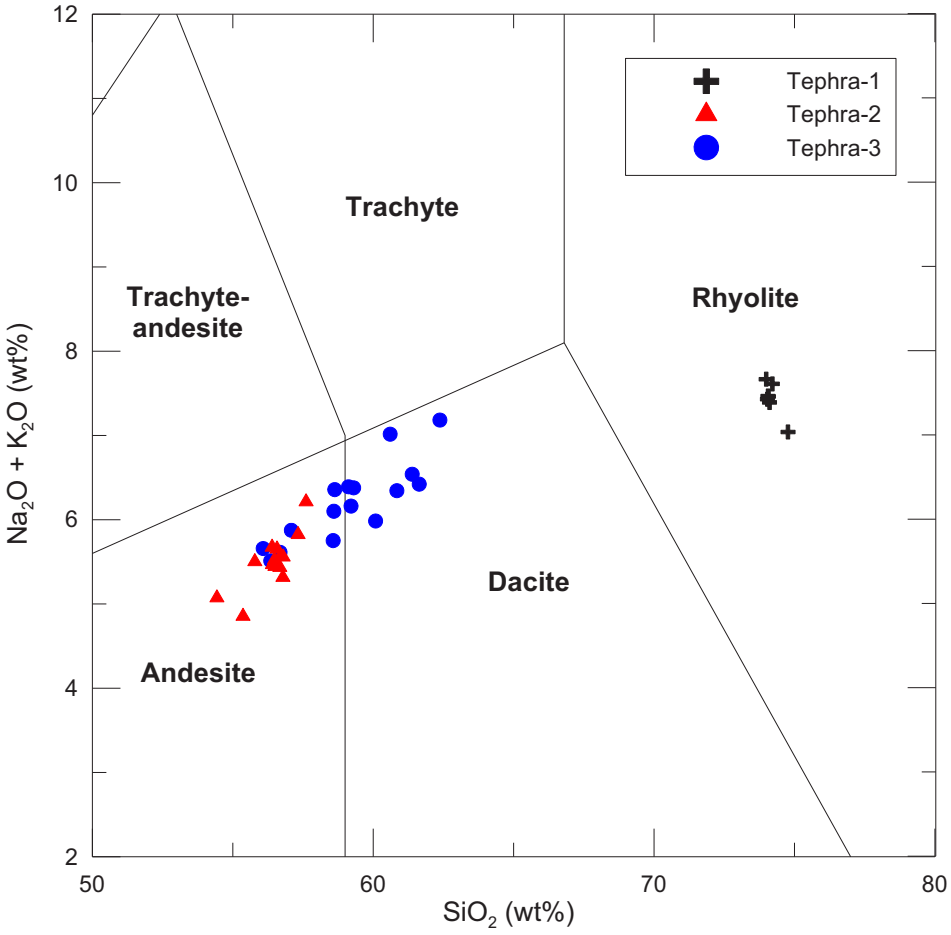

Figure 5.17. Compositional scheme adapted from Le Maitre (1984) showing composition of tephras from Lake Colenso. It should be noted that some values were excluded in this diagram; because they are thought to represent feldspar (andesine) based on the high aluminium, sodium and calcium values. Andesine is a common feldspar in rhyolitic tephras, and is commonly present as microlite inclusions in andesitic glass. Data recalculated to 100% on a volatile-free basis.

Tephra-1 falls into the rhyolitic composition zone of Le Maitre (1984) and it is possible to differentiate tephras of the same composition (e.g., Taupo and Okataina). Taupo-derived deposits are distinguished by their relatively lower SiO_2 (75 - 76 wt %) and higher FeO (1.7 - 2.0 wt %) content (Table 5.3) (Shane, 2000).

Tephra-2 and tephra-3 fall into the zone of dacitic-andesitic composition of Le Maitre (1984) suggesting a Tongariro or Taranaki provenance. These can be distinguished using a bi-plot of K_2O and SiO_2 (Shane, 2005); Taranaki-derived deposits generally have a high K_2O (>4 wt %) content (Fig. 5.18).

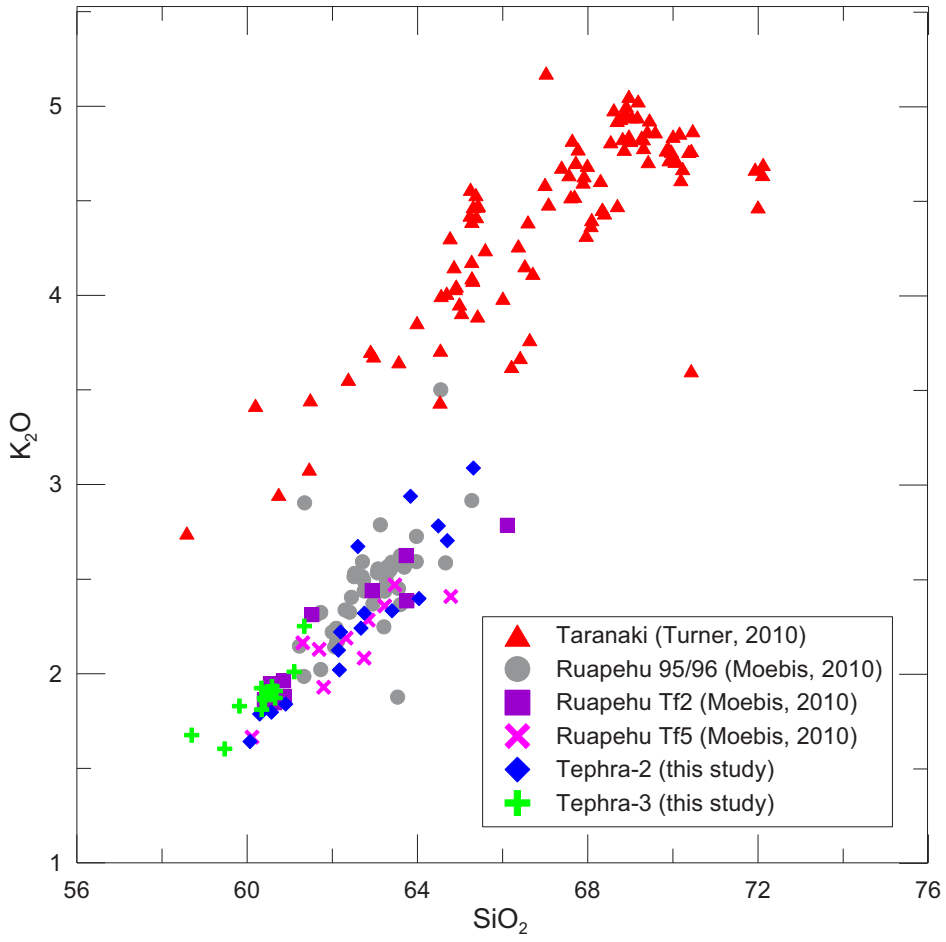

Figure 5.18. Bi-plot of K_2O and SiO_2 following the andesitic compositional scheme of Shane (2005). Data recalculated to 100% on a volatile-free basis. Tf refers to the Tufa Trig Formation (Donoghue *et al*., 1995).

However, tephras erupted from the same source volcano over short time periods (<20,000 years) are difficult to identify solely based on major glass chemistry (Lowe *et al*., 2008). The correlation of andesitic tephras is complicated due to the large range of andesitic units (Platz *et al*., 2007), the small amount of appropriate glass for probing (i.e. glass without microlite inclusions) and the high compositional variation of glass within individual tephras (Donoghue and Neall, 1996). However in some instances, tephras can be correlated to the composition of units in close proximity (Shane, 2000).

Summary

Tephras were identified based on a combination of physical characteristics, elemental composition, glass chemistry (Table 5.3), and radiocarbon dates. It is thought that tephra-1 is correlative to Taupo Pumice, tephra-2 is correlative to Tufa Trig Formation member 1 (Tf1), and tephra-3 is correlative to Tufa Trig Formation member 5 (Tf5) (Table 5.4)

The Tufa Trig Formation (Tf), outlined by Donoghue *et al*. (1995), comprises 19 members (Donoghue *et al*., 1997), deposited between 1717 cal yr BP (Lowe *et al*., 2008) and the present day. Tufa Trig Formation members are typically black to dark grey, ranging from coarse ash to lapilli grade tephras, and predominantly have dacitic glass chemistries (Donoghue *et al*., 1995). Tf5 is the most widespread member of the Tufa Trig Formation, occurring up to 130 km from source e.g., in Lakes Tutira and Rotonuiaha (Page and Trustrum, 1997; Wilmshurst, 1997). Member Tf5 is readily distinguished by its coarser grain size, greater thickness, and is typically comprised of black, olive and dark brown coarse ash and fine lithic lapilli, with small amounts of dark greyish brown fine pumice lapilli (Donoghue *et al*., 1995).

Tf5 was first identified by Donoghue *et al*. (1996) and has a minimum age of 611 ± 65 cal yr BP and a maximum age of 790 ± 119 cal yr BP. Page *et al*. (2010) used an estimated age of 650 ± 96 cal. yrs. B.P., Wilmshurst *et al*. (1997) used an age of 666 cal yr BP, while Moebis (2010) used the maximum age of 790 ± 119 cal yr BP. For a more reliable estimate it was decided to assume a constant sedimentation rate, deduced from the sedimentation rate (0.194 mm/yr) between the top of the core and radiocarbon date (NZA 35692). This gave the tephra an approximate age of 650 cal yr BP, correlative to what was used by Page *et al*. (2010).

There are two members (Tf1 and Tf2) within the Tufa Trig Formation which consist predominantly of scoriaceous lapilli, but are generally difficult to distinguish from one another based on physical characteristics (Donoghue *et al*., 1997) or glass chemistry (Moebis, 2010). Moebis (2010) obtained dates for the Tf1 and Tf2, 1555 ± 45 cal yr BP and 1338 ± 135 cal yr BP, respectively, and based on the stratigraphic position of tephra-2 in the Lake Colenso core it is likely that it is Tf1.

Table 5.3. Major glass elemental composition of tephras from Lake Colenso core (bold) and other studies.

		SiO_2	Al_2O_3	TiO_2	FeO	MnO	MgO	CaO	Na_2O	K_2O	Cl	H_2O	*n*
Tf1	**Mean**	**62.63**	**16.29**	**0.95**	**5.70**	**0.10**	**2.20**	**5.80**	**3.90**	**2.31**	**0.12**	**1.63**	**16**
	SD	***1.61***	***1.59***	***0.18***	***0.56***	***0.06***	***0.71***	***1.05***	***0.18***	***0.44***	***0.03***	***0.51***	
Tf5	**Mean**	**60.35**	**15.64**	**0.98**	**6.50**	**0.11**	**3.65**	**7.08**	**3.65**	**1.89**	**0.15**	**1.49**	**14**
	SD	***0.66***	***0.45***	***0.06***	***0.24***	***0.07***	***0.95***	***0.36***	***0.18***	***0.15***	***0.03***	***0.43***	
Tf5[b]	Mean	62.43	15.45	0.91	6.28	0.14	3.22	5.45	3.82	2.17	0.12	1.16	10
	SD	*1.30*	*0.18*	*1.92*	*1.37*	*0.06*	*2.24*	*0.82*	*0.37*	*0.24*	*0.05*	*1.07*	
Taupo	**Mean**	**75.15**	**12.90**	**0.33**	**1.94**	**0.07**	**0.25**	**1.52**	**4.55**	**2.89**	**0.26**	**2.54**	**7**
	SD	***0.22***	***0.13***	***0.06***	***0.12***	***0.60***	***0.57***	***0.29***	***0.18***	***0.06***	***0.03***	***0.78***	
Taupo[c]	Mean	75.04	13.45	0.30	1.99	0.07	0.22	1.47	4.49	2.85	0.19	4.63	19
	SD	*0.19*	*0.12*	*0.04*	*0.08*	*0.03*	*0.10*	*0.05*	*0.12*	*0.07*	*0.01*	*1.85*	

[a] Data recalculated to 100% on a volatile-free basis and shown as mean and standard deviation in wt%. Total iron expressed as FeO, water by difference from original analytical total

[b] Data from Moebis (2010)

[c] Data from Lowe *et al*. (2010)

n.b. all glass data is presented in Appendix 3

Table 5.4. Summary table showing distinguishable characteristics of tephras in the Lake Colenso core.

Defining characteristics	**Tephra-1**	**Tephra-2**	**Tephra-3**
Physical characteristics	Elongate vesicles, white-yellow pumice lapilli[a]	Scoriaceous pumice lapilli[b]	Distinctive black glass[b]
Elemental composition[c]	Rhyolite	Andesite	Dacite-andesite[d]
Glass chemistry	SiO_2 = 75.04[e] FeO = 1.99[e]	K_2O = 1.89[f]	K_2O = 2.31[f]
Radiocarbon bracketing ages[g]	<1799	1376-1799	>601
Conclusion	Taupo Pumice	Tufa Trig Formation member 1 [b]	Tufa Trig Formation member 5 [b]
Abbreviation used in text	-	Tf1	Tf5
Cal yr BP (mid-point 2σ)	1717 ± 13[h]	1555 ± 45[i]	650 ± 96[b]
Sample depth (cm)[k]	275	245	103

[a] Shane (2000
[b] Donoghue *et al*. (1997)
[c] Using the compositional scheme of Le Maitre (1984)
[d] Tufa Trig Formation members predominantly have dacitic glass chemistries (Donoghue *et al*., 1997)
[e] Taupo-derived deposits typically have lower SiO_2 (75-76 wt %) and higher FeO (1.7-2.0 wt %) content (Shane, 2000)
[f] Tongariro deposits generally have low K_2O (<4 wt %) content (Shane, 2005)
[g] From radiocarbon dates (Table 5.5)
[h] Lowe *et al*. (2008)
[i] Moebis (2010)
[k] Depth from composite core

Radiocarbon results

The surrounding lithology of the lake is thought to be responsible for difficulties in obtaining radiocarbon dates from the sediment cores. The majority of the dates align well stratigraphically (Table 5.5) and fit with ages derived from tephra layers. However, some samples (NZA 35748, NZA 35749 and NZA 34645) are consistently older than those from bracketing depth ranges and the identified tephra stratigraphy.

Table 5.5. Radiocarbon age data from composite core, Lake Colenso

Sample depth (cm) [a]	Lab code	$\delta^{13}C$ (‰)	^{14}C yr BP (1σ) [c]	Cal yr BP (mid-point 2 σ) [d]	Material dated
16A [b]	NZA 35748	-28.3 ‰	1159 ± 35	1007 ± 76	Pollen concentrate
16B [b]	NZA 35749	-28.4 ‰	2489 ± 60	2530 ± 181	Pollen concentrate
91	NZA 35692	-27.8 ‰	662 ± 15	601 ± 46	Pollen concentrate
104	NZA 34645	-30.9 ‰	2156 ± 20	2069 ± 72	Bulk sediment
196	NZA 35497	-28.6 ‰	1308 ± 15	1183 ± 89	Leaves
280	NZA 34331	-28.7 ‰	1923 ± 20	1799 ± 74	Leaves

[a] Corrected depth from composite core

[b] Two sub-samples were dated for this pollen concentrate sample because of the small measure of pollen in the sample

[c] Based on the half-life of 5730 years (Stuiver and Polach, 1977)

[d] AMS ^{14}C ages calibrated using OxCal 4.1 (Bronk Ramsey., 2001) and ShCal04 database (McCormac *et al*., 2004)

5.3.2 Sedimentology and dry bulk density

This section presents results from grain-size analyses of clastic sediments, where a selected part of the core was analysed. Also presented are the dry bulk density values as a measure of compaction in the sediment cores from Lake Colenso.

The percentage of clastic sediment and dry bulk density (Fig. 5.19) reflects the broad variation of lithological composition in the core, where clastic sediment percentage and dry bulk density increase at the silt and tephra layers in the core. The averages of the total percent of clastic sediment and dry bulk density between the base of the core at 328 cm and the lower peat boundary at 280 cm are ~75% and ~0.8 g/cm^3, respectively.

The peat is characterised by ~50% clastic sediment and ~0.6 g/cm^3 dry bulk density, also grain size is dominantly coarse (~30% silt, 70% sand). At the peat/lake sediment boundary (230 cm), the percentage of clastic sediment decreases to ~15%, and dry bulk density averages 0.3 g/cm^3. This continues toward the top of the core, with sudden increases at the silt layers where the percentage of clastic sediment rises to 30 - 50%. The silt layers (Fig. 5.15) contain >80% silt, while the tephra layers at 275, 245, and 103 cm depth are dominantly composed of the volcanic glass size fraction (63 – 125 μm), and <50% silt.

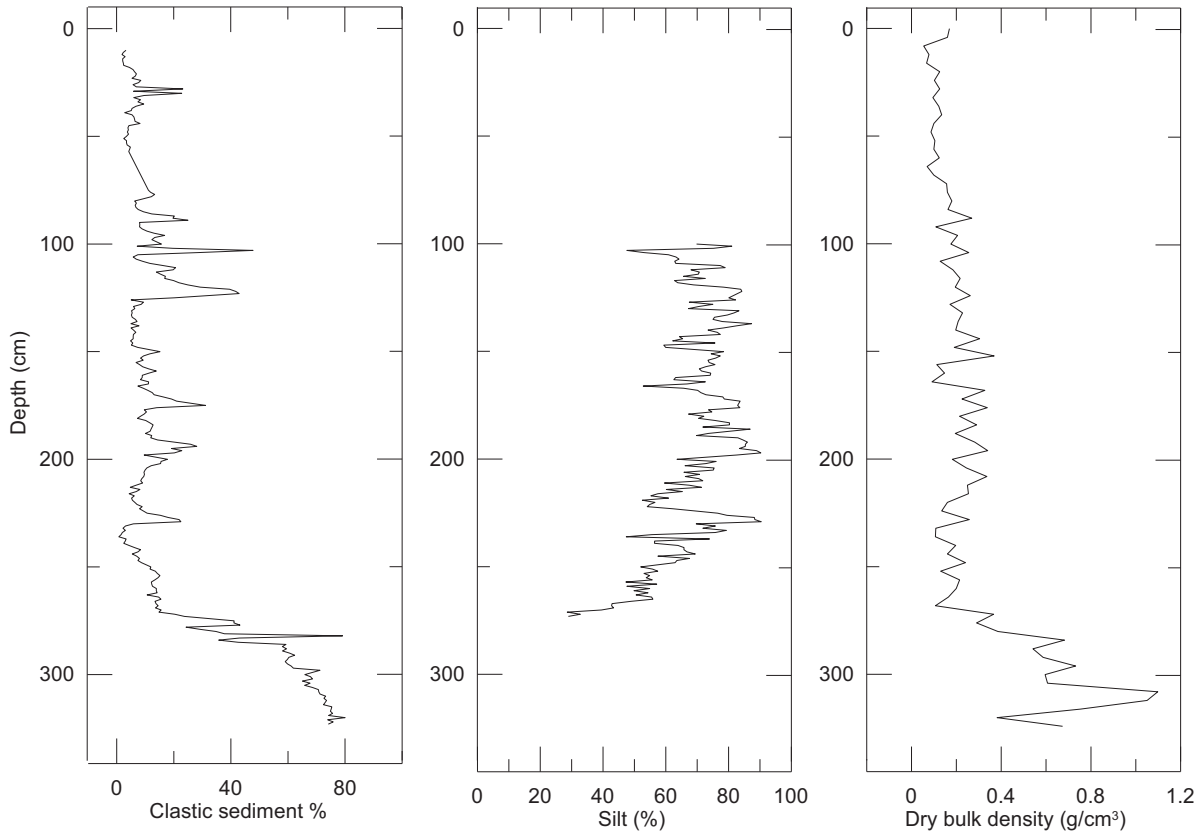

Figure 5.19. Total clastic percentage, total percentage silt and dry bulk density of the composite core, Lake Colenso.

5.3.3 Biogeochemistry

This section presents results from bulk geochemistry from the organic sediment and also stable isotope ($\delta^{18}O$ and $\delta^{13}C$) values from ostracods.

Bulk organic geochemistry

At 324 cm depth, organic matter content and the carbon:nitrogen (C:N) ratio is at a minimum (Fig. 5.20), representative of the mineral-rich reworked Tertiary material present in this part of the stratigraphy. There is a sustained rise in organic matter and in the C:N ratio after 281 cm, where the lithology changes to organic-rich peat material. The C:N ratio and organic matter content in the upper 230 cm is broadly synchronous with changes in lithology, where an increased ratio and organic matter content corresponds to silt and tephra layers. Overall, there is a decreasing trend in the C:N ratio.

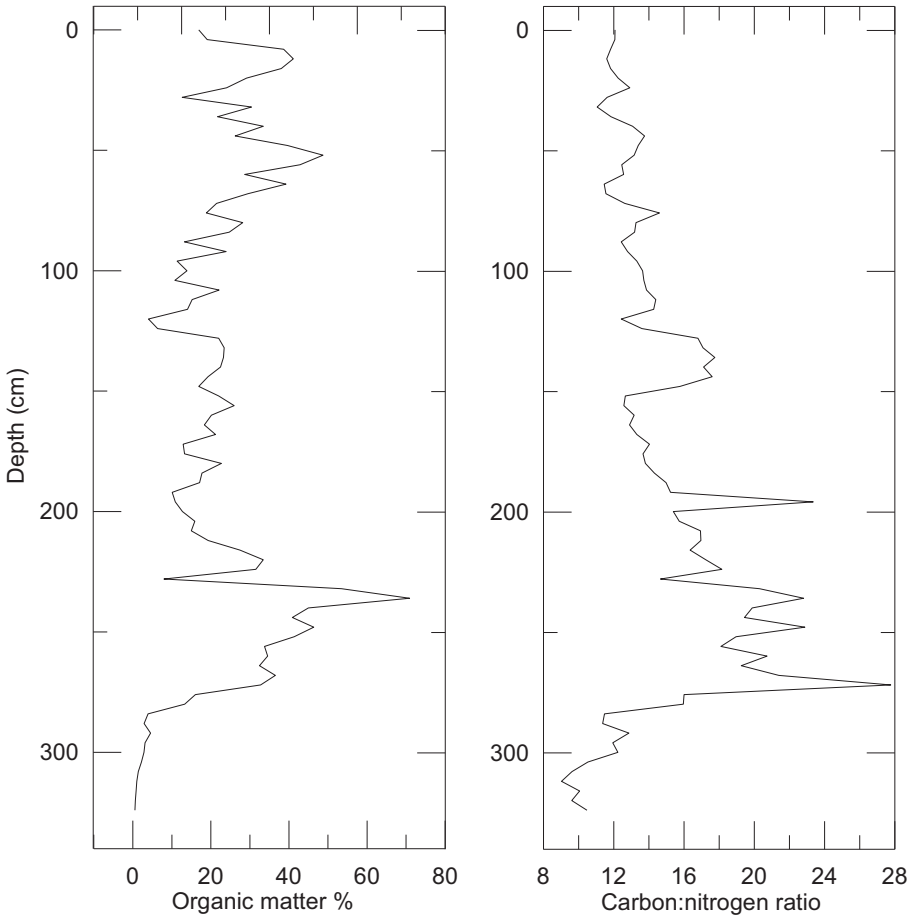

Figure 5.20. Bulk organic geochemistry measurements from the composite core showing the organic matter content and C:N ratio.

Stable isotope analysis

There was a notable absence of $CaCO_3$ from 70 to 20 cm, so no stable isotope values for ostracods were able to be obtained from this zone (Fig. 5.21). Values for $\delta^{18}O$ are variable throughout the record with values ranging from -5.91 to -2.64‰. There is a sudden increase at 186 cm depth, and also to a lesser extent at 142 and 16 cm. Values for $\delta^{13}C$ range from -10.48 to -4.84 ‰, generally decreasing towards the top of the core, and from 156 to 93 cm, there is variability but overall there is a decreasing trend. Additionally, there appears to be some covariance between $\delta^{18}O$ and $\delta^{13}C$ values.

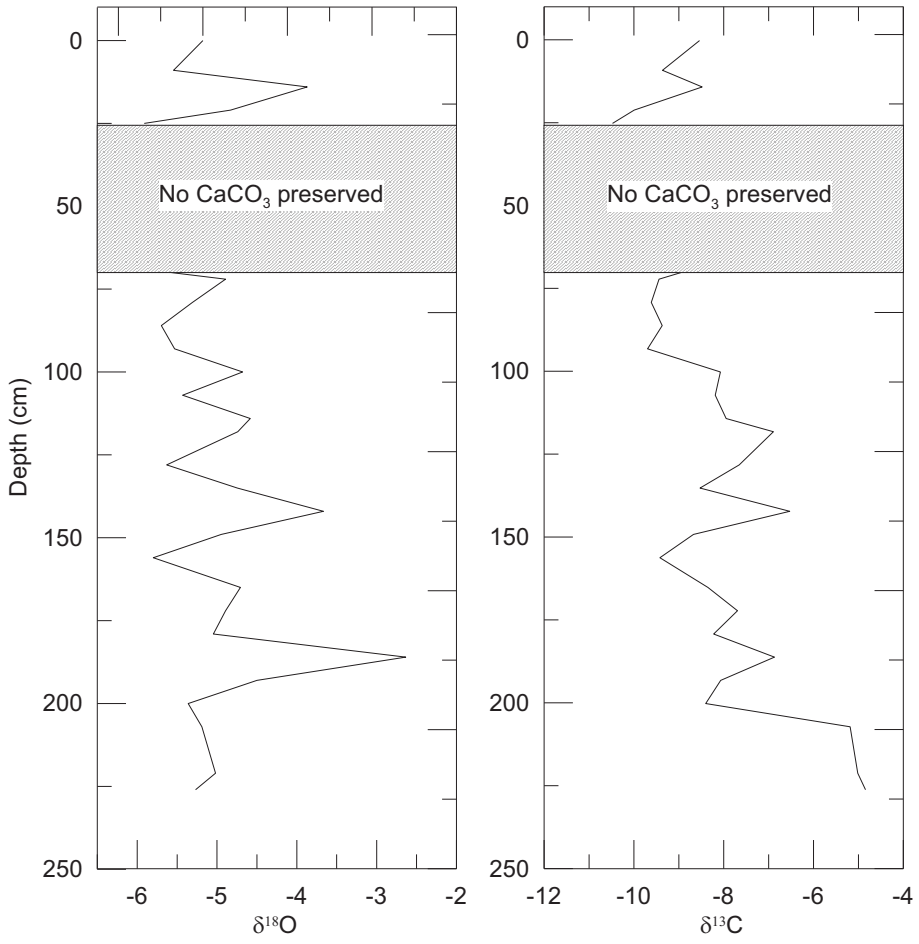

Figure 5.21. Stable isotope values of $\delta^{18}O$ and $\delta^{13}C$ extracted from ostracods (*Gomphocythere duffi*) from Lake Colenso. Raw stable isotope values are presented in Appendix 4.

5.3.4 Palynology, ostracods and molluscs

This section includes results from pollen, ostracod and mollusc analyses.

Palynology

A total of 66 pollen samples were analysed from the 280 cm profile. Broad changes in pollen composition are coincident with broad variation of lithological composition in the core (Fig. 5.22A).

Zone Pa 281 - 230 cm

The base of this zone is dominated by fern (*Isoetes,* Monolete fern spores*, Phymatosorus* and Cyathea) and wetland taxa (Cyperaceae and *Callitriche*). These fern and wetland taxa decrease collectively from ~50% to 20% over this zone (Fig. 5.22B). Podocarpaceae tend to be the dominant tree species in this zone, and the total percentage of tall trees range from 40% to 85%.

Zone Pb 230 - 70 cm

This zone is characterised by a significant increase up to ~90% in all tree taxa (Fig. 5.22C). Podocarpaceae appears to dominate the tall tree taxa (see Fuscaspora ratio in Fig. 6.3), and *Dacrydium cupressinum* and *Prumnopitys taxifolia* also increase slightly. Fern and wetland species are at a minimum (<15%) from this zone upwards, also noticeably *Haloragis* and *Isoetes* disappear. Additionally, *Libocedrus* disappears at 190 cm.

Zone Pc 70 - 0 cm

An increase of Fuscaspora is the main feature in this zone, as Podocarpaceae species tend to decrease in conjunction with *D. cupressinum* and *P. taxifolia*. *Weinmannia* appears at the start of this zone and remains steady until present day, also *Coprosma* and *Phymatosorus* increase in this zone. Fern taxa slightly increase from ~5% to ~10% in this zone (Fig. 5.22C).

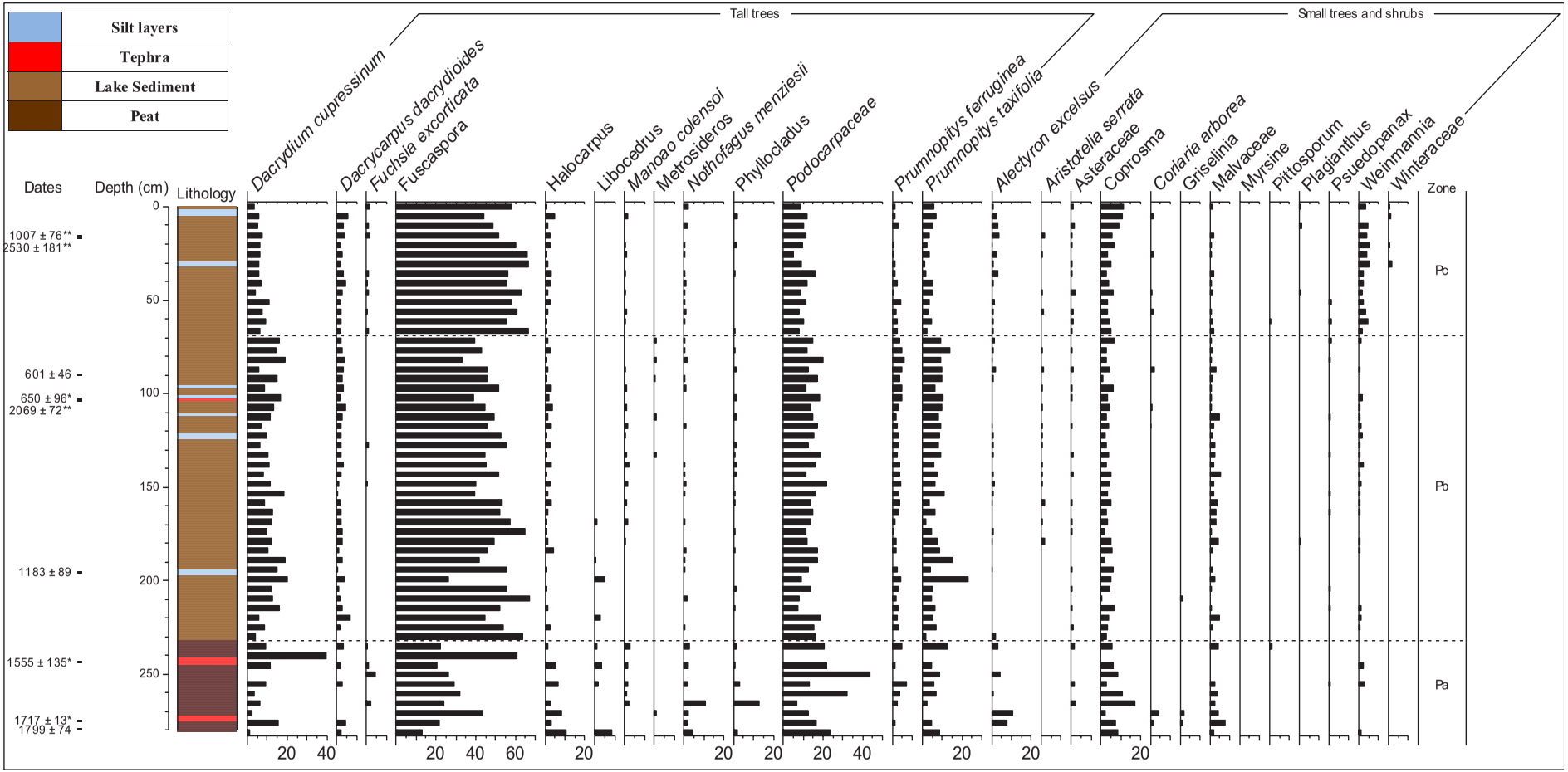

Figure 5.22. A. Relative pollen diagram from core 2 showing tall trees and small trees and shrubs. Dates are from radiocarbon and tephra samples and are presented in cal yr BP; * indicates it is a tephra-derived date and, ** indicate a radiocarbon date that has been affected by the hard-water effect, discussed in section 6.2.1.

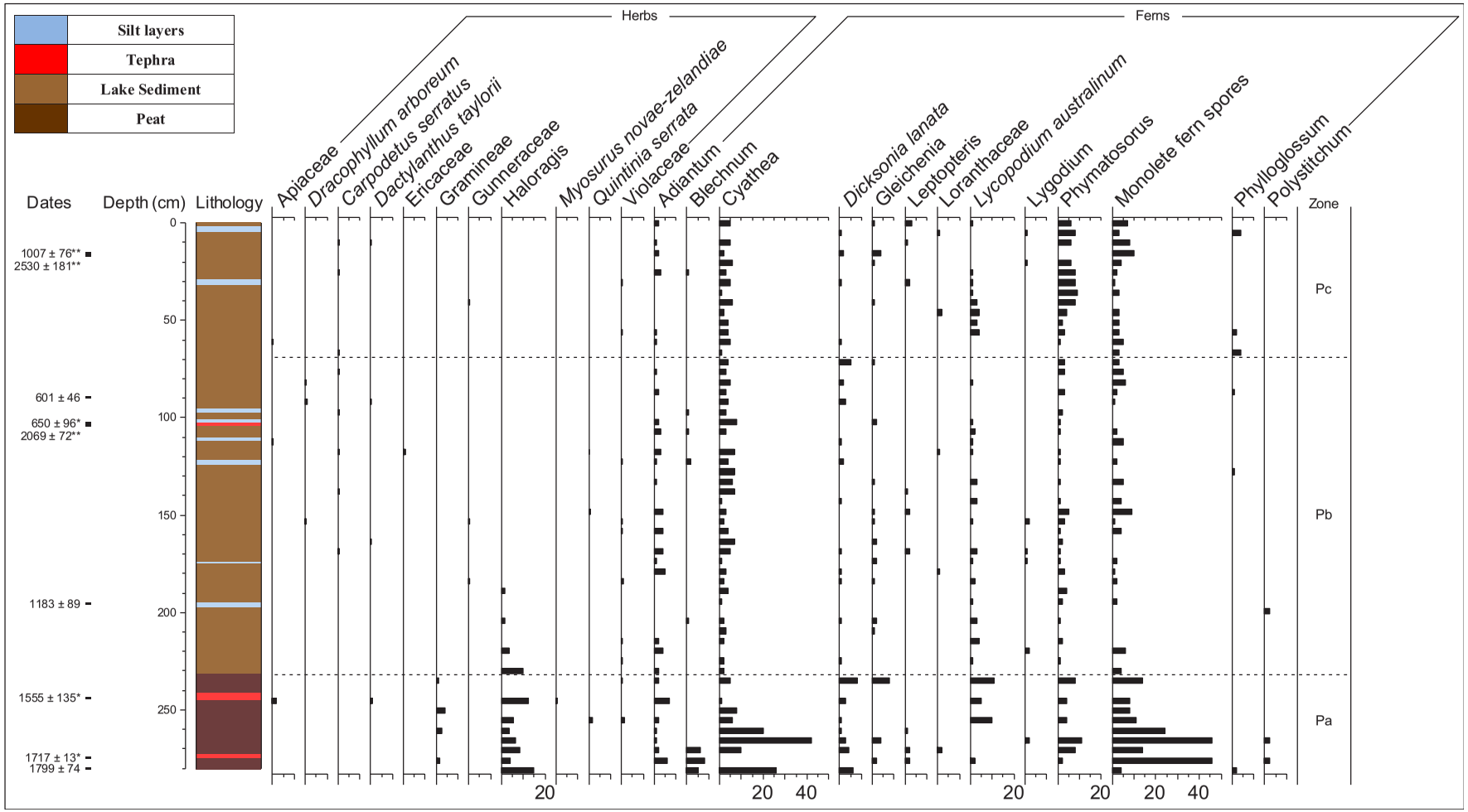

Figure 5.22. B. Relative pollen diagram from core 2 showing herbs and ferns. Dates are from radiocarbon and tephra samples and are presented in cal yr BP; * indicates it is a tephra-derived date and, ** indicate a radiocarbon date that has been affected by the hard-water effect, discussed in section 6.2.1.

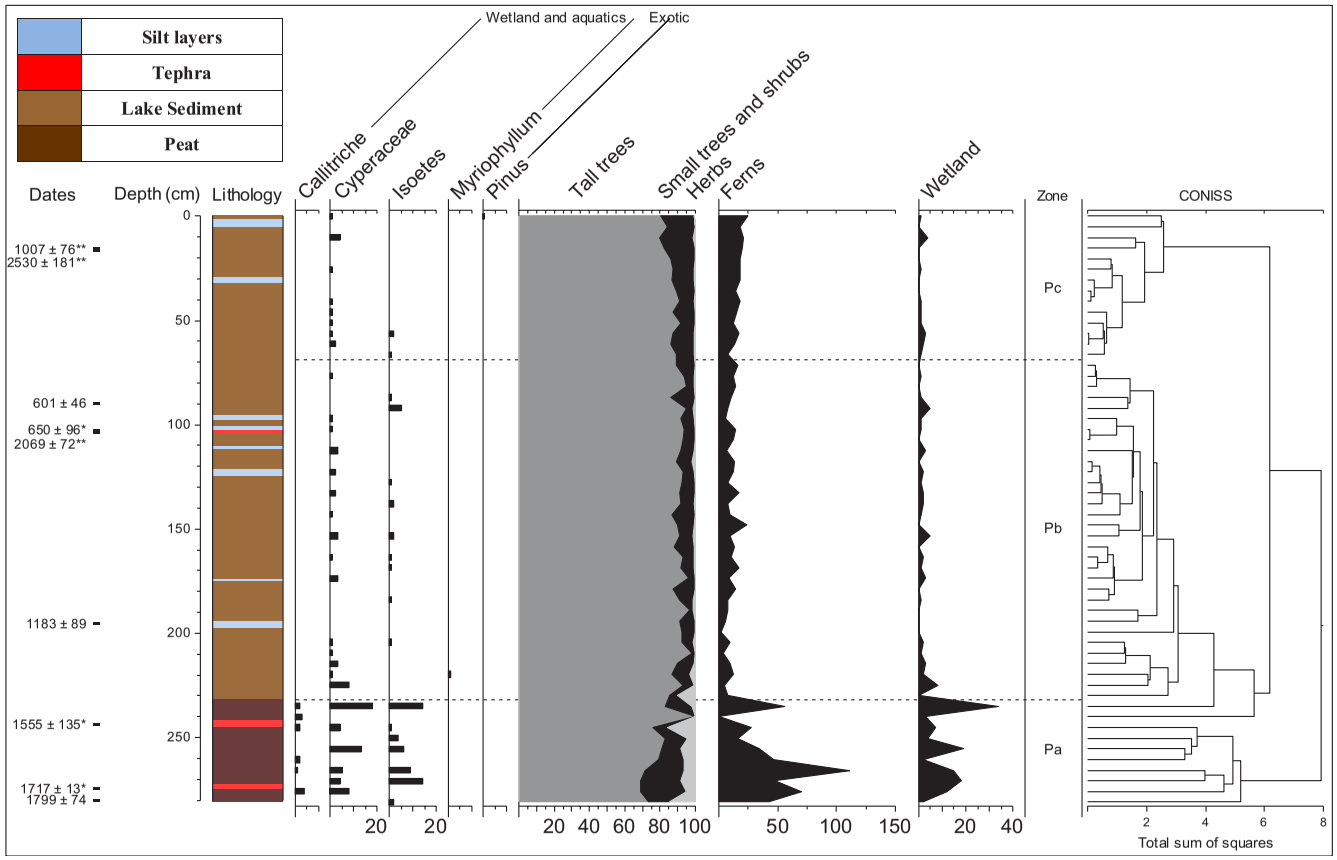

Figure 5.22. C. Relative pollen diagram from core 2 showing wetland and aquatic and exotic. Also, a summary vegetation diagram, total ferns and total wetland species excluded from the pollen sum. Dates are from radiocarbon and tephra samples and are presented in cal yr BP; * indicates it is a tephra-derived date and, ** indicate a radiocarbon date that has been affected by the hard-water effect, discussed in section 6.2.1.

Ostracods

Ostracods occur in the lake sediment (230 cm upwards) with only 2 taxa identified, *Gomphocythere duffi* (Barclay, 1968) and *Penthesilenula kohanga* (Eager, 1971). *G. duffi* is identifiable down to gender level and is displayed in addition to the species assemblage (Fig. 5.23). A total of 28 samples were analysed from the 230 cm profile.

Zone Oa 228 - 160 cm

This zone has a relatively low number of both species. *P. kohanga* suddenly increases at 214 cm to 114 valves/gm, although overall decreases throughout the zone with an average ~25 valves/gm. *G. duffi* shows no real trend and appears to have no significant change in this zone, with an average ~800 valves/gm. *G. duffi* males are dominant in this zone, averaging 1200 valves/gm. There is a notable absence of females between 166 and 181 cm, otherwise numbers are consistent averaging ~50 valves/gm.

Zone Ob 160 - 110 cm

G. duffi decreases toward the top of the zone while *P. kohanga* shows an overall increase, averaging ~200 valves/gm. *G. duffi* males increase to 1850 valves/gm and females increase to 130 valves/gm in this zone, although there is an overall decreasing number in both male and female. Female numbers disappear towards the top, and there is a marked rise at the top of the zone in males.

Zone Oc 110 - 70 cm

There is a significant increase in this zone of both species at 107 cm (*G. duffi* increases to 9250 valves/gm and *P. kohanga* increases to 450 valves/gm), though at 106 cm numbers taper off again in both species. The number of ostracods in this zone is still relatively high compared to other zones. *G. duffi* males increase to 8750 valves/gm and females increase to 500 valves/gm.

Zone Od 70 - 23 cm

There are no ostracods present in this zone.

Zone Oe 23 - 0 cm

There are low levels of ostracod numbers, *G. duffi* (<750 valves/gm) and *P. kohanga* (<50 valves/gm), in this zone, with an overall decreasing trend. *G. duffi* males are noticeable low (<600 valves/cm).

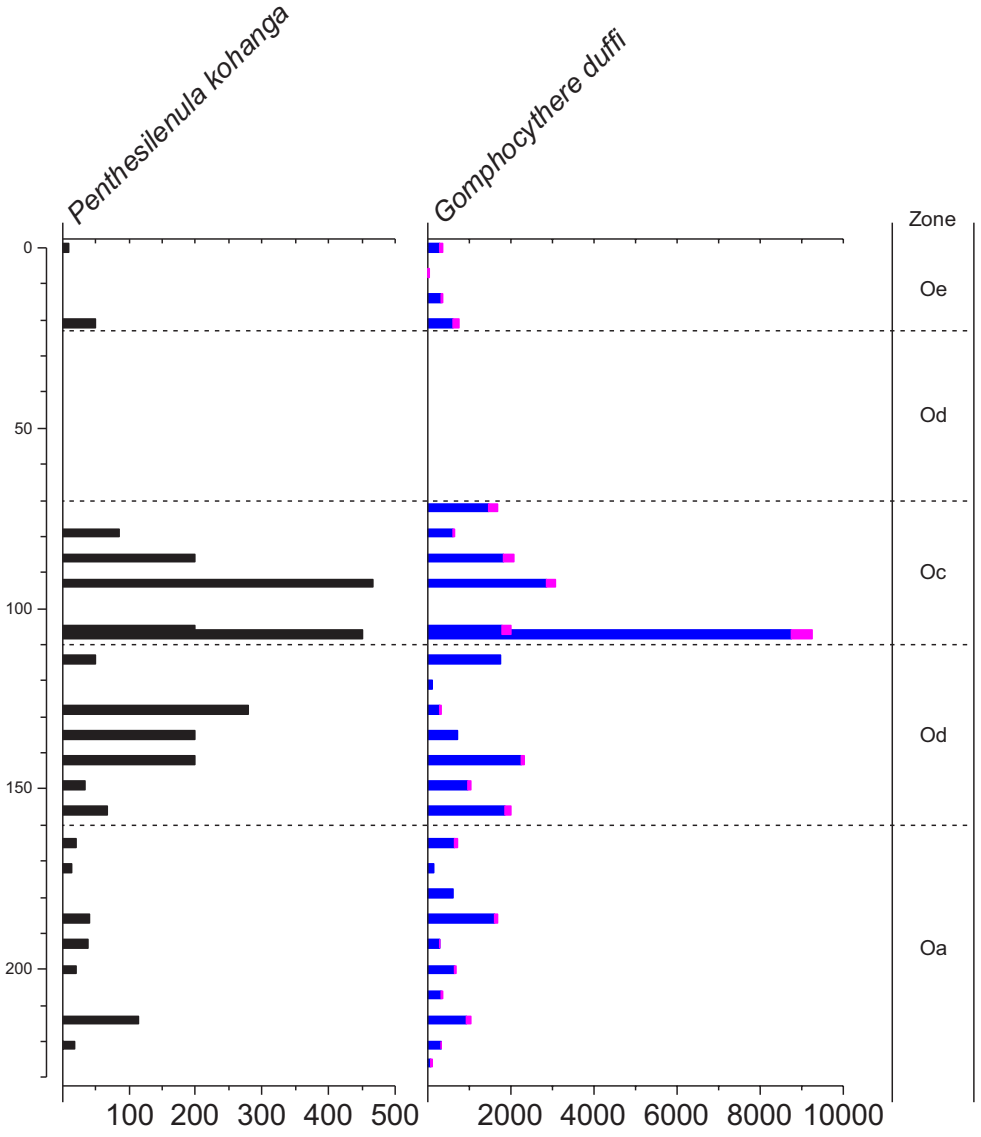

Figure 5.23. Ostracod species abundance represented as valves per gram of sediment. Variation in *G. duffi* gender also shown (male represented with blue, and female represented wih pink).

Molluscs

Similarly to the ostracods, molluscs occur in the lake sediment (230 cm upwards; Fig. 5.24), where only 2 taxa were identified, *Potamopyrgus antipodarum* (Gray, 1943) and *Pisidium novaezelandiae* (Prime, 1862). It is notable that adult specimens were relatively rare so the counts are predominantly of juvenile specimens.

Zone Ma 230 - 160 cm

This zone has a relatively low number of both species. *P. antipodarum* averages 110 valves/cm, while *P. novaezelandiae* averages 15 valves/gm.

Zone Mb 160 - 140 cm

This zone has a distinctly higher number of both species. *P. antipodarum* increases to 500 valves/gm and *P. novaezelandiae* increases to an average of 25 valves/gm and numbers remain steady throughout the zone.

Zone Mc 140 - 110 cm

In this zone, overall abundance of both species declines considerably with respect to the previous zone. *P. novaezelandiae* is mostly absent except for the top of the zone.

Zone Md 110 - 70 cm

P. antipodarum increases (1375 valves/gm) suddenly at 107 cm, but then decreases toward the top of the zone; *P. novaezelandiae* also has a peak (130 valves/gm) at 93 cm and decreases toward the top of the zone.

Zone Me 70 - 23 cm

There is a notable absence of any $CaCO_3$ in this zone.

Zone Mf 23 - 0 cm

Moderate numbers of *P. antipodarum* were counted in this zone, averaging 250 valves/gm, and *P. novaezelandiae* appears to have relatively high numbers in this zone averaging 55 valves/gm.

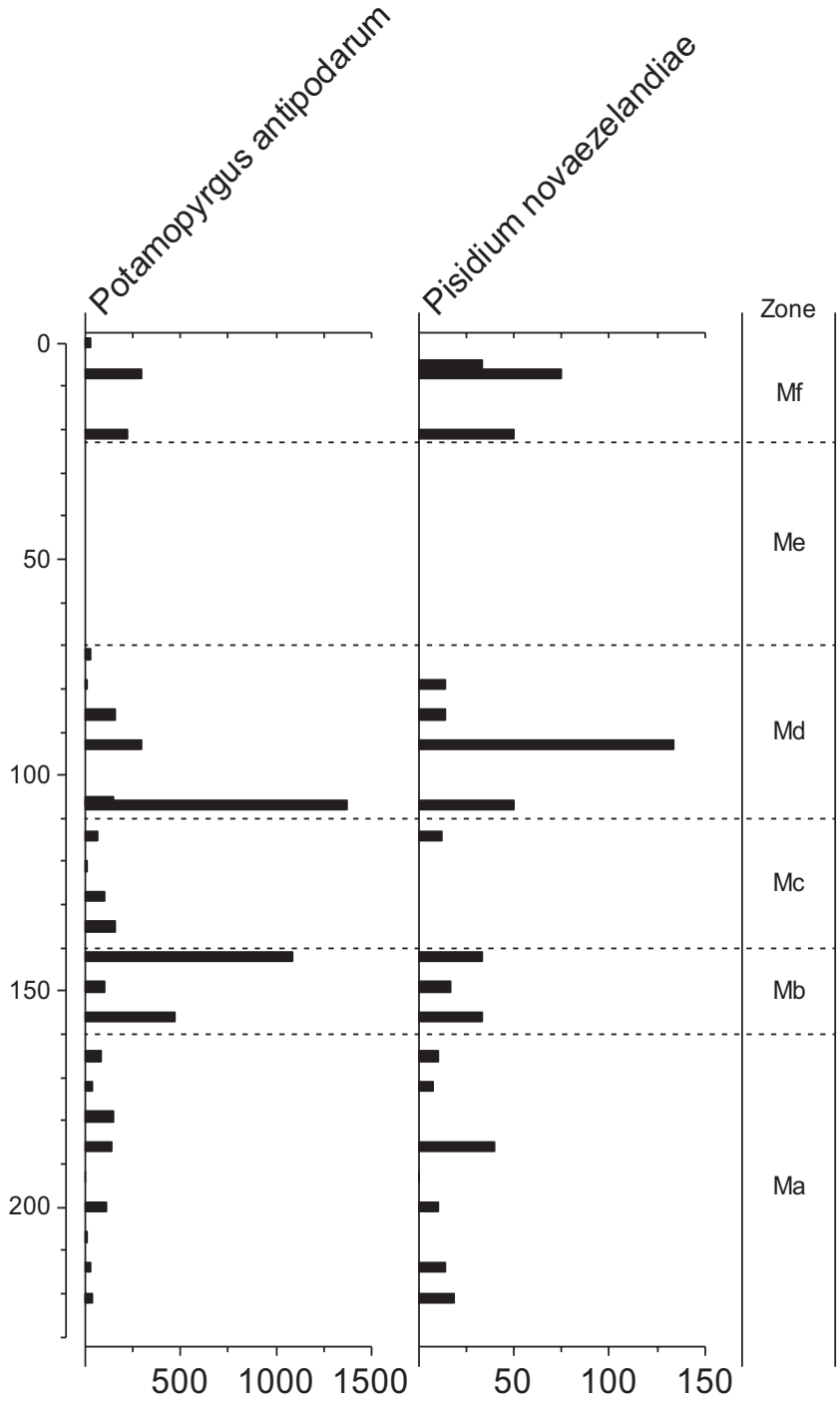

Figure 5.24. Mollusc abundance, represented as valves per gram of sediment.

5.3.5 Summary

Each lithotype (tephra, silt, organic layers, lake sediment, and peat) in the sediment cores can be distinguished by a range of properties (summarised in Table 5.6).

In review, the sedimentological, geochemical, pollen, ostrocod and mollusc results from Lake Colenso present a variable record of change, which allow an environmental record to be established. This variable record is discussed and put into context in the following chapter.

Table 5.6. Each lithotype can be distinguished by its separate properties and is summarised the accompanying table.

Lithotype	Texture	Thickness (cm)	Grain size (µm)	Dry bulk density	%C	%N	C/N ratio	Pollen conc.	Ostracod conc.	Mollusc conc.
Tufa Trig 5	Coarse ash	1	6-520	NA	NA	NA	NA	NA	NA	NA
Tufa Trig 1	Lapilli	1	6-1200	0.3	25%	1.3%	23	NA	NA	NA
Taupo Pumice	Lapilli	2	6-6000	0.7	20%	1.1%	28	NA	NA	NA
Leaf layer	Leaf material	1	6-230	0.35	6%	0.69	23	NA	NA	NA
Silt layers	Coarse silt	1.5–2	0-350	~0.3	5-10%	1-2%	11-13	NA	Medium	Medium
Organic lake mud (gyttja)	Silt-sand	2-65	0-350	0.1-0.2	15-25%	~1%	13-16	Medium	High	High
Mottled gyttja	Silt-sand	21.5	0–350	0.1-0.2	14%	0.6%	17	Medium	High	High
Peat	Organic material, including leaves and branches	49	0-350	0.2-0.5	10-35%	1-1.5%	16-20	High	NA	NA
Basal silt	Coarse silt	>47	NA	0.8	<1%	<0.2%	7-13	None	NA	NA

Chapter 6: Discussion

Due to the different approaches in this study, this chapter has been split into two sections: (1) addressing the evolution of the landscape with respect to the geology, geomorphology and formation of the lake; and, (2) an interpretation of the environmental history of the lake and the surrounding area since lake formation. Lastly, a synthesis of the paleoenvironmental record is presented summarizing results from this study.

6.1 Landscape evolution

This section aims to identify geological and geomorphological characteristics of the Lake Colenso area, and put them into a local and regional perspective. First, the geological history is discussed with a focus on the Plio-Pleistocene stratigraphy. Secondly, the tectonic history of the nearby faults and local significance to the development of the landscape is discussed.

6.1.1 Geological history

The Cenozoic stratigraphic record in the North Island is principally controlled by tectonism (Beanland *et al.*, 1998) and eustatic sea level fluctuations (Abbott and Carter, 1994). In the lower North Island, the Wanganui Basin comprises Plio-Pleistocene marine sediments (Fleming, 1953) that represent cyclothem deposits (Abbott and Carter, 1994).

Cenozoic sediments of the Mangaohane Plateau have an approximate age of 4 Ma (Browne, 1978), while the sediments of the Ngamatea Plateau to the north have an age of 6 Ma (Beu *et al*., 1981). It is suggested by Rogers (1987) that this coincides with a regressing shoreline and parallels the direction of retreat of the sea from the Wanganui Basin in a southwest direction. This explains the shallow and deep water stratigraphic relationships of the strata, such as the unconformities and erosional surfaces associated with transgression and regression.

The earliest Cenozoic deposit is the Basal conglomerate unit, thought to be early Opoitian in age, which rests unconformably on the Torlesse greywacke (Browne, 1978). The Basal conglomerate unit indicates a period of uplift where debris flows shed coarse-grained sediments from the adjacent fault-bounded Torlesse greywacke blocks (Browne, 2004b). This Pliocene uplift was a widespread event, with correlative units on the Mangaohane Plateau (Browne, 1978), Kuripapango region (Browne, 2004a) and southern Hawkes Bay (Lillie, 1953).

The overlying Mangatoro Formation (Lillie, 1953) is thought to be Opoitian in age, based on the foraminifera assemblage (Browne, 2004a). The occurrence of *Purpurocardia purpurata* (Deshayes, 1854), *Chlamys gemmulata* (Reeve, 1853) and *Fellaster zelandiae* (Gray, 1855) provide support for a littoral near-shore depositional environment (Beu and Maxwell, 1990). This formation is correlated with units elsewhere in the southern North Island (Beanland *et al*., 1991), and marks a period of subsidence recording the peak of transgressing sea levels where the Wanganui Basin is thought to have extended as far north as Waiouru (Beu *et al*., 1981).

The regressive phase is represented by the carbonate facies of the Kaumatua Formation (Erdman and Kelsey, 1992), known to be Mangapanian in age (Browne, 2004a). The sandstone lithofacies are interpreted to have been deposited in a high-energy shelf environment while the inter-bedded siltstones indicate periods of quiescence and low sediment supply (Browne, 2004a). The overlying clastic limestone units are thought to have been deposited within a high energy near-shore environment, while the siliciclastic sediments within the formation derived from the Torlesse greywacke suggest a local provenance (Browne, 2004a).

The Mangapanian-early Nukumaruan period is characterised as a regressive phase with regional uplift resulting in the absence of Waipipian sediments (Browne, 2004a), particularly in the northern Ruahine Range (Beu *et al*., 1981) and Kuripapango area (Browne, 2004b). This has formed an unconformity in the Lake

Colenso region, where Opoitian-Mangapanian deposits are tilted toward the north-west (Fig. 5.1) and the overlying deposits are relatively flat-lying (Fig. 5.7).

Chlamys delicatula (Hutton, 1873) found by Beu *et al*. (1981) indicates that the high peaks of the Ruahine Range (e.g., Te Rakaunuiakura and Aorangi) are capped by a thin outlier of Nukumaruan limestone (Beu *et al*., 1981). *C. delicutula* is an indicator species for the outer-shelf environment. This species requires cool water and starvation of terrigenous sediment, such as at the transition between highstand systems tracts and transgressive or lowstand system tracts (Orpin *et al*., 1998). The remnants of Nukumaruan rocks in the northern Ruahine Range suggest another period of uplift after this time, likely in Castlecliffian time (Beu *et al*., 1981). It has been suggested that an uplift rate of 1.7 mm/yr is applicable to the northern Ruahine Range as suggested by the highest peaks of marine sedimentary rock (Beu *et al*., 1981).

The Potae and Ohutu faults that bound the Mangaohane Plateau were initiated at separate times. It is possible that the Potae fault has been active since before the Pleistocene, as uplift provided a sediment source for deposition during and after this time (i.e. Basal conglomerate). The Ohutu fault is thought to have developed during the last period of uplift (Castlecliffian) as it offsets sediments deposited during the Pleistocene. A smaller en-echelon fault terminates the fault block at the Unknown Stream in the south, which has formed a half graben structure, termed here as the Colenso graben. The north-west trending uplifted fault block that makes up the Mangaohane Plateau is a dominant feature of the region (Browne, 1978), resulting in cuesta landforms (i.e. Potae) from the erosion-resistant limestone.

The apparent fit into the accepted model of the timing and development of the local and New Zealand landscape (Table 6.1) provides some confidence in the correlation of observed strata to other known units.

Table 6.1. Summary of main events as interpreted from the units found in the Lake Colenso study area (*discussed in the following sections).

Era	Epoch		Series	Stage	Geological phase	Deposits
Cenozoic	Holocene	Quaternary	Wanganui	Haweran	Uplift	Lake Colenso sediment*
						Landslide sediment*
	Pleistocene			Castlecliffian	Uplift	Not recorded
	Pliocene			Nukumaruan	Uplift/regression	Whariki Formation
					Trangression	Not recorded
				Mangapanian	Uplift/regression	Kaumatua Formation
				Waipipian	Unknown	Not present
				Opotian	Subsidence/ Transgression	Mangatoro Formation Basal Conglomerate
	Miocene		Taranaki	Kapitean	Erosion/weathering	Not present
				Tongaporutuan		
	Late Cretaceous-Oligocene				Erosion/weathering	Not present
Mesozoic	Early Cretaceous				Uplift (Rangitata Orogeny)	Not present
	Triassic-Jurassic				Subsidence	Torlesse greywacke

6.1.2 Geomorphology

Historic examples from elsewhere in New Zealand suggest that an earthquake origin should be considered for a landslide-dammed lake in a seismically active area (Adams, 1981). If the four landslide events in the Lake Colenso region are in fact caused by earthquakes then their ages (Table 5.2) give an approximation of the paleoseismicity of the area. This allows comparison with the reconstructed earthquake records (Table 3.2) of the Mohaka, Kaweka, Ruahine and Wellington Faults (Fig. 6.1; Hanson, 1998; Langridge *et al*., 2007). The correlation of landslide events with reconstructed seismic records must be approached with caution, as it is likely that an earthquake event may be localised, and it is likely that an earthquake 'signal' may not be recorded in all environments.

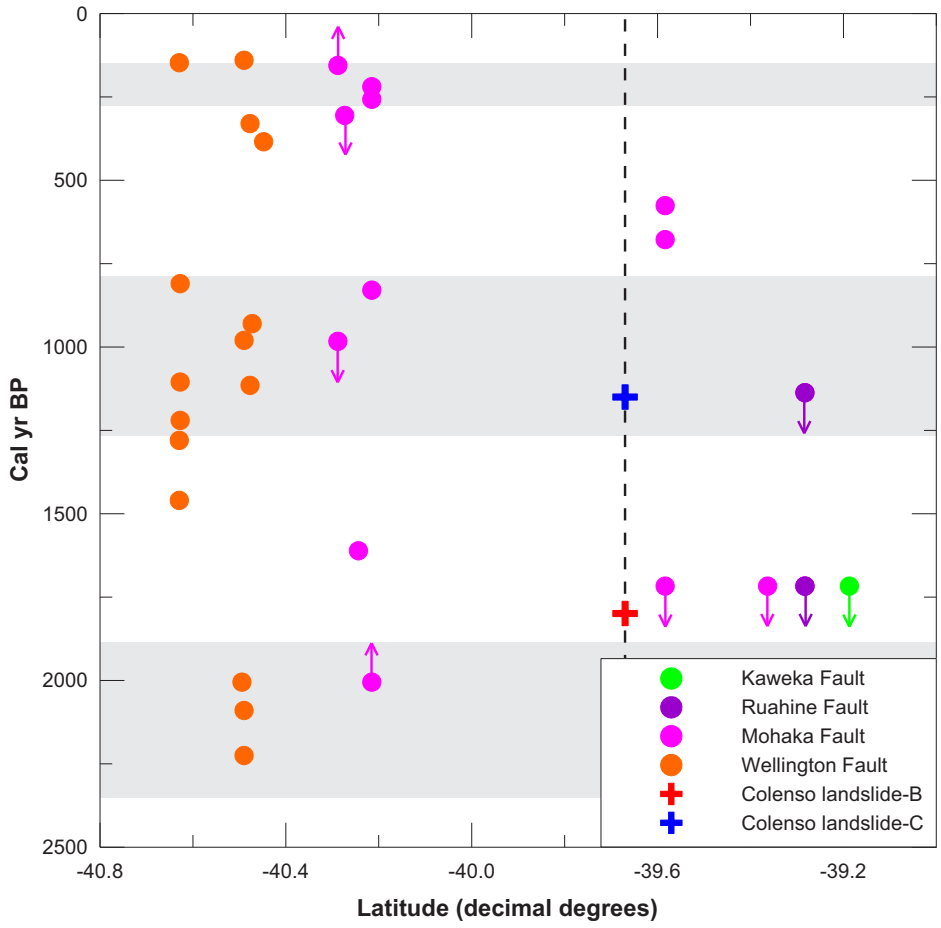

Figure 6.1. Paleoseismic records (Hanson, 1998; Langridge *et al*., 2007) for Kaweka, Ruahine, Mohaka and Wellington Faults plotted against latitude. Dashed line highlights the latitude of Lake Colenso. Arrows present minimum and maximum ages for seismic events (Hanson, 1998), i.e. an event on the Ruahine Fault that occurred >1717 cal yr BP is shown by a purple point at 1717 and arrow pointing downward. Shaded areas represent periods of increased seismic activity on the Pahiatua section of the Wellington Fault as put forward by Langridge *et al*. (2007).

There are no paleoseismic records that cover the period ~45,000 yr BP, so landslide-A can not be correlated to any earthquake events. There are a range of dates that correlate to the date of landslide-B (1799 ± 13 cal yr BP), i.e. post-Taupo (1717 cal yr BP; Lowe *et al*., 2008) in several locations on the Ruahine Fault, and also on the Mohaka and Kaweka Faults. Either these events presented by Hanson (1998) correlate to one event, or represent several fault movements on the Ruahine and Kaweka Faults. The timing of landslide-C (~1370 cal yr BP) is correlated to an event pre-1137 cal yr BP on the Ruahine Fault, an event post-983 cal yr BP on the Mohaka Fault (Hanson, 1998), and also events recorded on the Wellington Fault ~1250 cal yr BP. Landslide-D is small and may not have been triggered by an earthquake. Concieveably, it could have been initiated by a storm event. No date is available but it could possibly correlate to any of the events <500 yr BP.

These historic earthquake records from all four of the major proximal faults are commensurate with ages inferred for these latest landslide events, which provides confidence in the geomorphological model of landscape evolution and lake formation.

6.2 Lake Colenso

The lake was formed by three landslides. The first landslide (<45,172 ± 1261 yr BP) dramatically changed the geomorphology of the valley, and it appears (from evidence presented in this study) after the deposition of the second landslide (1799 ± 13 cal yr BP) that a swamp/peat environment formed in the hollows of the hummocky terrain. A third landslide (~1370 yr BP) later blocked valley drainage and initiated formation of the present-day Lake Colenso

6.2.1 Assessment of chronology

Several radiocarbon dates were obtained throughout the core using bulk sediment, plant macrofossil material and pollen concentrates, and three of the ^{14}C ages fit with the model of constant sedimentation (Fig. 6.2). However, there are apparent issues with some of the radiocarbon dates, these are discussed here.

The radiocarbon date (NZA 34645) taken directly below the Tf5 (650 ± 96 cal yr BP) and 15 cm below NZA 35692 (601 ± 46 cal yr BP), presents an age of 2071 ± 74 cal yr BP, approximately 1400 years older than expected. The tephra date for Tf5 is more reliable as it is based on several radiocarbon dates from other sites (Donoghue *et al*., 1995), so the tephra-derived chronology is deemed to be more dependable than that based solely on radiocarbon data. The 'hard-water reservoir effect' is the likely cause for the difficulties in dating using radiocarbon. This is a common complication in dating limnological samples (e.g., Olsson 1991). The catchment geology in this region (Fig. 3.5) is mostly limestone (Smale *et al*., 1978), and surface water entering the lake, along with terrigenous material is likely to contain dissolved carbon from the surrounding rocks. This affects the isotopic composition of carbon within the lake, as was found by Newnham *et al*. (1997), whereby contamination by inert carbon resulted in overestimation of age by ~1300 years.

Samples of pollen concentrate (NZA 35748 and NZA 35749) also presented varied results (Table 5.5); they resulted in ages (~800 and ~2300 years, respectively) considerably older than expected. A possible explanation for these divergent ages is

that older pollen has been brought into the lake catchment during deposition of silt layers in the lake (discussed in section 6.2.2). The sample volume of the pollen concentrates (NZA 35748 and NZA 35749) was very small, and so have a higher chance of being susceptible to contamination (older or younger). The inclusion of fine organic matter from aquatic plants that have incorporated older, dissolved carbonates from the surrounding limestone catchment (as outline above) is the likely cause. As in other studies (e.g., Olsson, 1991), the hard-water effect exhibited in Lake Colenso is shown to have a larger influence on small volume and bulk sediment samples.

Age model

Silt layers (discussed in 6.2.2) and volcanic ash is deposited relatively rapidly, usually over a period of days (Wilmshurst *et al*., 1997), and was subtracted from the total sediment core depth to prevent sedimentation rates being over-represented. Thus, the depth of each tephra and silt layer was corrected, and these were the depths from which the calendar ages were then derived (Table 6.2).

A near-constant sedimentation rate is assumed, and was derived from linear interpolation between radiocarbon and tephra dates, similar to what was done by Page *et al*. (2010). Stratigraphic boundaries or layers that were not dated were inferred from the calculation of sedimentation rates. For example, the age for the peat-lake sediment boundary has been calculated from sedimentation rates between Tf1 and NZA 35497, taking into account the different accumulation rate of peat and lake material (Fig. 6.2).

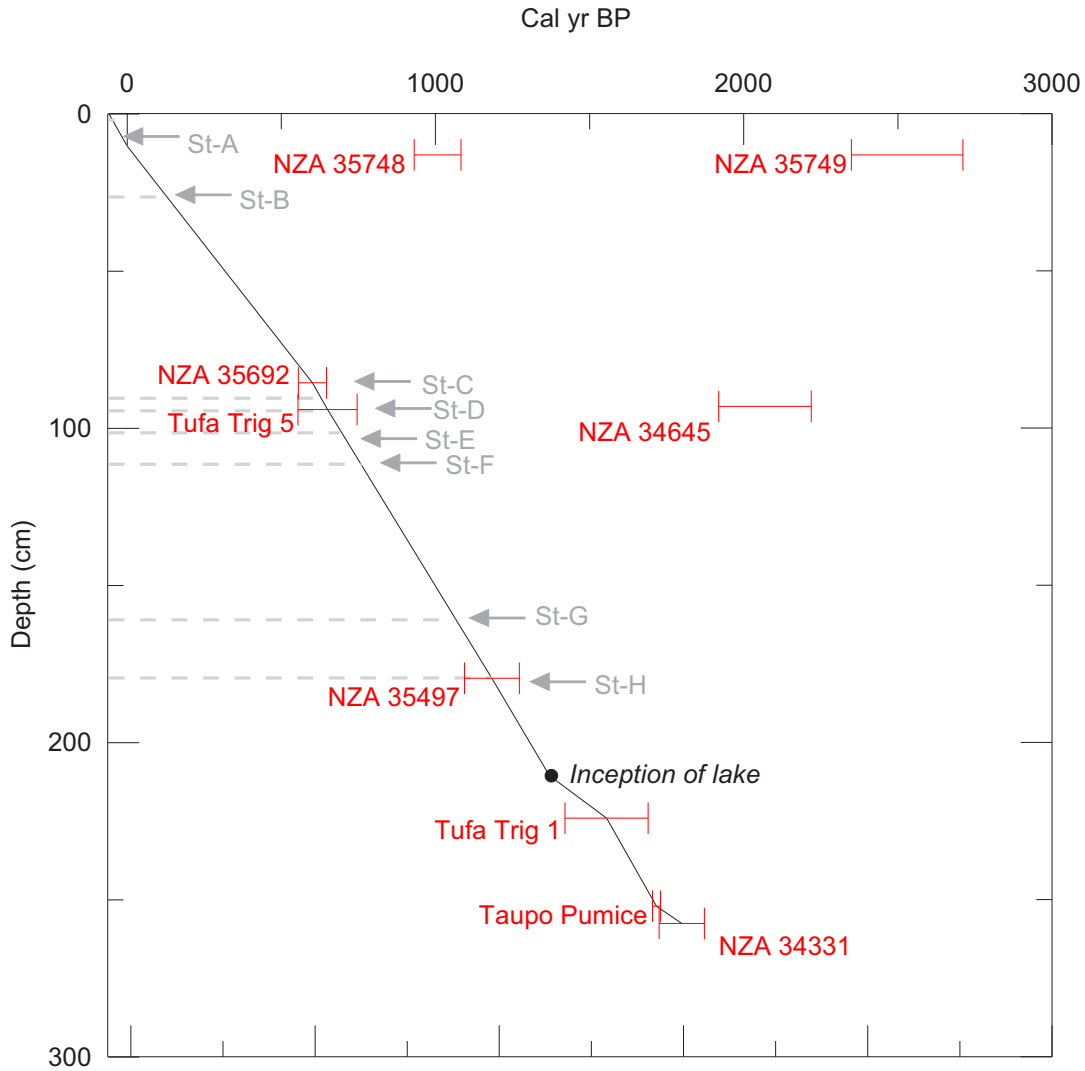

Figure 6.2. Age model for composite sediment core, based on tephra and radiocarbon dates. All ages are in cal yr BP, and have been calibrated using OxCal4.1 (Bronk Ramsey, 2001) and SHCAL04 dataset (McCormac et al., 2004). Storm ID numbers (e.g., St-A) and hashed lines shown here correspond to those in Table 6.2.

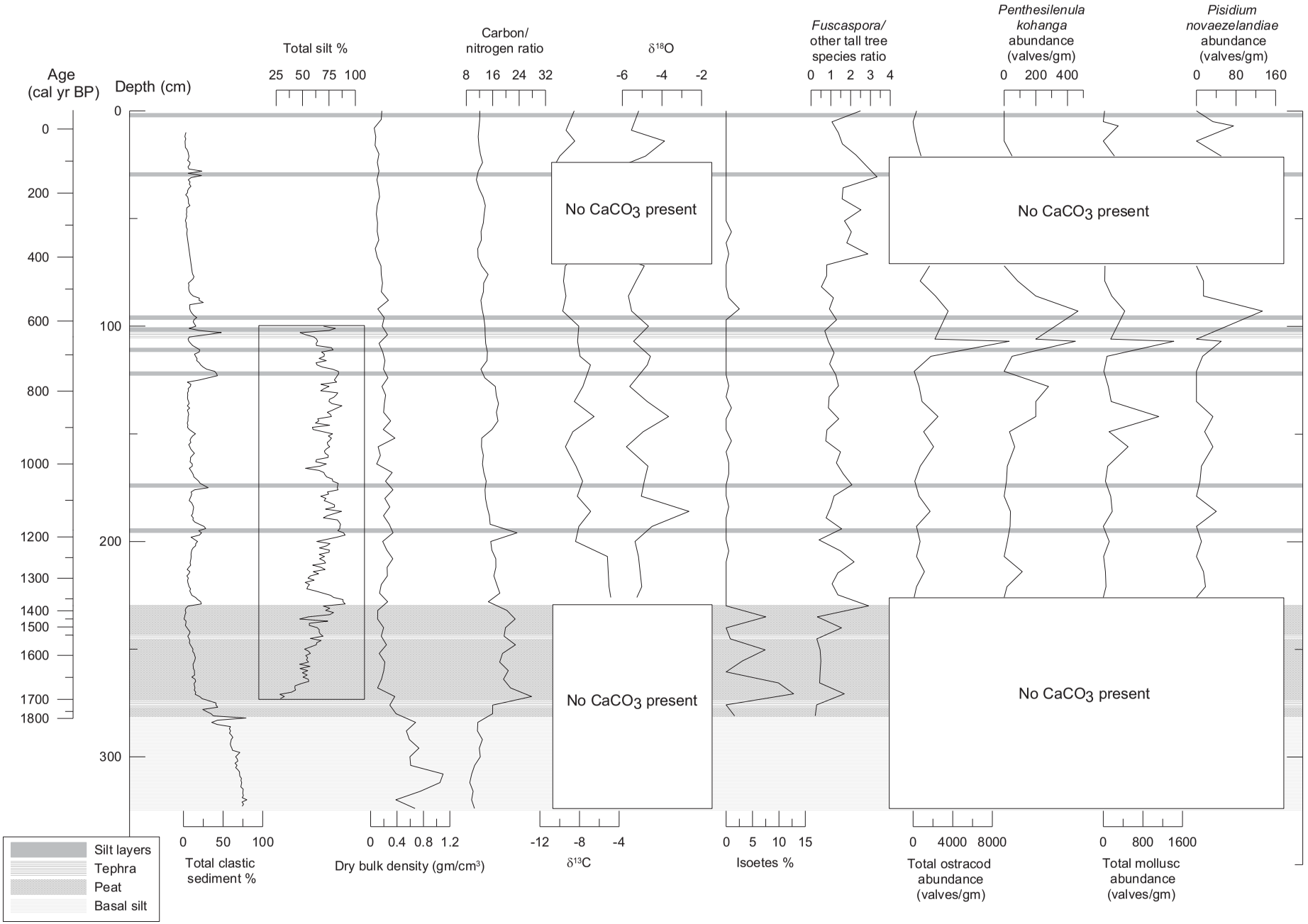

Figure 6.3. Summary diagram of results used to assess the environmental history of the Lake Colenso area.

6.2.2 Sediment analysis and interpretation of silt layers

The silt layers are one of the distinguishing features of the stratigraphy, and an interpretation of the processes responsible for their deposition provides insight into the stability of the lake catchment.

Using sedimentological and biogeochemical characteristics, it is possible to determine whether the silt layers are derived from within the lake or sourced from outside of the lake. The ratio of carbon and nitrogen (C:N) can be used to determine the origin of deposits (Meyers, 2003); sediment C:N ratio values of >20 reflect a terrestrial origin and a C:N ratio of between 4 and 10 is likely to have an in-lake origin (Augustinus *et al*., 2008). The C:N ratio of the peat material (1799 to 1370 cal yr BP.) ranges from 16 to 22 (Fig. 6.3), which suggests a terrestrial origin where land plants were dominant (Meyers and Lallier-Vergès, 1999).

The abrupt increase in the C:N ratio at 280 cm depth (Fig. 6.3) is a likely response to the eruption of the Taupo Pumice at 1717 ± 13 cal yr BP (Lowe *et al*., 2008). A marked decrease of the C:N ratio at 1370 cal yr BP (at the peat-lake sediment boundary) suggests the sudden onset of lake conditions. An abrupt departure at 1180 cal yr BP is correlated to the leaf layer preserved in the stratigraphy (Fig. 5.15).

A distinct and sustained rise in the C:N ratio is apparent from 920 to 780 cal yr BP which is correlated with the speckled sediment in this section of the sediment cores (Fig. 5.15). There are two plausible reasons for this increase in the C:N ratio; either (1) shallower lake levels, or (2) increased run-off introducing terrestrial organic matter and soil nutrients into the lake during times of wetter climate. A lower lake level would result in growth of aquatic macrophytes in closer proximity to the coring location (Moy *et al*., 2008), resulting in an increase in the C:N ratio. However, the paleohydrological record (discussed in section 6.2.3) and pollen assemblage (discussed in section 6.2.4) suggest that there was no significant change in lake level

at this time. The number of silt layers in this zone suggests that this part of the core reflects an episode of enhanced storminess. Additionally, high winds can form waves that cause mixing of littoral macrophytes and sediments in the centre of the lake (Moy *et al*., 2008), which would also cause an increase in C:N values.

Peng *et al.* (2005) used grain-size as a measure of precipitation in lake environments, and the dominance of the silt-size fraction reflected increased precipitation and associated sediment input from the surrounding landscape. Decreases in the C:N ratio at the silt layers indicates a terrestrial signal, and the increases in minerogenic matter, suggest that these silt layers have been washed in during episodes of erosion within the lake catchment. Collapse of deltaic sediment and turbidity currents triggered by seismic activity in this area are other likely causes for the emplacement of silt layers, though it appears this is not the case as there are no apparent unconformities or evidence of disturbance in the core stratigraphy.

Apart from these zones discussed above, there is a trend towards decreasing C:N ratio since lake formation and it is likely that this is due to the increased amount of lake algae, associated with a general increase in lake volume and overall lake stability.

The silt layers, which range from 1 to 4 cm in thickness, reflect sediment input from the surrounding landscape and are interpreted as a record of storms and periods of intense rainfall in the lake catchment. To reconstruct a storm history, ages for the individual silt layers have been calculated from the age model (Fig. 6.2) and presented in Table 6.2. Typically, studies that involve the reconstruction of storms from lacustrine sediments (e.g., Eden and Page, 1998; Wilmshurst *et al*., 1997; Page *et al*., 2010) use historic records to match recent storm layers, and then with the aid of radiocarbon dating and tephrochronology, construct an age model and extrapolate back to provide an age for older storms. A similar approach has been used here. Of course, the accuracy of such a record is limited by the dating resolution, which will result in greater uncertainty for the timing of some events.

Table 6. 2. Original and corrected depths, thicknesses and ages for storms layers.

Lower depth (cm)	Corrected depth (cm)	Layer thickness (cm)	Storm ID	Age (cal yr BP) [a]
5	2	3	St-A	-29 [b]
32	26.5	2.5	St-B	127
97.5	90.5	1.5	St-C	626
103	94.5	1.5	St-D	644
112	101.5	1	St-E	690
124.5	111.5	2.5	St-F	764
175	161	1	St-G	1065
197.5	179.5	4.0	St-H	1185

[a]Ages attained from Fig. 6.3.
[b]The age '-29' refers 29 years after 1950, i.e. 1979AD

The average frequency of storms is 1 in 150 years in the Lake Colenso record and storms occur on a centennial timescale with intervals between individual storms ranging from 18 to 499 years. It is apparent that there is a marked variability in the frequency and magnitude of storm layers and it appears that there are 3 distinct periods of storminess (1185 to 1065 cal yr BP, 764 to 626 cal yr BP, and 127 to -29 cal yr BP).

Page *et al*. (1994b) presented a plot of sediment thickness versus storm rainfall based on historic storm records, which had a correlation of $R^2 = 0.8$ (Page *et al*., 1994b). This relationship showed that sediment movement in steepland watersheds is principally caused by extreme storms and supports ideas put forward by other authors (Wolman and Gerson, 1978; De Rose *et al*., 1998). Eden and Page (1998) were then able to quantify the amount of sediment deposited depending on the intensity of the storm. Layers >0.4 cm thick represent storms with approximately 300 mm rainfall, and layers >1.0 cm thick represent storms with 400 – 450 mm rainfall. However, the relationship between the magnitude of storm rainfall and sediment yield is intricate, and depends on the frequency of events and the rate at which soil recovers (Trustrum and De Rose, 1988). A study into the amount of rainfall needed to trigger sediment movement was carried out in the landslide-prone Gisborne district by Hicks (1989). This study proposed that intensities of 100 mm

rainfall in a 24 hour period, 200 mm rainfall in a 48 hour period, or 300 mm rainfall in a 72 hour period were needed to act as a trigger. Prolonged low-intensity rainfall over an extended period of time can also have the same effect (Page *et al*., 2010).

The silt layers at Lake Colenso range from 1 to 4 cm in thickness, so if using the same sediment thickness-storm rainfall relationship of Eden and Page (1998), irrespective of the differences in catchment settings, each layer would have been deposited from a storm with greater than 400 mm rainfall. A major storm that is known to have had an effect in the Ruahine Range is Cyclone Alison (Grant *et al*., 1978) which occurred in 1975. Rainfall recordings from Pohangina Saddle show a total rainfall of 389 mm over a period of 24 hours, and 612 mm rainfall over a period of 72 hours (Grant *et al*., 1978). Although the age model from Lake Colenso presents the first storm layer (St-A) at ~1979 AD, it is likely that St-A is a correlative of the Cyclone Alison event.

During the 20th century there were at least 33 significant rainstorms that caused forest damage and erosion in selected parts of the Ruahine Range (Grant, 1991). Hence, based on the frequency of storm layers in the core (~1 storm every 150 years), it is apparent that only significantly large storms are recorded at Lake Colenso. There are no historical records beyond 127 yr BP (Grant, 1991), so it is difficult to assign other known storms to the silt layers recorded from Lake Colenso.

Erosion/storm history

With continued uplift and variable weather patterns, erosion is commonplace in the Ruahine Range. Erosion is, in part, a factor of the geology and as a result the terrain is steep and sharp-crested ridges are common (Rogers, 1987). Studies suggest an erosion rate of 1215m^3/ha/yr (Marden, 1984) in the Ruahine Range, comparable to erosion rates found elsewhere.

The key triggering mechanism for slope movement is the saturation of colluvium during major storm periods, where shallow translational slope movements dominate (Marden, 1984). Grant (1989) recognised eight periods of increased erosion and alluvial sedimentation in the Ruahine Range, which have tended to decrease in magnitude over time. Stages of erosion and alluvial sedimentation have been found not to correspond to the arrival of humans, but primarily from a sustained increase in the frequency of major rainstorms, related to long-term climatic fluctuation (Grant, 1989).

Comparison with other records/proxies

A summary of erosion periods as inferred from alluvial sedimentation (Hubbard and Neall, 1980; Grant, 1985), periods of increased precipitation from speleothem records (Lorrey *et al*., 2008), storm histories from lake sediments (Wilmshurst, 1997; Chester and Prior, 2004; Page *et al*., 2010), coastal deposition (McFadgen, 1989), periods of forest stand disturbance (Elder, 1963; Lusk and Ogden, 1992; Horrocks and Ogden, 1998), glacial advances (Schaefer *et al*., 2009), temperature derived from tree-rings (Cook *et al*., 2002; Palmer and Xiong, 2004) and speleothems (Williams *et al*., 2004) is displayed in Fig. 6.3. In comparing records, it must be kept in mind that there are likely to be inconsistencies in the timing of events associated with the uncertainties of age models in the various studies.

The period of storminess from 1186 to 1065 cal yr BP at Lake Colenso correlates to times of increased storminess put forward by Grant (1985), Page *et al*. (2010), and McFadgen (1989), and also correlates with a phase of increased precipitation inferred from speleothem records (Lorrey *et al.*, 2008). Also, there is a correspondence with the period of enhanced storminess (764 to 626 cal yr BP) at Lake Colenso with other records (Grant, 1985; McFadgen, 1989; Lusk and Ogden, 1992; Wilmshurst, 1997; Page *et al*., 2010). Temperatures at this time were warmer relative to the present day (Williams *et al*., 2004), which is supported by the $\delta^{18}O$ values data (discussed further in section 6.2.3) from Lake Colenso. The third period of storminess from Lake Colenso (127 to -39 cal yr BP) again correlates to episodes recorded by Grant (1985), and McFadgen (1989).

It appears that there is some correlation with the Waipawa, Waihirere and Pre-Kaharoa erosion periods (Grant, 1985), and a strong association with periods of coastal deposition (McFadgen, 1989) with the storm record from Lake Colenso. This suggests that these periods of increased erosion (Grant, 1985; McFadgen, 1989) are as regional and distinctive as originally thought, contrary to conclusions found by Wilmshurst (1997).

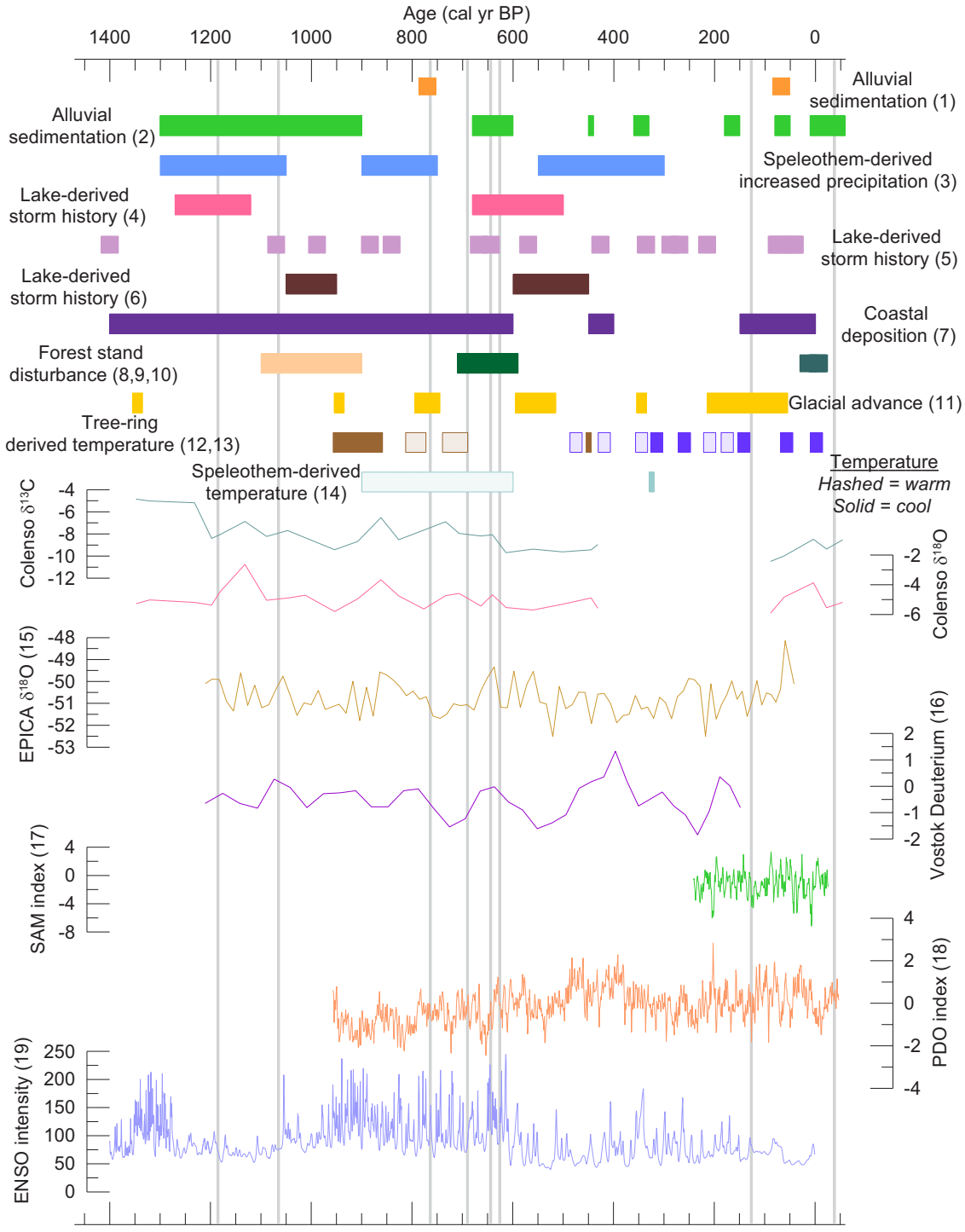

Figure 6.4. Summary graph showing $\delta^{18}O$ and $\delta^{13}C$ records from Lake Colenso and storm events (represented as grey lines) against periods of climatic change from a variety of proxies and environments discussed in text. (1) Hubbard and Neall (1980); (2) Grant (1985); (3) Lorrey *et al*. (2008); (4) Page *et al*. (2010); (5) Wilmshurst (1997); (6) Chester and Prior (2004); (7) McFadgen (1989); (8) Horrocks and Ogden (1988); (9) Lusk and Ogden (1992); (10) Elder (1963); (11) Schaefer *et al*. (2009); (12) Cook *et al*. (2002); (13) Palmer and Xiong, (2004); (14) Williams *et al*. (2004); (15) Jouzel *et al*. (2006); (16) Petit *et al*. (2001); (17) Stahle *et al*. (1998); (18) Macdonald and Case (2005); and (19) Moy *et al*. (2002).

Regional climatic drivers

Comparison of major storm periods with other New Zealand Holocene records indicates that the record from Lake Colenso has wider regional significance. New Zealand climate is the product of the interaction of sub-tropical and sub-polar atmospheric and oceanic systems (Schaefer *et al*., 2009). Hence, an assessment of the El Niño-Southern Oscillation (ENSO), Southern Annular Mode (SAM), and Pacific Decadal Oscillation (PDO), which are known to be the main driving forces of climatic variability in New Zealand (Ummenhofer *et al*., 2009), allows a further understanding of the factors controlling regional climate.

El Niño-Southern Oscillation (ENSO) is a quasi-decadal climate pattern that is characterised by variations in the temperature of the Pacific Ocean, where El Niño is associated with warming in the eastern Pacific Ocean and cooling in the western Pacific Ocean, and vice versa with La Niña (Shulmeister *et al*., 2004). The Southern Oscillation is the atmospheric component, and is the variation in surface air pressure between the eastern and western Pacific Ocean, the strength of which is measured by the Southern Oscillation Index (SOI; Lorrey *et al*., 2007). El Niño conditions in the eastern part of New Zealand tend to be characterised by enhanced south-westerly winds, cooler air and decreased precipitation, while La Niña is characterised by increased northerly winds, warmer air and increased precipitation (Lorrey *et al*., 2007).

The association of local rainfall records with the SOI (Fig. 3.4) suggests that variation in ENSO has an effect in the higher altitudes of the Ruahine Range. An increase in frequency and amplitude of the ENSO regime has been a feature of the late Holocene, which is thought to have been caused by the comparatively strengthened seasonality that enhances zonal circulation systems in the Southern Hemisphere (Shulmeister *et al*., 2006).

Moy *et al*. (2002) presents a record of the intensity and frequency of ENSO activity from the occurrence of clastic sediment (interpreted as in-wash from ENSO influenced storms) from Laguna Pallcacocha, Ecuador. Most of the storms (except for those at 644 and 626 cal yr BP) in the Colenso record show a correspondence (Fig. 6.4) with drier periods (less intense/frequent ENSO or La Niña) in the record put forward by Moy *et al*. (2002), similar to the conclusions of Page *et al*. (2010).

In addition to ENSO (Ummenhofer *et al*., 2009), precipitation is also influenced by Southern Annular Mode (SAM) which involves alternating periods of wind intensity and storminess (Renwick and Thompson, 2006), and is responsible for much of the climatic regime in high- to mid-latitudes in the Southern Hemisphere (Gillett *et al*., 2006). In its positive phase, SAM is characterised by weaker than normal westerly winds and settled climate in New Zealand with enhanced westerly winds and storminess in the Southern Ocean and vice versa in its negative phase (Ummenhofer *et al*., 2009). The positive phase is associated with cooler than average temperatures over continental Antarctica and warming over the Antarctic Peninsula, meaning drier than normal conditions in New Zealand due to the southward shift of the storm-track (Gillett *et al*., 2006). The deuterium-derived temperature record from Vostok (Petit *et al*., 2001) and $\delta^{18}O$ record from EPICA Dome C (Jouzel *et al*., 2006) can be used as a measure of temperature from Antarctica and, hence a measure of SAM where higher air temperatures in continental Antarctica correlate to negative phases of SAM.

The majority of storms in the Colenso record show an association with an increase in temperatures from Vostok and EPICA Dome C records (Fig. 6.4), which indicates a correlation with negative phases of SAM. This correlation of storm events with negative phases of SAM was also found by Page *et al*. (2010).

The Pacific Decadal Oscillation (PDO) is a pattern of Pacific climate variability, and while the spatial structure is similar to that of ENSO, the temporal patterns tend occur on an inter-decadal timescale (MacDonald and Case, 2005). During warm phases of PDO, the western and central Pacific Ocean is characterised by cooler than average temperatures while the eastern Pacific has higher than average temperatures, and vice-versa (Gedalof *et al.*, 2002). The location and strength of ENSO is strongly dependent on the conditions of PDO (Mantua *et al*., 1997), where warm/positive PDO is generally coincident with El Niño, and cool/negative PDO is coincident with La Niña (MacDonald and Case, 2005). There appears to be some correlation between most of the storms recorded at Lake Colenso (again except for those at 626 and 644 cal yr BP) and the reconstruction of PDO (Macdonald and Case, 2005), where storms occur during lower or negative PDO or periods of La Niña (Fig. 6.4).

The year of Cyclone Alison (1975) had a PDO index of -1.25 (D'Arrigo and Wilson, 2006) and SOI index of +13.6 (Bureau of Meteorology, 2011), which is indicative of a particularly strong La Niña phase. This is what is shown by the general trend of the record (Fig. 6.4) which shows that storms in the Colenso catchment typically occur during periods of La Niña. Also, the SAM index of -0.636 (Fogt *et al.*, 2009) in the same year is indicative of a negative SAM phase, again supporting the rest of the storm record, where storms typically occur in negative phases of SAM (Fig. 6.4).

It is likely that the Colenso storm record is influenced by a combination of atmospheric and oceanic systems and their individual frequency and variability. The inter-relationship between ENSO, SAM and PDO (Mantua *et al*., 1997; Fogt *et al.*, 2009) has a significant effect on the intensity of signals, making it harder to identify which of these, singularly or collectively, is the main driving force of regional precipitation patterns.

6.2.3 Paleohydrology

In this study, investigation of the $\delta^{13}C$ and $\delta^{18}O$ values from ostracods was exploratory, with the purpose of verifying if the concept is useful in a paleoenvironmental context. The isotopic signature of an ostracod is dominantly controlled by the isotopic composition of the lake water and the temperature of the water at the sediment-water interface during shell formation (Von Grafenstein *et al*., 1999). It is not influenced by in-washed carbonate (Finsinger *et al.*, 2008), which is useful in an area where the geology is dominated by carbonate-bearing rocks (Fig. 5.10).

The isotopic composition of lake water depends largely on the volume of the lake and the $\delta^{18}O$ of the input water, which is generally isotopically lighter than that of lake water (Li and Ku, 1997). Lake water becomes progressively enriched in $\delta^{18}O$ as evaporation dominates (Li *et al*., 1997), this process is typical in warmer summer months resulting in a seasonal variation in $\delta^{18}O$ (Escobar *et al*., 2010). When lake volume is stable, the $\delta^{18}O$ approaches a steady state as equilibrium is reached, and the magnitude of isotopic change is controlled by vapour exchange at the lake surface and also by the isotopic composition of the input water (Li *et al*., 1997). The $\delta^{18}O$ value of water, as determined by the evaporation and precipitation regime, is found to be relatively homogenous within shallow lakes where mixing is common (Escobar *et al*., 2010), with a slight trend toward negative values with increasing depth (Von Grafenstein *et al*., 1999).

The interpretation of $\delta^{13}C$ must be approached with caution, as the cycling of carbon in lakes is complex as fractionation occurs at different times (Andersson *et al*., 2010). Isotopic carbon can vary by several parts per thousand during a single year, due to input into the lake system from soil-derived CO_2 (-25‰), dissolution of local bedrock (-2 to +2‰), aquatic production by photosynthesizing plants, and the deposition and breakdown of organic material (deposition removes carbon from the system and breakdown releases ^{12}C-enriched CO_2; Andersson *et al*., 2010). Variability in $\delta^{13}C$ can also be attributed to seasonal variability, for example during summer when evaporation is dominant the lake water becomes isotopically heavier

with ^{13}C-enriched CO_2, as ^{12}C-enriched CO_2 is exchanged with the atmosphere (Li and Ku, 1997).

Discrepancies between the expected $\delta^{18}O$ and observed $\delta^{18}O$ suggest that ostracods do not form in isotopic equilibrium with the surrounding lake water, but that the differences are dependent on temperature (Von Grafenstein *et al*., 1999). Compositional variability between families is also common, where ostracods show an offset from assumed equilibrium, independent of water temperature; this is termed the 'vital offset' (Von Grafenstein *et al*., 1992). The varying processes in calcification between separate ostracod groups are believed to be the causal factor (Von Grafenstein *et al*., 1992). For example, an increase in $\delta^{18}O$ is positively correlated to the speed of the calcification process in freshwater ostracods. Hence, the smaller amount of time required for carapace development, the more enriched the $\delta^{18}O$ content of the carapace (Von Grafenstein *et al*., 1999).

Vital offset values are essential for the comparison and correlation using records from different species across different sites, and for comparison of fossil records with actual water isotope ratios (Von Grafenstein *et al*., 1999). Because of the relatively small isotopic fractionation of adult *Gomphocythere* (also known as *Limnocythere*; Eager, 1971), which has been shown to precipitate within $0.78 \pm 0.20‰$ of $\delta^{18}O$ (Von Grafenstein *et al*., 1999), the stable isotope results presented from Lake Colenso are not corrected. Therefore, it must be noted that the $\delta^{18}O$ values presented for *Gomphocythere duffi* may exaggerate the $\delta^{18}O$ for lake water by $0.78 \pm 0.20‰$.

Stable isotope values obtained from ostracods have been used in many studies, including provision of a paleohydrological record (Li and Ku, 1997), identification of periods of warming and cooling climate (Finsinger *et al*., 2008), and in the reconstruction of atmospheric circulation systems (Moy *et al*., 2008). Each lake has a unique trend in covariance, which is a function of the lake's morphology and its climatic and geographic setting (Talbot, 1990).

The covariance of $\delta^{13}C$ and $\delta^{18}O$ can be used as an indicator of paleohydrological change in closed lake systems (Li and Ku, 1997). Isotopic covariance is typical in hydrologically-closed basin lakes and any interruption or realignment of this trend is indicative of significant changes in basin hydrology (Talbot, 1990). A decrease in lake volume as a result of intense evaporation will result in an increase in $\delta^{18}O$, as $\delta^{16}O$ will preferentially go to the vapour phase. Also, $\delta^{13}C$ will increase if a decrease in volume is due to reduced freshwater input, meaning a strong $\delta^{13}C$ - $\delta^{18}O$ covariance (Li and Ku, 1997). The isotopic composition of a lake shows little variation if the lake volume is relatively stable or experiences slow changes, so $\delta^{13}C$ - $\delta^{18}O$ covariance is relatively weak (Li and Ku, 1997).

Here, terms of covariance are defined as the correlation coefficient (R), which is a measure of the strength of the linear relationship between two variables. The $\delta^{18}O$ values at Lake Colenso range from –5.80 to –2.64‰, with an average of –4.97‰, while $\delta^{13}C$ values range from -10.48 to -4.84‰ with an average of -8.16‰. This average $\delta^{18}O$ value is heavier than that of the modern lake water (–5.91‰), which suggests that Lake Colenso has remained a closed system since formation. The $\delta^{13}C$ - $\delta^{18}O$ covariance is weak ($R = 0.34$, $p < 0.01$), suggestive of a stable lake environment with no significant sustained rise or fall in lake level.

Interpretation of the individual $\delta^{13}C$ and $\delta^{18}O$ values can also be used to infer a record of hydrological change. $\delta^{13}C$ is used as a measure of precipitation (Moy *et al*., 2008) and by inference lake volume (McKenzie, 1985), and productivity (Fry and Sherr, 1984), with $\delta^{18}O$ used as a measure of temperature (Andersson, 2010). An increase of $\delta^{18}O$ is indicative of warmer temperature. In the Lake Colenso record $\delta^{18}O$ values begin relatively high then decrease rapidly from -8.40 to -5.19‰ at approximately 1200 cal yr BP and then decrease towards present day. This overall trend in decreasing values is punctuated by brief but significant increases at 1137, and from 860 to 634 cal yr BP, and minor increases at 1050, 427 and 8 cal yr BP. An increase of $\delta^{13}C$ is indicative of lower precipitation. These departures are found to

correlate with increases in $\delta^{18}O$ at 1137, 860 and 8 cal yr BP, and minor increases from 817 to 703, and at 634 and 447 cal yr BP.

The prolonged period of drier and warmer climate from 860 to 643 cal yr BP (Fig. 6.4) is correlated with warmer temperatures derived from speleothem (Williams *et al*., 2004) and tree-ring records (Cook *et al*., 2006). The seemingly anomalous values from 1355 to 1240 cal yr BP are likely related to the change from a peat bog to a lake environment and the colonization of ostracods. There also appears to be an overall decreasing trend in $\delta^{13}C$ during this time period, suggesting a progression towards deepening lake conditions. The relatively low values of $\delta^{18}O$ during this interval suggest a period of cooler temperatures resulting in decreased evaporation (Moy *et al*., 2008). Collectively, these results support the assertion made earlier that the storm events identified in the Lake Colenso record occurred during dry periods and less intense/frequent ENSO conditions.

6.2.4 Vegetation history

This section discusses the palynological record from Lake Colenso (where the interval between samples is ~30 years). Whether the pollen record represents a local or regional record is considered, and then followed by an account of vegetation changes and the possible causes.

Regional or localized record?

Pollen is known to travel long distances (Moar, 1969), such as the pollen found on Chatham Islands (Mildenhall, 1976; Dodson, 1976) from the two main islands of New Zealand. A lake is expected to collect pollen from local and regional sources, usually dependent on the size of the lake (Jacobson and Bradshaw, 1981). The pollen of *Pinus*, an exotic species, is susceptible to long distance dispersal because of its buoyant air sacs, and substantial production levels (Newnham *et al*., 1998). *Pinus* pollen is almost absent (<1%) from the Lake Colenso pollen profile, suggesting that the mountainous forested nature of the catchment has acted as a buffer for much of the regionally sourced pollen, as found by Newnham *et al.* (1998) at Lake Waikaremoana. Evidently, the paleovegetational record from Lake Colenso displays an undisturbed record of local changes in forest composition.

Interpretation of pollen

1799 to 1370 cal yr BP (Pollen zone Pa)

The pollen evidence from 1799 - 1370 cal yr BP (Fig. 5.22C) suggests a dominance of swamp/wetland taxa at the site. *Cyperaceae*, *Isoetes* and *Haloragis* can be used as a measure of available moisture (Brownsey and Smith-Dodsworth, 1989; Wilmshurst *et al*., 1999) as they prefer sites where water or moisture is in abundance, such as swamps, bogs, and lakes (Moore and Edgar, 1976). As *Isoetes* is typically restricted to water depths of 0 - 2 m (Vandergoes *et al*., 1997), its dominance in this zone implies water depth at this time did not exceed 2 m. *Prumnopitys taxifolia* is also a useful indicator of wetness (Vandergoes *et al*., 1997). *P. taxifolia* is predominant in areas prone to drought (Leathwick and Whitehead, 2001), and therefore low numbers is taken to represent a wet climate (Horrocks and Ogden, 1998). The relatively low levels of *P.taxifolia* during pollen zone Pa compared to other pollen zones provides further evidence for relatively wet conditions during this time.

The presence of *Cyathea* tree ferns is likely to indicate a local record at this time, as this genus prefers moist climate though characteristically does not inhabit very wet substrates, such as the peat bog surface that would have been present in the Colenso basin. So, *Cyathea* was likely present in the forest either adjacent or surrounding the swamp environment.

An interesting feature of this pollen zone is the high number of *Podocarpaceae* compared to Fuscaspora and the overall lower values of tree taxa. There are several plausible reasons that may explain this;

1) The vegetation of the swamp environment was contributing the majority of the pollen rain to the site, and diluting the pollen from the nearby forest and wider area.
2) Response to geomorphic disturbance (discussed in section 6.1.2) where the landslide (1799 ± 13 cal yr BP) damaged a large area of forest. It is possible that the landslide, which caused an opening in the forest canopy, allowed pollen from

wider regional sources to be incorporated explaining the diversity of species in pollen zone Pa (e.g., the presence of sub-alpine species such as *Halocarpus*, *Libocedrus* and *Phyllocladus*). However, the absence of *Weinmannia*, which is an indicator for disturbance, suggests this is not the case.

3) A response to a change in climate conditions. Though there is no significant climate change at this time suggested in other North Island records (Lees, 1986).

The first reason is the most likely, as the zone is dominated by swamp/bog taxa and related podocarps that probably grew around the swampy margins of the peat environment.

1370 to 396 cal yr BP (Pollen zone Pb)

The Pa/Pb zone boundary at 1370 cal yr BP reflects the change from a swamp to a lake environment following landslide-B (discussed in 6.1.2), with the decrease of *Isoetes* indicating the deepening of water as lake volume increased. An increase in tall tree species suggests there was an increase in abundance of tall trees in the lake catchment, perhaps in association with favourable climate which is supported by the decrease in *Nothofagus menziesii*. The decrease of *Halocarpus* and *Phyllocladus*, and the gradual absence of *Libocedrus* indicate either that the higher abundance of tall trees prevented much of this upland pollen reaching the site, or that the tree line retreated in response to climate. The decrease in *Cyathea* can be explained by the increased pollen production to the site, associated with the increased proportion of tall tree species.

A conifer-hardwood forest dominates the local environment at this time, as the canopy was predominantly composed of *Nothofagus*, with other conifer emergents, such as *Prumnopitys taxifolia*, *Podocarpus* (most likely *Podocarpus totara*, based on its occurrence in the present day forest), and *Dacrydium cupressinum.*

396 cal yr BP to present (Pollen zone Pc)

Vegetation appears relatively stable until ~396 cal yr BP, where Fuscaspora increases at the expense of other tall tree species (see Fuscaspora ratio in Fig. 6.2), suggestive of a shift towards cooler climate, while the decline of *P. taxifolia* and *Dacrydium cupressinum* suggest a change to a drier conditions. The understory species *Coprosma* and *Weinmannia* noticeably increase at this time. This vegetation assemblage persisted until present time, and there are several factors which could have contributed to this change in vegetational composition, as discussed in the next section.

Possible reasons for change at ~396 cal yr BP

Weinmannia and Fuscaspora are often used as indicators of disturbance due to their ability to colonize rapidly (Stewart and Veblan, 1982; Hubbard and Neall, 1980). There are several mechanisms that could have caused disturbance at this time: (1) an anthropogenic impact; (2) a direct climatically induced change; or (3) geomorphic disturbance in the vicinity, which itself may be an indirect result of a climatic phenomenon. These three scenarios are discussed below.

1. *Anthropogenic forest clearance*

   It is thought that continual forest clearance in coastal areas started ~600 years ago by the early Maori and ~150 years ago by Europeans (Wilmshurst, 1997). An age of ~391 cal yr BP has been put forward for the commencement of temporary forest clearance at Lake Waikaremoana. So far, this is the youngest record of pre-European anthropogenic impact (Newnham *et al*., 1998), and earlier than initial colonization of inland areas in the model of generally accepted anthropogenic forest impact (McGlone and Wilmshurst, 1999).

The period of vegetation change at Lake Colenso shows correspondence to the date of anthropogenic forest clearance put forward by Newnham *et al*. (1998). If the change at Colenso is due to anthropogenic impact, then this correlation suggests a migration of Maori to inland mountainous areas at this time. It is known that there was Maori settlement at Mokai Patea by at least 1844, the time at which William Colenso visited (Colenso, 1884). While there are no records of any settlements in the Lake Colenso catchment during this time, it is known that Maori used this as part of the route to the Hawkes Bay during the 19th century (Colenso, 1884; Aston, 1914), and likely sometime before:

> *"And, also though many years before, -a famed ancestor of theirs, named Te Rangitauira, who, in peacefully travelling from* [*Mokai-*] *Patea, to Hawke's Bay (Colenso, 1884)."*

A paper titled "The wars at Mokai Patea", suggests that passage to this region was frequent (Best, 1912). It is likely that the Mokai Patea people altered the nearby forest, evident by the abundance of *Coriaria* near Mokai Patea observed by William Colenso in 1847 (Colenso, 1884). Fire was a common method for clearance of land, and there is evidence of fires in the area in 1847 and during the 1880's, the latter date more likely a European influence (Elder, 1963). Based on radiocarbon evidence and age of *Libocedrus* stands, Rogers (1987) suggested a major period of deforestation in the Northern Ruahine Range by fire from 530 - 550 cal yr BP, which is thought to be from early Maori rather than volcanism (Elder, 1965).

The criteria for anthropogenic forest clearance discussed by McGlone (1983) include the decline in tall tree taxa, a sustained rise in successional vegetation (i.e. *Pteridium esculentum*), and an increase in charcoal. While the timing of this early burning event suggests that Maori were present in the area; the absence of charcoal, no significant decrease in forest taxa, no notable rise in seral taxa, and absence of *P. esculentum* in the pollen profile, suggests that Maori did not have a significant effect in the Lake Colenso catchment.

2. Climate variability

A cooler climate in New Zealand at this time is suggested by tree-ring derived temperature records (Palmer and Xiong, 2004), consistent with palynological records in the Ruahine Range. A sustained increase in *Olearia* in the West Tamaki catchment suggests a persistence of cooler and wetter climate since ~300 yr BP to present day (Lees, 1986). The reconstruction of climatic regimes from speleothem records, from eastern North Island and western South Island, suggest that the period 450 - 300 cal yr BP was particularly harsh (Lorrey *et al*., 2008). This is supported by an apparent increase in storminess as shown in lake-derived storm histories (Wilmshurst, 1997; Chester and Prior, 2004; Page *et al*., 2010), and amplified alluvial sedimentation (Grant, 1985). The $\delta^{13}C$ speleothem record from Hawke's Bay indicates that the following period (300 to 50 cal yr BP) was one of lower precipitation (Lorrey *et al*., 2008); and is also characterized by glacial advances in the Southern Alps (Schaefer *et al*., 2009; Winkler, 2010) and at Mt Taranaki (Brook *et al*., *in press*), these glacial advances are thought to be a result of change to a period of enhanced south-westerly airflow (Shulmeister *et al*., 2004).

It is apparent that climate has been variable throughout the late Holocene and that a significant cooling occurred regionally around ~396 cal yr BP, coeval with the Little Ice Age (LIA, 600 - 150 cal yr BP; Hendy *et al*., 2002), and within the Ruahine Range at least, these conditions have persisted to present day (Lees, 1986). It is possible that this is the sole factor for vegetation change in the Lake Colenso catchment. Podocarp forests, which are generally intolerable to harsh conditions, deteriorated and *Nothofagus* expanded at the initial onset of the LIA (Newnham *et al*., 1998). This led to a downwards adjustment in altitudinal vegetation patterns to take advantage of the disturbance in podocarp-hardwood forest (Newnham *et al*., 1998). Once present, *Nothofagus* tends to dominate the forest canopy as its dense growth habit creates low-light conditions, creating a difficult environment for the regeneration and growth of smaller species such as podocarps (June and Ogden, 1978), which explains the persistence of increased *Nothofagus* in the pollen profile.

3. Landscape disturbance

The active environment in the Ruahine Range provides several possible causes for forest disturbance. Disturbance events from natural causes have been recognised in many late Holocene pollen diagrams (Wilmshust *et al*., 1997), and have been attributed to a variety of factors. These include vegetation damage from cyclones (Shaw, 1983), tree damage during heavy snowfall (Grant, 1991) or drought (Grant, 1984), forest deterioration or mass movement caused by heavy rainfall or earthquakes (Marden, 1984), or burning, smothering and defoliation of vegetation from volcanism (Wilmshurst and McGlone, 1996).

An assessment of the processes of canopy regeneration suggests that forest seems to recover fairly rapidly following catastrophic destruction, and that regeneration will create a mosaic of species, as the openness of the forest will render it susceptible to other invasive species (June and Ogden, 1978). A number of possible landscape disturbance scenarios are discussed below:

- Cyclonic storms are not a major cause of disturbance to lowland podocarp/hardwood forests in the Hawke's Bay region (Wilmshurst *et al*., 1997), but are found to have caused considerable damage to forests in the Ruahine Range (Grant, 1991). The lack of correlation between erosion pulses and changes in pollen composition suggests that storms did not cause major forest disturbance in the Lake Colenso catchment during the pre-European era. While it is noted that the pollen sampling resolution is not high enough to record effects of individual storms, it is probable that the vegetational change at ~396 cal yr BP in vegetation was not caused by a single cyclone event.

- Forest damage in the Ruahine Range has been recorded from snowfall and drought (Grant, 1991), though it is difficult to reconstruct a record of this nature because there is no preservation of such changes in the

environment. Hence, there is no record of this prior to 180 cal yr BP (Grant, 1991).

- Mass movement caused by increased rainfall has been found to cause forest deterioration in the Ruahine Range (Marden, 1984; Grant, 1985). Periods of increased alluvial sedimentation triggered by increased rainfall have been studied by Grant (1985). However, he did not recognise a period of alluvial sedimentation at ~396 cal yr BP.

  There are areas of recent alluvial sedimentation in the Upper Kawhatau River and more locally in the upper Mangatera River (Tony Gates, *pers. comm.*). However these sites are not dated and a correlation with an event ~396 cal yr BP could not be made with confidence. Also, there are no storm-derived silt layers in the Lake Colenso stratigraphy at this time.

  Seismic activity is also a major cause of mass movement (discussed in section 6.1.2). Reconstructions of paleoseismicity show that there was an event at 385 cal yr BP on the northern section of the Wellington Fault (Langridge *et al*., 2007). It is possible that if mass movement from this earthquake, or a period of increased rainfall, did cause mass movement in the vicinity of Lake Colenso that *Weinmannia* (a colonizing species) and *Nothofagus fusca* would have colonized the newly exposed ground. A similar increase in *Weinmannia* at around this time was found at West Tamaki, where it is suggested that the rise was due to establishment of the species on freshly exposed ground (Lees, 1986).

- A response to volcanism in this case is unlikely as no tephras were recorded in the Lake Colenso sediment, and there were no significant events from Mt. Ruapehu (Donoghue *et al*., 1997) or other centres (Lowe *et al*., 2008) at this time.

In summary, it is difficult to conclude with any certainty the exact causes of vegetational change at Lake Colenso. It seems plausible to assume a model of an initial disturbance at ~396 cal yr BP, either caused by harsh cooling climate which would have certainly caused a downward movement of the tree-line, explaining the expansion of *Fuscaspora*, or by a geomorphic disturbance. While there is no apparent increase of *Nothofagus menziesii* at this time which would indicate a cooler climate, there is evidence from regional-wide proxies, including pollen in the Ruahine Range (Lees, 1986) and at Lake Waikaremoana (Newnham *et al*., 1998), that suggest a cooling at this time (Palmer and Xiong, 2002; Lorrey *et al*., 2008). This initial disturbance probably resulted in erosion associated with either cooling and/or increased precipitation, or an earthquake (385 cal yr BP; Langridge *et al*., 2007), would present fresh surfaces for the colonization of *Weinmannia* and *Nothofagus fusca*. While the levels of *Cyathea* are consistent over this period of change, suggesting no change in the precipitation regime, there is evidence for a drier climate around this time as indicated by Lorrey *et al*. (2008).

This mountainous Lake Colenso appears to have remained pristine and relatively isolated from human disturbance. Anthropogenic impacts at many other sites in New Zealand have tended to obscure natural variability in many late Holocene records (Wilmshurst, 1997). Hence, the site offers a rare opportunity to investigate undisturbed natural environmental change, particularly in recording the ecological response to changes in climate.

6.2.5 Lake paleoecology

Ostracods and molluscs have long been known to be indicators of past environments (Holmes, 2001), and are particularly responsive to salinity, oxygen levels, substrate and depth (Eager, 1999). An ostracod and mollusc assemblage typically shows a record of water depth, although other environmental factors that also influence water level mean it is difficult to quantify changes in lake level (Alin *et al*., 2003). However, if used with other proxies, it is possible to assess the timing and magnitude of fluctuations in the watershed. The genders of *Gomphocythere duffi* are not well understood, and so it is hard to use this information to show paleoenvironmental changes.

An absence of any ostracods and molluscs was noticeable between 427 - 87 cal yr BP (Fig. 6.2), and this zone corresponds to an increase in the percentage of sedimentary organic matter. The high organic matter concentration is a likely explanation for the absence of $CaCO_3$ matter, as degradation of organic matter releases organic acids and carbon dioxide, which lowers pH and can dissolve sedimentary carbonates (Dean, 1999), as found by Alin *et al*. (2003) and Andersson (2010).

Gomphocythere is most abundant in early summer as calcification predominantly occurs from late spring to early autumn and is found to be relatively rare in winter months (Von Grafenstein *et al*., 1999). *Penthesilenula* is present all year round but generally more abundant in late summer when reproduction is thought to occur (Von Grafenstein *et al*., 1999). So, an increase in either of these species suggests either a prolonged summer, or phase of warmer climate. The only significant increase occurs at 670 cal yr BP in both species (Fig. 5.24) which may be indicative of warmer climate. This agrees with the previously interpreted period of drier and warmer climate from 860 to 643 cal yr BP as inferred from the stable isotope values of the ostracods in this study, and warmer temperatures derived from speleothems (Williams *et al*., 2004).

An increase in oxygen content causes an increase in *Pisidium* sp. (Holopanien and Jónasson, 1983), and so this species is particularly responsive to eutrophication (Jónasson, 1972). A prolonged lack of oxygen can cause heavy mortality in *Pisidium* (Holopanien and Jónasson, 1983). Some lakes tend to have a seasonal variation in oxygen, with less oxygen during warmer periods and increased evaporation (Jónasson, 1972). So, an increase in *Pisidium novaezelandiae* is likely to represent times where oxygen supply is abundant.

6.3 Synthesis of environmental change in the Lake Colenso area

The geological history presented here provides further evidence for an early Pliocene uplift phase followed by a marine transgression during mid-late Pliocene time, and subsequent uplift and erosion of the area throughout the Quaternary. Tectonism has been and continues to be a major factor in the Ruahine Range. Results discussed here provide further understanding, not only into the paleoseismicity of the region, but also an increased understanding into the complex processes involved in the construction of a landslide-dammed lake.

The environmental history of the Lake Colenso catchment, particularly for the last 1370 years, can be divided into three distinct periods as inferred from the multi-proxy analysis (summarised in Fig. 6.5). The period from 1799 to 1370 cal yr BP is thought to be a period of wetter climate as inferred from the dominance in *Cyperaceae*, *Haloragis*, *Cyathea*, *Prumnopitys taxifolia* and *Podocarpaceae* in the pollen record. A change in the vegetation composition towards generally warmer and drier climate, or a change in landscape conditions, is apparent at 1370 cal yr BP, as suggested by the decrease in *N. menziesii*, *Halocarpus*, *Phyllocladus*, *Libocedrus* and *Cyathea* in the pollen record. This period coincides with a landslide event at 1370 cal yr BP, which blocked valley drainage and caused lake formation.

The period from 1197 to 1065 cal yr BP, is characterised by increased variability in the storm record, with storms occurring at 1185 and 1065 cal yr BP. This period also has lower precipitation as inferred from stable isotope values at 1137 and 1050 cal yr BP, and increased temperatures at 1137 cal yr BP. This period (Fig. 6.5) is coeval with the Medieval Warm Period (MWP; 1150-750 cal yr BP) as defined by Broecker (2001). Also, correlative with the warm period put forward by Williams *et al*. (2004), which is thought to result from enhanced north-easterly circulation explaining the association with an increased intensity in ENSO (Moy *et al*., 2002).

A period of quiescence followed until 860 cal yr BP. A period of drier conditions as inferred from $\delta^{13}C$ occurred from 860 to 634 cal yr BP, and a period of warmer

temperatures, as inferred from $\delta^{18}O$ from 703 to 817, and at 634 cal yr BP. Storm events occurred at 764, 690, 644 and 626 cal yr BP. Also, an increase in molluscs and ostracods is representative of a warmer climate at 670 cal yr BP. It is likely that this period of warmer climate continued until 630 cal yr BP. and is followed by a phase of seemingly stable climatic conditions. There is a short phase of warmer climate and decreased precipitation from 450 to 425 cal yr BP, as suggested by the $\delta^{18}O$ and $\delta^{13}C$ values respectively.

A distinct change towards cooler climate is apparent at 396 cal yr BP, and is shown by the increase in Fuscaspora, *Weinmannia, Coprosma*, and also the decrease in *Prumnopitys taxifolia* and *Dacrydium cupressinum*. It is likely that an initial period of harsh climate caused the primary change, and this caused or coincided with some geomorphic disturbance in the area. This is also the point at which there is no $CaCO_3$ in the sedimentary record. This cool period is coeval with the Little Ice Age (LIA, 600 - 150 cal yr BP; Hendy *et al*., 2002) (Fig. 6.5), which has been recorded in tree-ring (Palmer and Xiong, 2004) and speleothem-derived temperature records (Lorrey *et al*., 2008), glacial advances (Schaefer *et al*., 2009) and is locally supported by palynological records in the southern Ruahine Range (Lees, 1986). Lorrey *et al*. (2008) characterized this period as being influenced by a trough regime in the eastern North Island and western South Island (Lorrey *et al*., 2008), and is thought to result from enhanced westerly airflow (Shulmeister *et al*., 2004).

This apparent cooling persists to present time, and there are no records of storms from 396 to 120 cal yr BP, which correlates with findings by Lorrey *et al*. (2008), showing a period of drier climate from 300 to 50 cal yr BP. A short period of variability in the storm record is evident from 127 to -29 cal yr BP, and a departure toward warmer climate, as shown by the stable isotope values, at -8 cal yr BP during a period of seemingly cooler conditions.

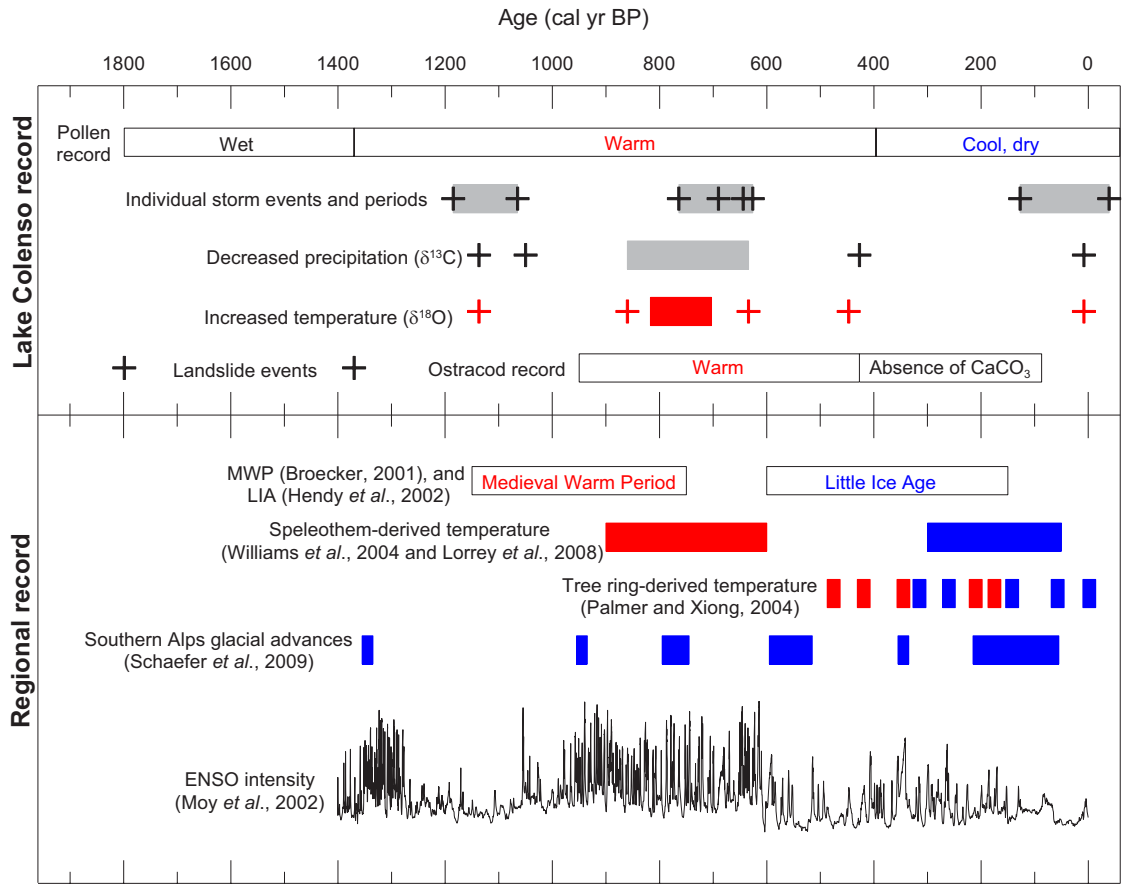

Figure 6.5. Comparison of the paleoenvironmental record at Lake Colenso against regional proxies showing change in the late Holocene. Red indicates a warm period while blue indicates cool periods, where applicable.

Lorrey *et al*. (2008) suggests that cooler periods over the late Holocene are associated with stronger westerlies, and that warm periods are linked with northerly and easterly circulation as influenced by subtropical processes. The results from Lake Colenso which show a record of environmental change on decadal to centennial timescales, confirm that climate throughout the Holocene has been highly variable (Mayewski *et al*., 2004). The record preserved at Lake Colenso is broadly synchronous with regional variability (Fig. 6.5), such as the Medieval Warm Period and Little Ice Age, and these results will aid in constraining the timing for regional climatic changes during the Late Holocene, useful for the continuing investigation into climate change in New Zealand (Alloway *et al*., 2007).

Chapter 7: Conclusion

7.1 Environmental significance

This chapter presents a summary of the main findings in this study, and also discusses potential direction for future research.

The geological history of the study area strengthens findings by Browne (1978; 2004a), showing alternating periods of subsidence and uplift throughout the Plio-Pleistocene which resulted in the deposition of Wanganui Basin sediments in the region. The correlation between separate landslide events and paleoseismic records (Hanson, 1998; Langridge *et al*., 2007) presents a further understanding into the evolution of the landslide-dammed Lake Colenso, and by inference, the paleoseismicity of the area.

Lake Colenso contains a ~1800 cal yr BP high-resolution record of environmental change. The multi-proxy approach has been beneficial in constructing a comprehensive environmental record, where various proxies have been found to respond differently to climate.

Storm periods recorded at Lake Colenso are related to the interaction between regional atmospheric circulation systems, El Niño Southern Oscillation, Southern Annular Mode and the Pacific Decadal Oscillation, and correlate with the other regional records of climate over the late Holocene, highlighting the effect of regional climatic forcing.

This study has proved valuable, particularly in the palynological record, in showing a record of natural environmental change unaffected by anthropogenic impact, which is useful in New Zealand where human impact typically obscures natural variability throughout the late Holocene (Wilmshurst, 1997).

Overall, the environmental record at Lake Colenso is characterised by broad changes that correlate to the regionally distinctive Medieval Warm Period and Little Ice Age periods. This paleoenvironmental record from an isolated site aids in constraining the timing for regional climatic changes and is a valuable resource for future paleoenvironmental reconstruction over this time period, both locally and regionally. The wide array of methods used shows potential for wider use, and the record presented here is important in its contribution to existing knowledge of the late Holocene in New Zealand.

7.2 Future research

There are four main areas for future research, which would enhance the value of this record.

Geology

Future research into the geology of the area through the identification of macroscopic shells, and also microscopic biota, such as foraminifera and pollen, would provide better association with known formations and chronological constraints.

Chronology

In most paleoenvironmental reconstructions, there are often some uncertainties associated with the chronology, particularly where events of interest are dated by interpolation. For a more accurate record of variability particularly with respect to the storms and environmental changes, it would be beneficial to obtain more dates, particularly toward the top of the record to better constrain the age model.

Stable isotope values

For a more reliable determination of paleohydrological conditions and associated fluctuations in lake levels, the study of an independent proxy such as diatoms, would provide a useful measure of lake volume and allow comparisons to be made. Paleoclimatic reconstructions based on stable isotope measurements from ostracods should ideally use multiple carapaces from each stratigraphic level, so that variability contained in the measurement of single valves is reduced (Escobar *et al.*, 2010). However, together with the information used from other proxies, results seem promising. The correlation of the temperature and precipitation record from Lake Colenso inferred from the stable isotope values with other studies highlights the potential of this method. Results from this pilot study allow only a low-resolution record of variability over the last 1370 years. A higher sampling resolution on a sub-decadal scale would allow a thorough exploration into the concept and provide more insight into the climate over the late Holocene, which would be of regional significance.

Palynology, ostracods and molluscs

Sampling for pollen at a higher resolution would prove useful to attain an in-depth record of vegetation change in response to climate variability over a period where high-resolution natural records are scarce (Schaefer *et al*., 2009).

The investigation into ostracods and molluscs, in combination with other proxies, has provided some insight to the value of this method for paleoenvironmental reconstruction. The main limitation in this study has been that the ecology of these particular species is not well understood. A study into the present day ecology could prove useful for this proxy in a paleoenvironmental context.

References

Abbott, S. T., and Carter, R. M. (1994). The sequence architecture of mid-Pleistocene (0.35-0.95 Ma) cyclothems from New Zealand: facies development during a period of known orbital control on sea-level cyclicity. In P. L. de Boer and D. G. Smith (Eds.), *Orbital Forcing and Cyclic Sequences* (pp. 367-394). International Association of Sedimentologists Special Publication 19.

Adams, J. (1981). Earthquake-dammed lakes in New Zealand. *Geology*, 9, 215-219.

Adkin, G. L. (1949). The Tararua Range as a unit of the geological structure of New Zealand. *Transactions of the Royal Society of New Zealand*, 77, 5, 260-272.

Alin, S. R., and Cohen, A. S. (2003). Lake-level history of Lake Tanganyika, East Africa, for the past 2500 years based on ostracode-inferred water-depth reconstruction. *Palaegeography, Palaeoclimatology, Palaeoecology*, 199, 1-2, 31-49.

Alloway, B. V., Lowe, D. J., Barrell, D. J. A., Newnham, R. M., Almond, P. C., and Augustinus, P. C. (2007). Towards a climate event stratigraphy for New Zealand over the past 30 000 years (NZ-INTIMATE project). *Journal of Quaternary Science,* 22, 1, 9-35.

Andersson, S., Rosqvist, G., Leng, M. J., Wastegard, S., and Blaauw, M. (2010). Late Holocene climate change in central Sweden inferred from lacustrine stable isotope data. *Journal of Quaternary Science*, 25, 8, 1305-1316.

Armon, J. W. (1974). Radiocarbon age for freshwater mussel shells from Taumutu, Lake Ellesmere, New Zealand. *New Zealand Journal of Marine and Freshwater Research*, 8, 1, 229 - 232.

Aston, B. C. (1914). Notes on the Phanerogamic flora of the Ruahine mountain chain, with a list of the plants observed thereon. *Transactions and Proceedings of the New Zealand Institute*, 46, 40-54.

Augustinus, P., Bleakley, N., Deng, Y., Shane, P., and Cochran, U. (2008). Rapid change in early Holocene environments inferred from Lake Pupuke, Auckland City, New Zealand. *Journal of Quaternary Science*, 23, 5, 435-447.

Augustinus, P., Reid, M., Andersson, S., Deng, Y., and Horrocks, M. (2006). Biological and geochemical record of anthropogenic impacts in recent sediments from Lake Pupuke, Auckland City, New Zealand. *Journal of Paleolimnology*, 35, 4, 789-805.

Barclay, M. H. (1968). Additions to the freshwater ostracod fauna of New Zealand. *New Zealand Journal of Marine and Freshwater Research*, 2, 67–80.

Beanland, S., and Berryman, K. R. (1991) Paleoseismicity of the Wellington Fault northeast of the Tararua Ranges. *Geological Society of New Zealand Newsletter*, 93, 42-46.

Beanland, S., Melhuish, A., Nicol, A., and Ravens, J. (1998). Structure of the inner forearc region, Hikurangi subduction margin, New Zealand, from seismic reflection and outcrop data. *New Zealand Journal of Geology and Geophysics*, 41, 325-342.

Belis, C. A., Finsinger, W., and Ammann, B. (2008). The late glacial-Holocene transition as inferred from ostracod and pollen records in the Lago Piccolo di Avigliana (Northern Italy). *Palaeogeography, Palaeoclimatology, Palaeoecology*, 264, 3-4, 306-317.

Berryman, K. (1990). Late Quaternary movement on the Wellington Fault in the Upper Hutt area, New Zealand. *New Zealand Journal of Geology and Geophysics*, 33, 2, 257-270.

Best, E. (1912). Nga whawhai o Mokai-Patea [The wars at Mokai-Patea]. *The Journal of the Polynesian Society*, 21, 3, 89-89.

Beu, A.G. (1995). *Pliocene limestones and their scallops: lithostratigraphy, pectinid biostratigraphy and paleogeography of eastern North Island Late Neogene limestone* (Institute of Geological and Nuclear Sciences monograph 10; New Zealand Geological Survey paleontological bulletin 68). Lower Hutt: Institute of Geological and Nuclear Sciences.

Beu, A. G., Browne, G. H., and Grant-Taylor, T. L. (1981). New *Chlamys delicatula* localities in the Central North Island and uplift of the Ruahine Range. *New Zealand Journal of Geology and Geophysics*, 24, 1, 127-132.

Beu, A. G., and Maxwell, P. A. (1990). *Cenozoic Mollusca of New Zealand*. Lower Hutt: New Zealand Geological Survey.

Boomer, I. (2002). Environmental Applications of Marine and Freshwater Ostracoda. In S. K. Haslett (Ed.), *Quaternary Environmental Micropalaeontology* (pp. 138-155). New York: Oxford University Press.

Broecker, W. S. (2001). Was the Medieval Warm Period Global? *Science*, *291*, 5508, 1497-1499.

Bronk Ramsey, C. (2001). Development of the radiocarbon calibration program OxCal. *Radiocarbon*, 43, 2A, 355-363.

Brook, M. S., Neall, V. E., Stewart, R. B., Dykes, R. C., and Birks, D. L. (*in press*). Recognition and Paleoclimatic implications of Late Holocene glaciation on Mt Taranaki, North Island, New Zealand. *The Holocene*.

Browne, G. H. (1978). Wanganui strata of the Mangaohane Plateau, northern Ruahine Range, Taihape. *Tane*, 24, 199-210.

Browne, G. H. (2004a). Late Neogene sedimentation adjacent to the tectonically evolving North Island axial ranges: Insights from Kuripapango, western Hawke's Bay. *New Zealand Journal of Geology and Geophysics*, 47, 4, 663-674.

Browne, G. H. (2004b). The Miocene-Pliocene interior seaway of the central North Island: sedimentary patterns and tectonic styles in the Kuripapango Strait (pp. 89-109). *Field trip guide: Geological Society of New Zealand Miscellaneous Publication 117B*.

Brownsey, P. J., and Smith-Dodsworth, J. C. (1989). *New Zealand ferns and allied plants*. Auckland: David Bateman.

Bureau of Meteorology: Australian Government. (2011). *SOI graph and archives*. Retrieved March 8, 2011 from http://www.bom.gov.au/climate.

Chapman, M. A. (1963). A Review of the Freshwater Ostracods in New Zealand. *Hydrobiologia*, 22, 1-40.

Chester, P.I., and Prior, C.A. (2004). An AMS ^{14}C pollen-dated sediment and pollen sequence from the late Holocene at Round Lake, southern coastal Hawkes Bay. *Radiocarbon*, 46, 2, 721-731.

Colenso, W. (1884). *In memoriam: an account of visits to and crossings over, the Ruahine mountain range, New Zealand, and of the natural history of that region*. Napier: Daily Telegraph.

Cook, E. R., Buckley, B. M., Palmer, J. G., Fenwick, P., Peterson, M. J., and Boswijk, G. (2006). Millennia-long tree-ring records from Tasmania and New Zealand: a basis for modelling climate variability and forcing, past, present and future. *Journal of Quaternary Science*, 21, 7, 689-699.

Cook, E. R., Palmer, J. G., and D'Arrigo, R. D. (2002). Evidence for a 'Medieval Warm Period' in a 1,100 year tree-ring reconstruction of past austral summer temperatures in New Zealand. *Geophysical Research Letters*, 29, 14, 1667, 12-1 – 12-4.

Costa, J. E., and Schuster, R. L. (1988). The formation and failure of natural dams. *Geological Society of America Bulletin*, 100, 1054-1068.

Cotton, C. S. (1916). Fault coasts in New Zealand. *Geographical Review*, 1 (1), 20-47.

Crozier, M. J. (1997). The climate–landslide couple: a Southern Hemisphere perspective. In Matthews, J. A., Brunsden, D., Frenzel, B., Gläser, B., and Weib, M. M. (Eds.), *Rapid mass movement as a source of climatic evidence for the Holocene* (pp. 333-354). Stuttgart: Gustav Fischer.

Cunningham, A. (1979). A century of change in the forests of the Ruahine Range, North Island, New Zealand: 1870-1970. *New Zealand Journal of Ecology*, 2, 11-21.

Cunningham, A., and Stribling, P. W. (1978). *The Ruahine Range* (Water and Soil Technical Publication No. 13). Wellington: National Water and Soil Conservation Organisation and New Zealand Forest Service.

Daly, B. K. (2000). *Total/Organic Carbon Measurement & Carbonate and the affect of shells or limestone on LECO-C measurements* (Validation Report No. 1 for Methods 114 & 152). Landcare Research: Palmerston North.

De Rose, R.C., Gomez, B., Marden, M., and Trustrum, N.A. (1998). Gully erosion in Mangatu Forest, New Zealand, estimated from digital elevation models. *Earth Surface Processes and Landforms*, 23, 1045-1053.

D'Arrigo, R., and Wilson, R. (2006), On the Asian expression of the PDO. *International Journal of Climatology*, 26, 1607–1617.

Dean, W. E. (1999). The carbon cycle and biogeochemical dynamics in lake sediments. *Journal of Paleolimnology*, 21, 4, 375-393.

Department of Conservation. (2008). *Western Ruahine Forest Park*. Retrieved February 18, 2010 from http://www.doc.govt.nz/parks-and-recreation/places-to-visit/manawatu-whanganui/manawatu-area/western-ruahine-forest-park/features/

Deshayes, G. P. (1854). Descriptions of twenty new species of the genus Cardita from the collection of Hugh Cuming, Esq. *Proceedings of the Zoological Society of London*, 20, 100-103.

Dodson, J. R. (1976). Modern pollen spectra from Chatham Island, New Zealand. *New Zealand Journal of Botany*, 14, 341-347.

Donoghue, S. L., and Neall, V. E. (1996). Tephrostratigraphic studies at Tongariro Volcanic Centre, New Zealand: An overview. *Quaternary International*, 34-36, 13-20.

Donoghue, S. L., Neall, V. E., and Palmer, A. S. (1995). Stratigraphy and chronology of late Quaternary andesitic tephra deposits, Tongariro Volcanic Centre, New Zealand. *Journal of the Royal Society of New Zealand*, 25, 2, 115-206.

Donoghue, S. L., Neall, V. E., Palmer, A. S., and Stewart, R. B. (1997). The volcanic history of Ruapehu during the past 2 millennia based on the record of Tufa Trig tephras. *Bulletin of Volcanology*, 59, 2, 136-146.

Eager, S. H. (1971). A checklist of *Ostracoda* of New Zealand. *Journal of the Royal Society of New Zealand*, 1, 53–64.

Eager, S. H. (1999). Distribution of *Ostracoda* around a coastal sewer outfall: a case study from Wellington, New Zealand. *Journal of the Royal Society of New Zealand*, 29, 257-264.

Eden, D. N., and Page, M. J. (1998). Palaeoclimatic implications of a storm erosion record from late Holocene lake sediments, North Island, New Zealand. *Palaeogeography, Palaeoclimatology, Palaeoecology*, 139, 1-2, 37-58.

Elder, N. L. (1962). Vegetation of the Kaimanawa ranges. *Transactions of the Royal Society of New Zealand*, 2, 1, 1-37.

Elder, N. L. (1963). Evidence of climatic change from the vegetation of the North Island. *Proceedings of the New Zealand Ecological Society*, 45-48.

Elder, N. L. (1965). Vegetation of Ruahine Range: An introduction. *Transactions of the Royal Society of New Zealand*, 3, 3, 13-66.

Erdman, C. F., and Kelsey, H. M. (1992). Pliocene and Pleistocene stratigraphy and tectonics, Ohara Depression and Wakarara Range, North Island, New Zealand. *New Zealand Journal of Geology and Geophysics*, 35, 177-192.

Escobar, J., Curtis, J., Brenner, M., Hodell, D., and Holmes, J. (2010). Isotope measurements of single ostracod valves and gastropod shells for climate reconstruction: evaluation of within-sample variability and determination of optimum sample size. *Journal of Paleolimnology*, 43, 4, 921-938.

Faegri, K., and Iversen, J. (1989). *Textbook of Pollen analysis*. New York: John Wiley and Sons.

Finsinger, W., Belis, C., Blockley, S., Eicher, U., Leuenberger, M., and Lotter, A. (2008). Temporal patterns in lacustrine stable isotopes as evidence for climate change during the late glacial in the Southern European Alps. *Journal of Paleolimnology*, 40, 3, 885-895.

Feldmeyer, A. E., Jones, B. C., and Firth, J. (1943). *Geology of the Palmerston—Wanganui Basin, "West Side"* Wellington: Institute of Geological and Nuclear Sciences.

Fleming, C. A. (1953). *The geology of Wanganui Subdivision* (New Zealand Geological Survey bulletin 52). Wellington: New Zealand Geological Survey.

Fogt, R. L., Perlwitz, J., Monaghan, A. J., Bromwich, D. H., Jones, J. M., and Marshall, G. J. (2009). Historical SAM Variability. Part II: 20th century variability and trends from reconstructions, observations, and the IPCC AR4 Models. *Journal of Climate*, 22, 5346–5365.

Froggatt, P. C. (1983). Toward a comprehensive upper Quaternary tephra and ignimbrite stratigraphy in New Zealand using electron microprobe analysis of glass shards. *Quaternary Research*, 19, 2, 188-200.

Froggatt, P. C., and Gosson, G. J. (1982). *Techniques for the preparation of tephra samples for mineral and chemical analysis and radiometric dating*. Wellington: Victoria University.

Froggatt, P. C., and Rogers, G. M. (1990). Tephrostratigraphy of high altitude peat bogs along the axial ranges. *New Zealand Journal of Geology and Geophysics*, 33, 111-124.

Fry, B., and Sherr, E. B. (1984). $\delta^{13}C$ measurements as indicators of carbon flow in marine and freshwater ecosystems. *Contributions in Marine Science*, 27, 13-47.

Gedalof, Z., Mantua, N. J., and Peterson, D. L. (2002). A multi-century perspective of variability in the Pacific Decadal Oscillation: new insights from tree rings and coral. *Geophysical Research Letters*, 29, 24, 2204.

Gellatly, A. F., Chinn, T. J. H., and Rothlisberger, F. (1988). Holocene glacier variations in New-Zealand: a review. *Quaternary Science Reviews*, 7, 2, 227-242.

Geological and Nuclear Science. (2010). *Geological Map of New Zealand*. Retrieved 4 March, 2010 from http://data.gns.cri.nz/geoatlas.

Gillett, N. P., Kell, T. D., and Jones, P. D. (2006). Regional climate impacts of the Southern Annular Mode. *Geophysical Research Letters*, 33, 23, L23704.

Goldin, A. (1987). Reassessing the use of loss-on-ignition for estimating organic matter content in noncalcareous soils. *Communications in Soil Science and Plant Analysis*, 18, 10, 1111 - 1116.

Grant, P. J. (1983). *Recently increased erosion and sediment transport rates in the upper Waipawa River basin, Ruahine Range*. Palmerston North: Ministry of Works and Development.

Grant, P. J. (1984). Drought effect on high-altitude forests, Ruahine Range, North Island, New Zealand. *New Zealand Journal of Botany*, 22, 1, 15-27.

Grant, P. J. (1985). Major periods of erosion and alluvial sedimentation in New Zealand during the Late Holocene. *Journal of the Royal Society of New Zealand,* 15, 67-121.

Grant, P. J. (1989). Effects on New Zealand Vegetation of Late Holocene Erosion and Alluvial Sedimentation. *New Zealand Journal of Ecology*, 12, 131-144.

Grant, P. J. (1991). Disturbance in the forests of the Ruahine Range since 1770. *Journal of the Royal Society of New Zealand*, 21, 4, 385-404.

Grant, P. J. (1996). *Forests of Yesterday*. Wellington. P. J. Grant.

Grant, P. J., Hawkins, N. V., and Christie, W. (1978). *Rainfalls and floods of Cyclone Alison, March 1975, on the north-eastern Ruahine Range* (Water and Soil Miscellaneous Publication, No. 1). Wellington: Ministry of Works and Development.

Gray, J. E. (1834). Catalogue of the species of Molluscs & their shells, which have hitherto been recorded as found at New Zealand, with the description of some lately discovered species on the fossil shells from New Zealand. In E. Dieffenbach (Ed.). *Travels in New Zealand; with contributions to the geography, geology, botany and natural history of that country* (pp. 228-265). Volume 2. London: John Murray.

Grimm, E. C. (1987). CONISS: a FORTRAN 77 program for stratigraphically constrained cluster analysis by the method of incremental sum of squares. *Computers and GeoSciences*, 13, 1, 13-35.

Hancox, G. T. and Perrin, N. D. (1994). Green Lake landslide: a very large ancient rock slide in Fiordland, New Zealand. In R. Oliveira, L. F. Rodrigues, A. G Ceolho, and A. P. (Eds.) *Proceedings Seventh International Congress International Association of Engineering Geology*, 5–9 September 1994, Lisboa, Portugal, 1677–1689.

Hancox, G. T., Perrin, N. D., and Dellow, G. D. (1997*). Earthquake-induced landsliding in New Zealand and implications for MM intensity and seismic hazard assessment* (Client Report 43601B). Lower Hutt: Institute of Geological and Nuclear Sciences.

Hanson, J. A. (1998). *The neotectonics of the Wellington and Ruahine faults between the Manawatu Gorge and Puketitiri, North Island, New Zealand*. Unpublished doctoral thesis, Massey University, Palmerston North, New Zealand.

Hayward, B. W., Wilson, K., Morley, M. S., Cochran, U., Grenfell, H. R., and Sabaa, A. T. (2010). Microfossil record of the Holocene evolution of coastal wetlands in a tectonically active region of New Zealand. *The Holocene*, 20, 3, 405-421.

Heiri, O., Lotter, A. F., and Lemcke, G. (2001). Loss on ignition as a method for estimating organic and carbonate content in sediments: reproducibility and comparability of results. *Journal of Paleolimnology*, 25, 1, 101-110.

Hendy, E. J., Gagan, M. K., Alibert, C. A., McCulloch, M. T., Lough, J. M., and Isdale, P. J. (2002). Abrupt decrease in tropical Pacific Sea surface salinity at end of Little Ice Age. *Science*, 295, 5559, 1511-1514.

Hicks, D. L. (1989). *Some ways to estimate the frequency of erosion-inducing rainfall*. Lower Hutt; Department of Scientific and Industrial Research, Land and Soil Science.

Holmes, J. A. (1998). A late Quaternary ostracod record from Wallywash Great Pond, a Jamaican marl lake. *Journal of Paleolimnology*, 19, 2, 115-128.

Holmes, J. A. (2001). Ostracoda. In J. P. Smol, H. J. B. Birks and W. M. Last (Eds.), *Tracking Environmental Change using Lake Sediments* (Volume 4: Zoological Indicators (pp 125-152). Dordrecht: Kluwer Academic Publishers.

Holopainen, I. J., and Jónasson, P. M. (1983). Long-term population-dynamics and production of Pisidium (bivalvia) in the profundal of Lake Esrom, Denmark. *Oikos*, 41, 1, 99-117.

Hornibrook, N. de B. (1955). Ostracoda in the deposits of the Pyramid Valley swamp. *Records of the Canterbury Musuem. 6*, 4*,* 267-277.

Horrocks, M., and Ogden, J. (1998). The Effects of the Taupo Tephra Eruption of c. 1718 BP on the Vegetation of Mt Hauhungatahi, Central North Island, New Zealand. *Journal of Biogeography*, 25, 4, 649-660.

Hubbard, C. B., and Neall, V. E. (1980). A reconstruction of late Quaternary erosional events in the West Tamaki River catchment, southern Ruahine Range, North Island, New Zealand. *New Zealand Journal of Geology and Geophysics*, 23, 5-6, 587-593.

Hull, A. G. (1983). *Trenching of the Mohaka Fault near Hautapu River, Hawkes Bay*. (Report number 831/26). Wellington: New Zealand Geological Survey.

Hutton, F. W. (1873). *Catalogue of the Marine Mollusca of New Zealand, with diagnoses of the species*. Wellington: Government Printer.

Jacobson, G. L., and Bradshaw, R. H. W. (1981). The selection of sites for paleovegetational studies. *Quaternary Research*, 16, 1, 80-96.

James, I. L. (1973). Mass Movements in the Upper Pohangina Catchment, Ruahine Range. *Journal of Hydrology*, 12, 2, 92-102.

Jónasson, P. M. (1972). Ecology and production of the profundal benthos. *Oikos*, *14*, 1-148.

Jouzel, J., Masson-Delmotte, V., Cattani, O., Dreyfus, G., Falourd, S., Hoffmann, G., Minster, B., Nouet, J., Barnola, J. M., Chappellaz, J., Fischer, H., Gallet, J. C., Johnsen, S., Leuenberger, M., Loulergue, L., Luethi, D., Oerter, H., Parrenin, F., Raisbeck, G., Raynaud, D., Schilt, A., Schwander, J., Selmo, E., Souchez, R., Spahni, R., Stauffer, B., Steffensen, J. P., Stenni, B., Stocker, T. F., Tison, J. L., Werner, M., and Wolff. E. W. (2007). Orbital and Millennial Antarctic Climate Variability over the Past 800,000 Years. *Science*, 317, 5839, 793-797.

June, S. R. and J. Ogden (1978). Studies on the vegetation of Mount Colenso, New Zealand. 4. An assessment of the processes of canopy maintenance and regeneration in a red beech (*Nothofagus fusca*) forest. *New Zealand Journal of Ecology*, 1, 7-15.

Katz, H. R. (1979). Alpine uplift and subsidence of foredeeps. In R. I. Walcott, and M. M. Cresswell (Ed.). The origin of the Southern Alps. *Bulletin of the Royal Society of New Zealand*, 18, 121-130.

Keatings, K., Hawkes, I., Holmes, J., Flower, R., Leng, M., and Abu-Zied, R. (2007). Evaluation of ostracod-based palaeoenvironmental reconstruction with instrumental data from the arid Faiyum Depression, Egypt. *Journal of Paleolimnology*, 38, 2, 261-283.

Kingma, J. T. (1959). The Tectonic History of New Zealand. *Ibid*, 2, 1-55.

Kingma, J. T. (1962). *Sheet 11 Dannevirke* (Geological Map of New Zealand 1:250000; 1st ed.). Wellington: Department of Scientific and Industrial Research.

Korup, O. K. (2002). Recent research on landslide dams: a literature review with special attention to New Zealand. *Progress in Physical Geography*, 26, 2, 206-235.

Lamb, S. H., and Vella, P. (1987). The last million years of deformation in part of the New Zealand plate boundary zone. *Journal of Structural Geology*, 19, 877-891.

Land Information New Zealand (2010). *Aerial Images and Orthophotos*. Retrieved November 18, 2010 from http://www.linz.govt.nz/topography/aerial-image/index.aspx.

Landridge, R. M., Berryman, K. R., and Van Dissen, R. J. (2005). Defining the geometric segmentation and Holocene slip rate of the Wellington Fault, New Zealand: The Pahiatua section. *New Zealand Journal of Geology and Geophysics*, 48, 4, 591-607.

Langridge, R. M., Berryman, K. R., and Van Dissen, R. J. (2007). Late Holocene paleoseismicity of the Pahiatua section of the Wellington Fault, New Zealand. *New Zealand Journal of Geology and Geophysics*, 50, 3, 205-226.

Large, M. F., and Braggins, J. E. (1991). Spore atlas of New Zealand ferns and fern allies. *New Zealand Journal of Botany*, 21, 1-168.

Le Maitre, R.W. (1984). A proposal by the IUGS Subcommission on the Systematics of Igneous Rocks for a chemical classification of volcanic rocks based on the total alkali silica (TAS) diagram. *Australian Journal of Earth Sciences*, 31, 243–255.

Leathwick, J. R., and Whitehead, D. (2001). Soil and atmospheric water deficits and the distributions of New Zealand's indigenous tree species. *Functional Ecology*, 15, 233-242.

Lees, C. M. (1981). *Some Aranuian (postglacial) organic deposits in the south eastern Ruahine Range, North Island, New Zealand, investigated by*

palynological methods. Unpublished masterate thesis. Massey University, Palmerston North, New Zealand.

Lees, C. M. (1986). Late Quaternary palynology of the southern Ruahine Range, North Island, New Zealand. *New Zealand Journal of Botany*, 24, 2, 315-329.

Li, H. C., and Ku, T. L. (1997). $\delta^{13}C$-$\delta^{18}O$ covariance as a paleohydrological indicator for closed-basin lakes. *Palaeogeography Palaeoclimatology Palaeoecology*, 133, 1-2, 69-80.

Li, H. -C., Ku, T. -L., Stott, L. D., and Anderson, R. F. (1997). Stable Isotope Studies on Mono Lake (California). $\delta^{18}O$ in Lake Sediments as a Proxy for Climatic Change During the Last 150 Years. *Limnology and Oceanography*, 42, 2, 230-238.

Lillie, A. R. (1953). *The Geology of the Dannevirke Subdivision* (New Zealand Geological Survey Bulletin no. 46). Wellington: Department of Scientific and Industrial Research.

Livingston, M. E., Biggs, B. J., and Gifford, J. S. (1986). *Inventory of New Zealand lakes*. Wellington: Water and Soil miscellaneous publication.

Loizeau, J. -L., Arbouille, D., Santiago, S., and Vernet, J. -P. (1994). Evaluation of a wide range laser diffraction grain size analyser for use with sediments. *Sedimentology*, 41, 2, 353-361.

Lorrey, A., Fowler, A. M., and Salinger, J. (2007). Regional climate regime classification as a qualitative tool for interpreting multi-proxy palaeoclimate data spatial patterns: A New Zealand case study. *Palaeogeography Palaeoclimatology Palaeoecology*, 253, 3-4, 407-433.

Lorrey, A., Williams, P., Salinger, J., Martin, T., Palmer, J., and Fowler, A. (2008). Speleothem stable isotope records interpreted within a multi-proxy framework and implications for New Zealand palaeoclimate reconstruction. *Quaternary International*, 187, 52-75.

Lowe, D. J., and Green, J. D. (1987). Origins and development of the lakes. In A. B. Viner. *Inland Waters of New Zealand*. DSIR Bulletin, 241, 1-164.

Lowe, D. J., and Green, J. D. (1992). Lakes. In J. M. Soons and M. J. Selby (Eds.). *Landforms of New Zealand* (2nd ed.)(pp. 107-143). Auckland. Longman Paul.

Lowe, D. J., Shane, P. A. R., Alloway, B. V., and Newnham, R. M. (2008). Fingerprints and age models for widespread New Zealand tephra marker beds erupted since 30,000 years ago: a framework for NZ-INTIMATE. *Quaternary Science Reviews*, 27, 1-2 95-126.

Lowe, J. L. and Walker, M. (1997). *Reconstructing Quaternary environments* (2nd ed.). New Jersey: Prentice Hall.

Lusk, C. H., and Ogden, J. (1992). Age structure and dynamics of a podocarp-broadleaf forest, Tongariro National Park, New Zealand. *Journal of Ecology* 80, 379–393.

MacDonald, G. M., and Case, R. A. (2005). Variations in the Pacific Decadal Oscillation over the past millennium. *Geophysical Research Letters*, 32, 8, L08703.

Mantua, N. J., Steven, R. H., Zhang, Y., Wallace, J. M., and Francis, R. C. (1997). A Pacific interdecadal climate oscillation with impacts on salmon production. *Bulletin of the American Meteorological Society*, 78, 1069-1079.

Marden, M. (1984). *Geology and Its Relationship to Erosion in the Southern Ruahine Range, North Island, New Zealand*. Unpublished doctoral thesis, Massey University, Palmerston North, New Zealand.

Mayewski, P. A., Rohling, E. E., Stager, J. C., Karlén, W., Maasch, K. A., Meeker, L. D., Meyerson, E. A., Gasse, F., van Kreveld, S., Holmgren, K., Lee-Thorpe, J., Rosqvist, G., Rack, F., Staubwasser, M., Schneider, R. R., and Steig, E. J. (2004). Holocene climate variability. *Quaternary Research*, 62, 243–255.

McCormac, F. G., Hogg, A. G., Blackwee, P. G., Buck, C. C., Higham, T. F. G., and Reimer, P. J. (2004). SHCAL04 Southern Hemisphere calibration, 0–11.0 cal kyr BP. *Radiocarbon*, 46, 3, 1087-1092.

McGlone, M. S. (1983). Holocene pollen diagrams, Lake Rotorua, North Island, New Zealand. *Journal of the Royal Society of New Zealand*, 13, 53-65.

McGlone, M. S., and Moar, N. T. (1977). The Ascarina decline and post-glacial climatic change. *New Zealand Journal of Botany*, 15, 485-489.

McGlone, M. S., Salinger, M. J., and Moar, N. T. (1993). Palaeovegetation studies of New Zealand's climate since the Last Glacial Maximum. In H. E. Wright, J. E. Kutzbach, I. T. Webb, W. F. Ruddiman, F. A. Street-Perrott, and P. J. Bartlein (Eds.), *Global Climates Since the Last Glacial Maximum* (pp. 294-317). Minneapolis: University of Minnesota Press.

McGlone, M. S., and Topping, W. W. (1977). Aranuian (post-glacial) pollen diagrams from the Tongariro region, North Island, New Zealand. *New Zealand Journal of Botany*, 15, 749-760.

McGlone, M. S., and Topping, W. W. (1983). Late Quaternary vegetation, Tongariro region, central North Island, New Zealand. *New Zealand Journal of Botany*, 21, 53–76.

McGlone, M. S., and Wilmshurst, J. M. (1999). Dating initial Maori environmental impacts in New Zealand. *Quaternary International*, 59, 5-16.

McFadgen, B. G. (1985). Late Holocene stratigraphy of coastal deposits between Auckland and Dunedin, New Zealand. *Journal of the Royal Society of New Zealand*, 15, 27-65.

McFadgen, B. G. (1989). Late Holocene depositional episodes in coastal New Zealand. *New Zealand Journal of Ecology*, 12, 145-149.

McIntyre, A. P., and Kamp, P. J. J. (1998). Late Pliocene (2.8 -2.4 Ma) cyclothemic shelf deposits, Parikino, Wanganui Basin, New Zealand: Lithostratigraphy and correlation of cycles. *New Zealand Journal of Geology and Geophysics*, 41, 1, 69-84.

McKay, A. (1892). *On the Geology of Marlborough and South-east Nelson*. Wellington: New Zealand Geological Survey Report.

McKelvey, R. J., and Murton, K. (1992). Landslide damage on the east-coast region arising from tropical Cyclone Bola, March 1988. Rotterdam: Balkema.

McKenzie, J. A. (1985). Carbon isotopes and productivity in the lacustrine and marine environment. In W. Stumm (Ed.), *Chemical processes in lakes* (pp. 99-118). New Jersey: Wiley.

McLaren, P. (1981). An interpretation of trends in grain size measures. *Journal of Sedimentary Research*, 51, 2, 611-624.

Meyers, P. A. (2003). Applications of organic geochemistry to paleolimnological reconstructions: a summary of examples from the Laurentian Great Lakes. *Organic Geochemistry*, 34, 2, 261-289.

Meyers, P. A., and Lallier-Vergés, E. (1999). Lacustrine Sedimentary Organic Matter Records of Late Quaternary Paleoclimates. *Journal of Paleolimnology*, 21, 3, 345-372.

Mildenhall, D. C. (1976). Exotic pollen rain on the Chatham Islands during the late Pleistocene. *New Zealand Journal of Geology and Geophysics*, 19, 327-333.

Mischke, S., Aichner, B., Diekmann, B., Herzschuh, U., Plessen, B., and Wünnemann, B., (2010). Ostracods and stable isotopes of a late glacial and Holocene lake record from the NE Tibetan Plateau. *Chemical Geology*, 276, 1-2, 95-103.

Mischke, S., and Holmes, J. A. (2008). Applications of lacustrine and marginal marine Ostracoda to palaeoenvironmental reconstruction. *Palaeogeography, Palaeoclimatology, Palaeoecology,* 264, 3-4, 211-212.

Moar, N.T. (1956). Peat on Mokai Patea, Ruahine Range, North Island, New Zealand. *New Zealand Journal of Science and Technology*, 37, 419-426.

Moar, N. T. (1961). Contributions to the Quaternary history of the New Zealand flora: 4. Pollen diagrams from the Western Ruahine Ranges. *New Zealand Journal of Science,* 4, 350-359.

Moar, N. T. (1967). Contributions to the Quaternary history of the New Zealand flora: 5. Pollen diagrams from No Man's Land bog, Northern Ruahine Ranges. *New Zealand Journal of Botany*, 5, 394-399.

Moar, N. T. (1969). Possible long-distance transport of pollen to New Zealand. *New Zealand Journal of Botany*, 7, 424-426.

Moar, N. T. (1993). *Pollen grains of New Zealand dicotyledonous plants*. Lincoln: Manaaki Whenua Press.

Moebis, A. (2010). *Understanding the Holocene explosive eruption record of the Tongariro Volcanic Centre, New Zealand*. Unpublished doctoral thesis, Massey University, Palmerston North, New Zealand.

Moore, L. B., and Edgar, E. (1976). Flora of New Zealand: Volume 2. Wellington: Government Printer.

Moy, C. M., Dunbar, R. B., Moreno, P. I., Francois, J.-P., Villa-Martínez, R., and Mucciarone, D. M. (2008). Isotopic evidence for hydrologic change related to the westerlies in SW Patagonia, Chile, during the last millennium. *Quaternary Science Reviews*, 27, 13-14, 1335-1349.

Moy, C. M., Seltzer, G. O., Rodbell, D. T., and Anderson, D. M. (2002). Variability of El Nino/Southern Oscillation activity at millennial timescales during the Holocene epoch. *Nature*, 420, 6912, 162-165.

Murray, M. R. (2002). Is laser particle size determination possible for carbonate-rich lake sediments? *Journal of Paleolimnology*, 27, 2, 173-183.

National Institute of Water and Atmospheric research (2011). *The National Climate Database*. Retrieved February 20, 2011 from http://cliflo.niwa.co.nz.

Newnham, R. M., Lowe, D. J., and Matthews, B. W. (1998). A late-Holocene and prehistoric record of environmental change from Lake Waikaremoana, New Zealand. *The Holocene*, 8, 4, 443-454.

Newnham, R. M., Lowe, D. D., and Williams, P. P. (1999). Quaternary environmental change in New Zealand: a review. *Progress in Physical Geography*, 23, 4, 567-610.

Newnham, R. M., Vandergoes, M. J., Garnett, M., Lowe, D. J., Prior, C., and Almond, P. C. (2007). Test of AMS 14C dating of pollen concentrates using tephrochronology. *Journal of Quaternary Science*, 22, 37-51.

Olsson, I. U. (1991). Accuracy and precision in sediment chronology. *Hydrobiologia*, 214, 25-34.

Orpin, A. R., Carter, L., Page, M. J., Cochran, U. A., Trustrum, N. A., and Gomez, B. (2010). Holocene sedimentary record from Lake Tutira: A template for upland watershed erosion proximal to the Waipaoa Sedimentary System, northeastern New Zealand. *Marine Geology*, 270, 1-4, 11-29.

Orpin, A. R., Gammon, P. R., Naish, T. R., and Carter, R. M. (1998). Modern and ancient Zygochlamys delicatula shellbeds in New Zealand, and their sequence stratigraphic implications. Sedimentary *Geology*, 122, 1-4, 267-284.

Page, M. J., Trustrum, N. A., and De Rose, R. C. (1994a). A high resolution record of storm-induced erosion from lake sediments, New Zealand. *Journal of Paleolimnology*, 11, 3, 333-348.

Page, M. J., Trustrum, N. A., and Dymond, J. R. (1994b). Sediment budget to assess the geomorphic effect of a cyclonic storm, New Zealand. *Geomorphology*, 9, 3, 169-188.

Page, M. J., and Trustrum, N. A. (1997). A late Holocene lake sediment record of the erosion response to land use change in a steepland catchment, New Zealand. *Zeitschrift für Geomorphologie*, 41, 369–392.

Page, M. J., Trustrum, N. A., Orpin, A. R., Carter, L., Gomez, B., and Cochran, U. A. (2010). Storm frequency and magnitude in response to Holocene climate variability, Lake Tutira, North-Eastern New Zealand. *Marine Geology*, 270, 1-4, 30-44.

Palmer, J. G., and Xiong, L. M. (2004). New Zealand climate over the last 500 years reconstructed from Libocedrus bidwillii Hook. f. tree-ring chronologies. *The Holocene*, 14, 2, 282-289.

Peng, Y., Xiao, J., Nakamura, T., Liu, B., and Inouchi, Y. (2005). Holocene East Asian monsoonal precipitation pattern revealed by grain-size distribution of core sediments of Daihai Lake in Inner Mongolia of north-central China. *Earth and Planetary Science Letters*, 233, 3-4, 467-479.

Perrin, N. D. and Hancox, G. T. 1992: Landslide-dammed lakes in New Zealand preliminary studies on their distribution, causes and effects. In Bell, D.H., (Ed.) *Landslides. Glissements de terrain. Proceedings of the Sixth International Symposium, 10–14 February 1992, Christchurch, 1457–1466.*

Petit, J. R., Jouzel, J., Raynaud, D., Barkov, N. I., Barnola, J. M., Basile, I., Bender, M., Chappellaz, J., Davis, J., Delaygue, G., Delmotte, M., Kotlyakov, V. M., Legrand, M., Lipenkov, V., Lorius, C., Pépin, L., Ritz, C., Saltzman, E., and Stievenard, M. (1999). Climate and Atmospheric History of the Past 420,000 years from the Vostok Ice Core, Antarctica. *Nature*, 399, 429-436.

Platz, T., Cronin, S. J., Smith, I. E. M., Turner, M. B., and Stewart, R. B. (2007). Improving the reliability of microprobe-based analyses of andesitic glasses for tephra correlation. *The Holocene*, 17, 5, 573-583.

Pocknall, D. T. (1981). Pollen morphology of the New Zealand species of Dacrydium solander, Podocarpus L'Heritier, and Dacrycarpus endlicher (Podocarpaceae). *New Zealand Journal of Botany*, 19, 67-95.

Prime, J. (1862) *Pisidium novaezelandiae*. In Beu, A. G., and Maxwell, P. A. (1990). *Cenozoic Mollusca of New Zealand*. Lower Hutt: New Zealand Geological Survey.

Read, S. A. L., Beetham, R. D., and Riley, P. B. (1992). Lake Waikaremoana barrier-a large landslide dam in New Zealand. In D. H. Bell (ed.), *Landslides* (pp. 1481-1487). Rotterdam, Balkema.

Reeve, L. A. (1853). C*hlamys gemmulata*. In Beu, A. G., and Maxwell, P. A. (1990). *Cenozoic Mollusca of New Zealand*. Lower Hutt: New Zealand Geological Survey.

Reeves, J. M., Chivas, A. R., Garcia, A., and De Deckker, P. (2007). Palaeoenvironmental change in the Gulf of Carpentaria (Australia) since the last interglacial based on Ostracoda. *Palaeogeography, Palaeoclimatology, Palaeoecology*, 246, 2-4, 163-187.

Renwick, J. A., and Thompson, D. (2006). The Southern Annular Mode and New Zealand climate. *Water and Atmosphere (New Zealand)*, *14*, 24-25.

Rijske, W. C. (1979). *Soils of part Urewera-Waikaremoana area, North Island, New Zealand* (New Zealand Soil Survey Report 45). Wellington, Department of Scientific and Industrial Research.

Rogers, G. M. (1987). *Landscape history of Moawhango Ecological District*. Unpublished doctoral thesis, Victoria University of Wellington, Wellington, New Zealand.

Rogers, G. M. (1989). Beech and Conifer Community Interactions in Moawhango Ecological Region, North Island, New Zealand. *New Zealand Journal of Ecology*, 12, 47-61.

Rogers, G. M., and Leathwick, J. R. (1997). Factors predisposing forests to canopy collapse in the southern Ruahine Range, New Zealand. *Biological Conservation*, 80, 3, 325-338.

Rogers, G. M., and McGlone, M. S. (1989). A postglacial vegetation history of the southern-central uplands of North Island, New Zealand. *Journal of the Royal Society of New Zealand*, 19, 3, 229-248.

Rogers, G. M. and McGlone, M. S. (1994). A history of Kaiparoro clearing and the limits of Nothofagus in the northern Tararua Range, New Zealand. *New Zealand Journal of Botany*, 32, 463-482.

Rose, N. L., Golding, P. N. E., and Battarbee, R. W. (1996). Selective concentration and enumeration of tephra shards from lake sediment cores. *The Holocene*, 6, 2, 243-246.

Rossetti, G., Eagar, S. H., and Martens, K. (1998). On two new species of the genus Darwinula (Crustacea, Ostracoda) from New Zealand. *Italian Journal of Zoology*, 65, 3, 325 - 332.

Schaefer, J. M., Denton, G. H., Kaplan, M., Putnam, A., Finkel, R. C., Barrell, D. J. A., Andersen, B. G., Schwartz, R., MacKintosh, A., Chinn, T., and Schlüchter, C. (2009). High-Frequency Holocene Glacier Fluctuations in New Zealand Differ from the Northern Signature. *Science*, 324, 5927, 622-625.

Shane, P. (2000). Tephrochronology: a New Zealand case study. *Earth-Science Reviews*, 49, 1-4, 223-259.

Shane, P. (2005). Towards a comprehensive distal andesitic tephrostratigraphic framework for New Zealand based on eruptions from Egmont volcano. *Journal of Quaternary Science*, 20, 45–57.

Shaw, W. B. (1983). Tropical cyclones: Determinants of pattern and structure in New Zealand's indigenous forests. *Pacific Science*, 37, 405-414.

Shulmeister, J., Goodwin, I., Renwick, J., Harle, K., Armand, L., and McGlone, M. S. (2004). The Southern Hemisphere westerlies in the Australasian sector over the last glacial cycle: a synthesis. *Quaternary International*, 118, 23-53.

Shulmeister, J., Rodbell, D. T., Gagan, M. K., and Seltzer, G. O. (2006). Inter-hemispheric linkages in climate change: paleo-perspectives for future climate change. *Climate of the Past*, 2, 2, 167-185.

Smale, D., Houghton, B. F., McKellar, I. C., Mansergh, G. D., Moore, P. R., Grant-Taylor, T. L., and Te Punga, M. T. (1978). *Geology and erosion in the Ruahine Range. New Zealand* (Geological Survey Report G20). Wellington: Department of Scientific and Industrial Research.

Sperazza, M., Moore, J. N., and Hendrix, M. S. (2004). High-resolution particle size analysis of naturally occurring very fine-grained sediment through laser diffractometry. *Journal of Sedimentary Research*, 74, 5, 736-743.

Stahle, D. W., D'Arrigo, R. D., Krusic, P. J., Cleaveland, M. K., Cook, E. R., Allan, R. J., Cole, J. E., Dunbar, R. B., Therrell, M. D., Gay, D. A., Moore, M. D., Stokes, M. A., Burns, B. T., Villanueva-Diaz, J., and Thompson, L. G. (1998). Experimental dendroclimatic reconstruction of the Southern Oscillation. *Bulletin of the American Meteorological Society*, 79, 2137-2152.

Steen-McIntyre, V. (1977). *A manual for tephrochronology*. Colorado: V. Steen-McIntyre.

Stewart, G. H., and Veblen, T. T. (1982). Regeneration patterns in southern rata (Metrosideros umbellata) – kamahi (Weinmannia racemosa) forest in central Westland, New Zealand. *New Zealand Journal of Botany*, 20, 55-72.

Stuiver, M., and Polach, H. A. (1977). Discussion: Reporting of ^{14}C Data. *Radiocarbon*, 19, 3, 355-363.

Sturman, A. P. P., McGowan, H. A. A., and Spronken-Smith, R. A. A. (1999). Mesoscale and local climates in New Zealand. *Progress in Physical Geography*, 23, 4, 611-635.

Suggate, R. P. (1978). Torlesse Supergroup. In R. P. Suggate, G. R. Stevens, and M.T. Te Punga, (Eds.). *The geology of New Zealand* (pp. 254-255). Wellington, Government Printer.

Talbot, M. R. (1990). A review of the palaeohydrological interpretation of carbon and oxygen isotopic ratios in primary lacustrine carbonates. *Chemical Geology: Isotope Geoscience section,* 80, 4, 261-279.

Thornton, J. (2009). *The Field Guide to New Zealand Geology: An introduction to rocks, minerals and fossils*. Auckland: Penguin NZ.

Trustrum, N.H., and De Rose, R.C. (1988). Soil depth-age relationship of landslides on deforested hillslopes, Taranaki, New Zcaland. *Geomorphology*, 1, 143-160.

Trustrum, N.A., Gomez, B., Page, M.J., Reid, L.M., and Hicks, D.M. (1999). Sediment production, storage and output: the relative role of large magnitude events in steepland catchments. *Zeitschrift für Geomorphologie*, 115, 71–86.

Turner, M. (2010). *Developing an integrated eruption record over the last 10,000 years at Mt Taranaki/Egmont, New Zealand*. Unpublished doctoral thesis, Massey University, Palmerston North.

Ummenhofer, C. C., Sen Gupta, A., and England, M. H. (2009). Causes of late twentieth-century trends in New Zealand precipitation. *Journal of Climate*, 22, 3–19.

Vaasma, T. (2008). Grain-size analysis of lacustrine sediments: a comparison of pre-treatment methods. *Estonian Journal of Ecology*, 57, 4, 231-243.

Van Dissen, R. J., and Berryman, K. R. (1996). Surface rupture earthquakes over the last ~1000 years in the Wellington region, New Zealand, and implications for ground shaking hazard. *Journal of Geophysical Research*, 101(B3), 5999-6019.

Van Dissen, R. J., Berryman, K. R., Pettinga, J. R., and Hill, N. L. (1992). Paleoseismicity of the Wellington: Hutt Valley Segment of the Wellington

Fault, North Island, New Zealand. *New Zealand Journal of Geology and Geophysic*s, 35, 2, 165-176.

Vandergoes, M. J., Fitzsimons, S. J., and Newnham, R. M. (1997). Late glacial to Holocene vegetation and climate change in the eastern Takitimu Mountains, western Southland, New Zealand. *Journal of the Royal Society of New Zealand*, 27, 1, 53-66

Von Grafenstein, U., Erlenkeuser, H., Brauer, A., Jouzel, J., and S. J. Johnsen. (1999). A mid-European decadal isotope–climate record from 15,500 to 5000 years B.P. *Science*, 284, 1654-1657.

Von Grafenstein, U., Erlenkeuser, H., Muller, J., and Kleinmann-Eisenmann, A. (1992). Oxygen records of benthic ostracods in Bavarian lake sediments. *Naturwissenschaften*, 79, 145-152.

Waksman, S. A., and Stevens, K. R. (1930). A Critical Study of the Methods for Determining the Nature and Abundance of Soil Organic Matter. *Soil Science*, 30, 2, 97-116.

Wang, N., and Grapes, R. (2008). Infrared-stimulated luminescence dating of late Quaternary aggradation surfaces and their deformation along an active fault, southern North Island of New Zealand. *Geomorphology*, 96, 1-2, 86-104.

Wardle, J. (1970). The ecology of Nothofagus solandri: the distribution and relationship with other major forest and scrub species. *New Zealand Journal of Botany*, 8, 494-531.

Wellman, H. W. (1953). Data for the Study of Recent and late Pleistocene Faulting in the South Island of New Zealand. *New Zealand Journal of Science and Technnology*, B33, 270-288.

Whitehouse, I. E. (1983). Distribution of large rock avalanche deposits in the central Southern Alps, New Zealand. *New Zealand Journal of Geology and Geophysics*, 26, 272-279.

Williams, P. W. (1991). Tectonic geomorphology, uplift rates and geomorphic response in New Zealand. *Catena*, 18, 5, 439-452.

Williams, P. W., King, D. N. T., Zhao, J.-X., and Collerson, K. D. (2004). Speleothem master chronologies: combined Holocene ^{18}O and ^{13}C records from the North Island of New Zealand and their palaeoenvironmental interpretation. *The Holocene,* 14, 2, 194-208.

Wilmshurst, J. M. (1997). The impact of human settlement on vegetation and soil stability in Hawke's Bay, New Zealand. *New Zealand Journal of Botany*, 35, 97-111.

Wilmshurst, J. M., Eden, D. N., and Froggatt, P. C. (1999). Late Holocene forest disturbance in Gisborne, New Zealand: A comparison of terrestrial and marine pollen records. *New Zealand Journal of Botany*, 37, 3, 523-540.

Wilmshurst, J. M., and McGlone, M. S. (1996). Forest disturbance in the central North Island, New Zealand, following the 1850 BP Taupo eruption. *The Holocene*, 6, 4, 399-411.

Wilmshurst, J. M., McGlone, M. S., and Charman, D. J. (2002). Holocene vegetation and climate change in southern New Zealand: linkages between forest composition and quantitative surface moisture reconstructions from an ombrogenous bog. *Journal of Quaternary Science*, 17, 7, 653-666.

Wilmshurst, J. M., McGlone, M. S., and Partridge, T. R. (1997). A late Holocene history of natural disturbance in lowland podocarp/hardwood forest, Hawke's Bay, New Zealand. *New Zealand Journal of Botany*, 35, 79-96.

Wilson, A. T., Hendy, C. H., and Reynolds, C. P. (1979). Short-term climate change and New Zealand temperatures during the last millennium. *Nature*, 279, 5711, 315-317.

Winkler, S. (2000). The 'Little Ice Age' maximum in the Southern Alps, New Zealand: preliminary results at Mueller Glacier. *The Holocene*, 10, 5, 643-647.

Wolman, M. G., and Gerson, R. (1978). Relative scales of time and effectiveness of climate in watershed geomorphology. *Earth Surface Processes and Landforms*, 3, 2, 189-208.

Zittel, K. A. (1864). II. Fossile Mollusken und Echinoderm aus Neu-Seeland. Nebst beitragen von den Herren Bergrath Franz Ritter V. Hauer und Professor Eduard Suess. In F. von Hochstetter, M. Hornes, F. Ritter von Hauer (Eds.) Palaontologie von Neu-Seeland. Beitrage zur Kenntniss der Fossilen Flora und Flora der Provinzen Auckland und Nelso. Reise cer Osterreichischen Fergatte Novara um die Erde. *Geologiser Theil*. *1*, 2, 15-68.

Appendices

Appendix 1 - Core logs

Core 1

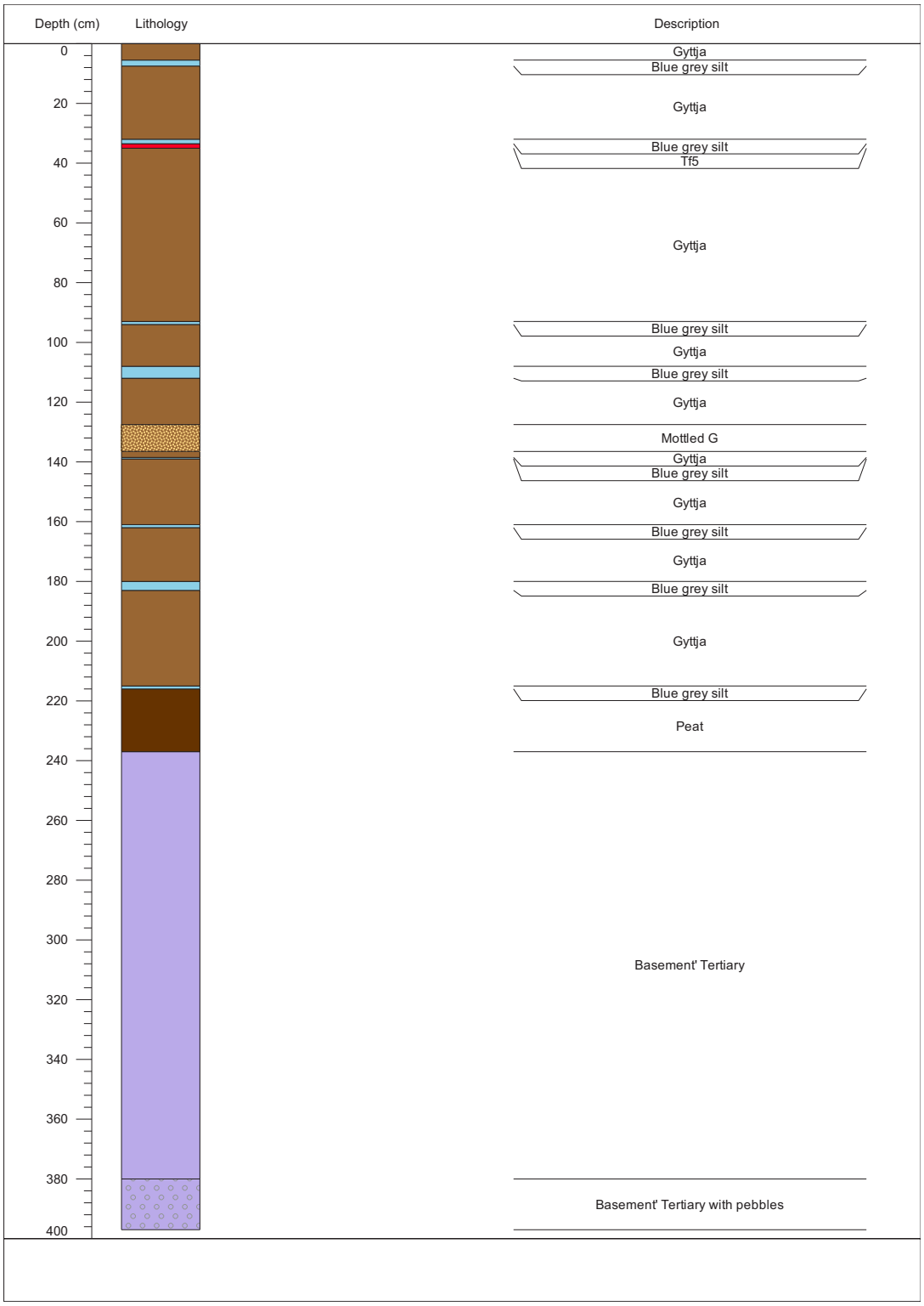

Core 2

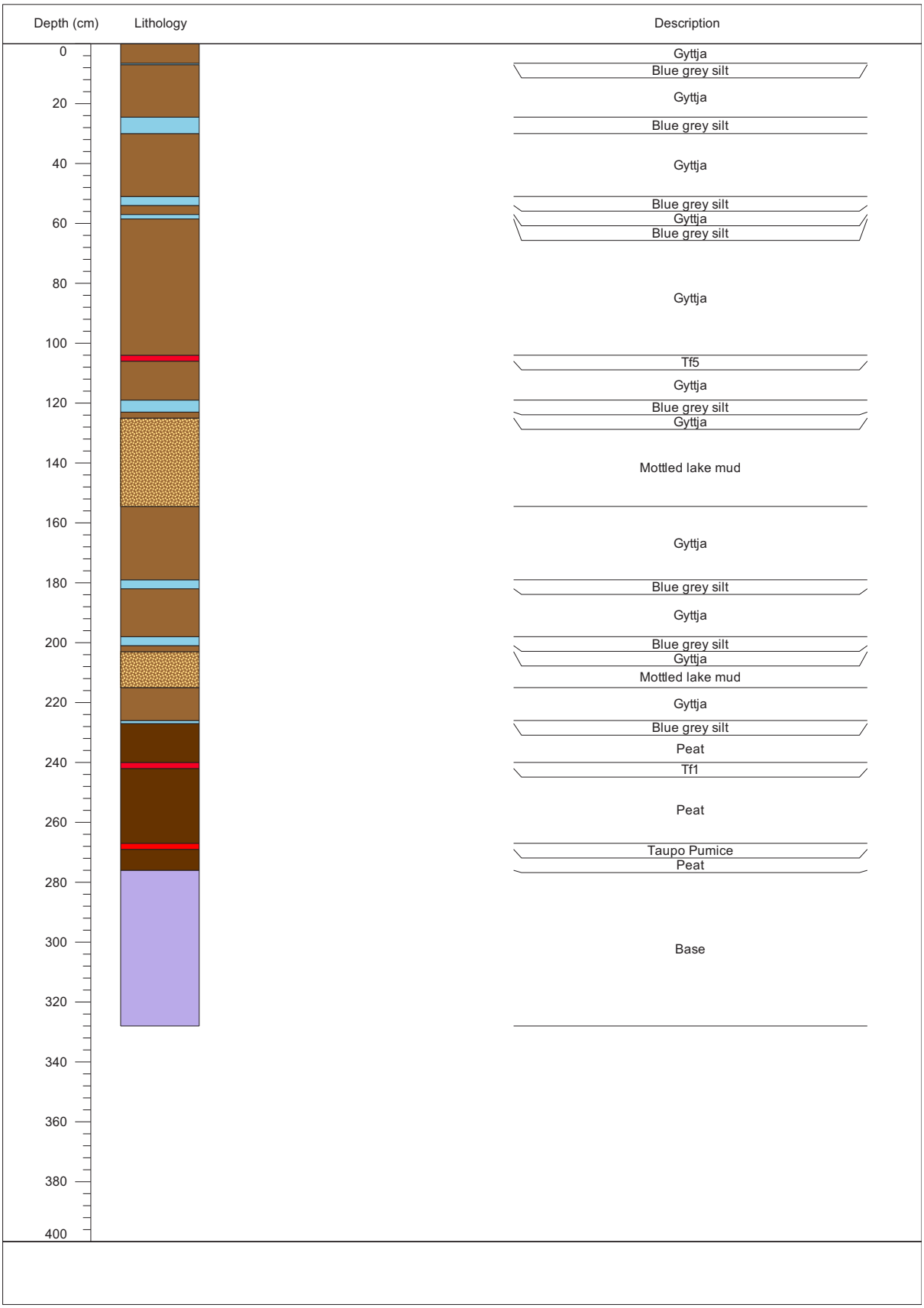
Depth (cm)
Lithology
Description
0
20
40
60
80
100
120
140
160
180
200
220
240
260
280
300
320
340
360
380
400
Gyttja
Blue grey silt
Gyttja
Blue grey silt
Gyttja
Blue grey silt
Gyttja
Blue grey silt
Gyttja
Tf5
Gyttja
Blue grey silt
Gyttja
Mottled lake mud
Gyttja
Blue grey silt
Gyttja
Blue grey silt
Gyttja
Mottled lake mud
Gyttja
Blue grey silt
Peat
Tf1
Peat
Taupo Pumice
Peat
Base

Core 3

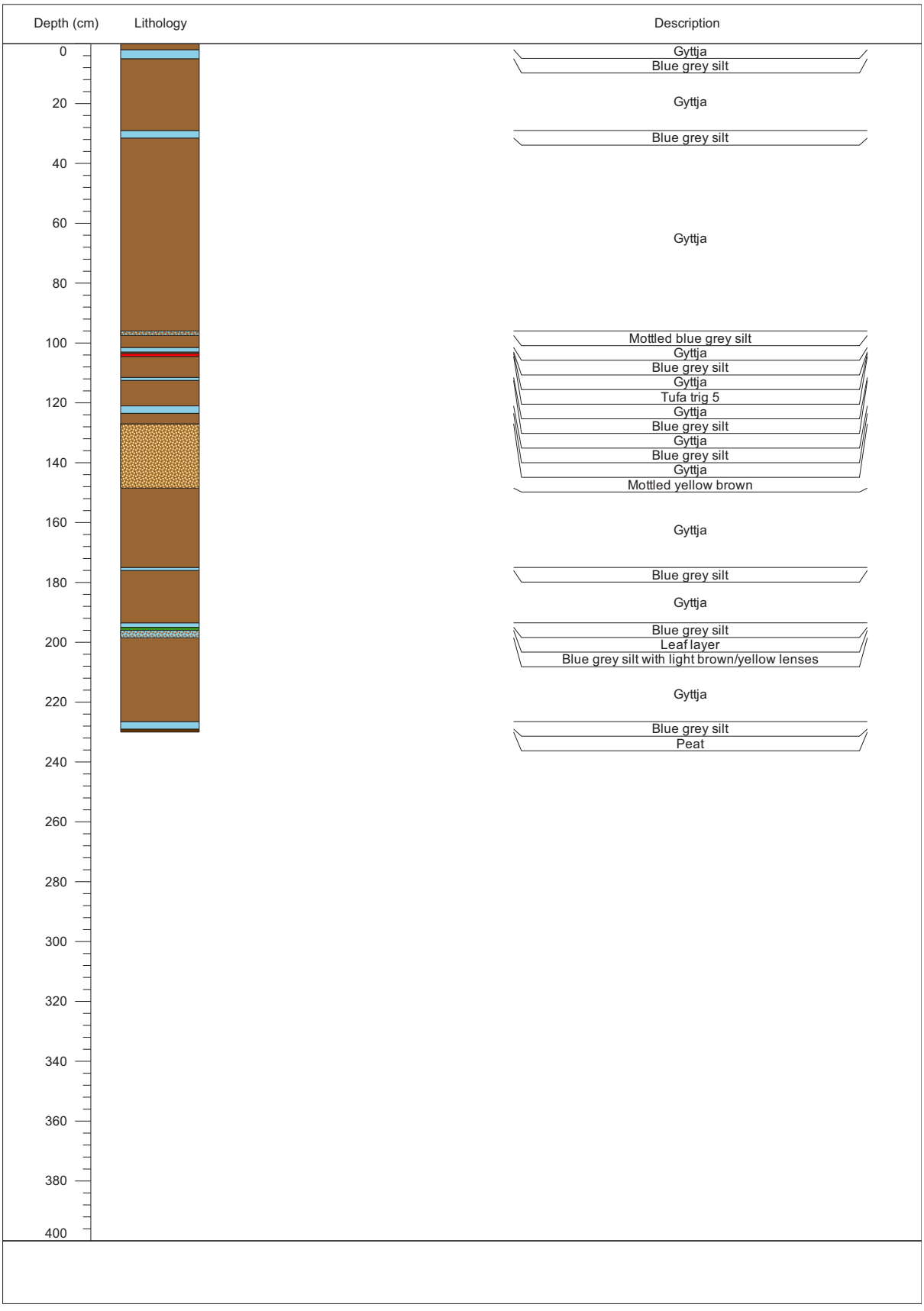
Depth (cm)
Lithology
Description
0
20
40
60
80
100
120
140
160
180
200
220
240
260
280
300
320
340
360
380
400
Gyttja
Blue grey silt
Gyttja
Blue grey silt
Gyttja
Mottled blue grey silt
Gyttja
Blue grey silt
Gyttja
Tufa trig 5
Gyttja
Blue grey silt
Gyttja
Blue grey silt
Gyttja
Mottled yellow brown
Gyttja
Blue grey silt
Gyttja
Blue grey silt
Leaf layer
Blue grey silt with light brown/yellow lenses
Gyttja
Blue grey silt
Peat

Core 4

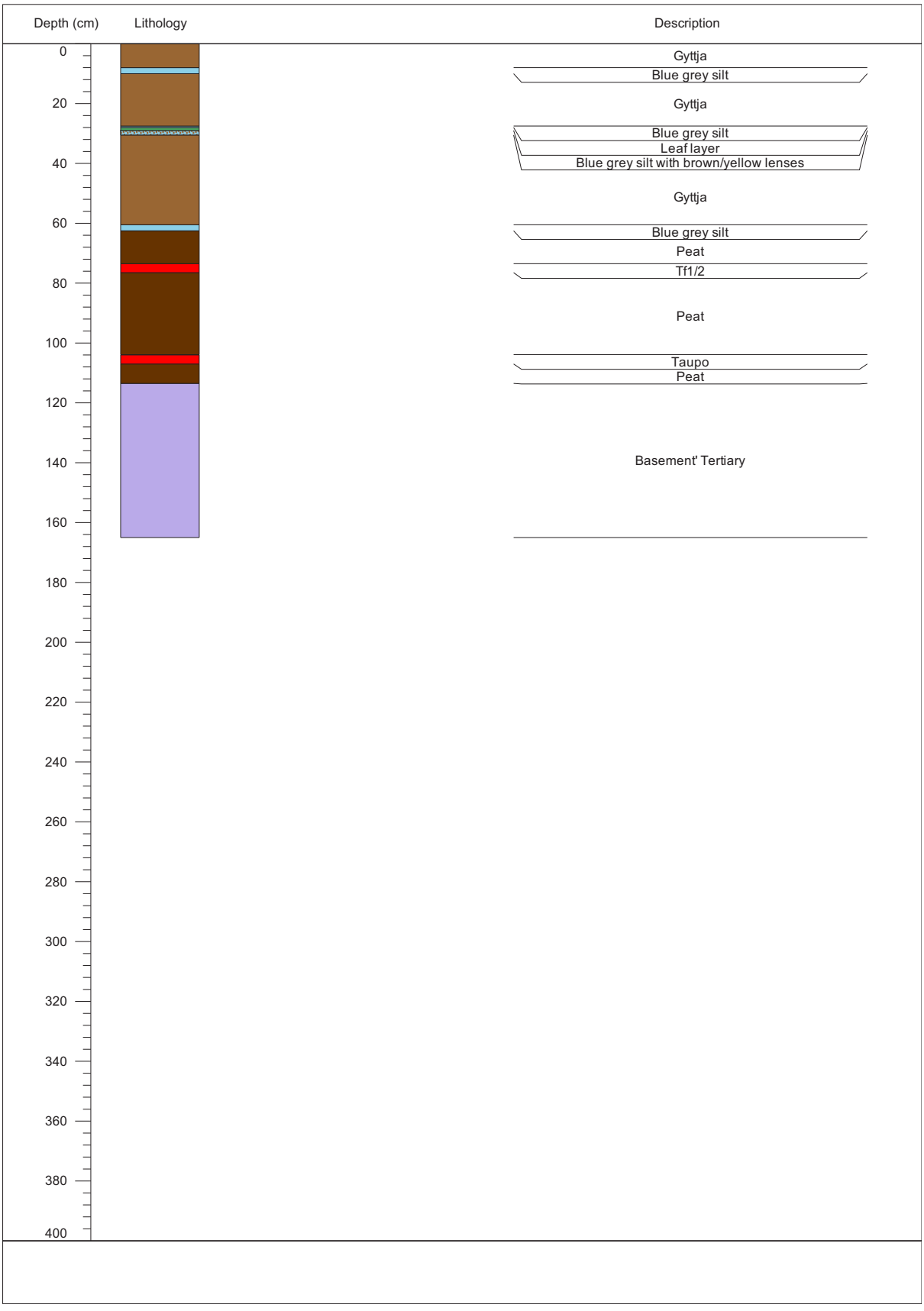
Depth (cm)
Lithology
Description
0
20
40
60
80
100
120
140
160
180
200
220
240
260
280
300
320
340
360
380
400
Gyttja
Blue grey silt
Gyttja
Blue grey silt
Leaf layer
Blue grey silt with brown/yellow lenses
Gyttja
Blue grey silt
Peat
Tf1/2
Peat
Taupo
Peat
Basement' Tertiary

Core 5

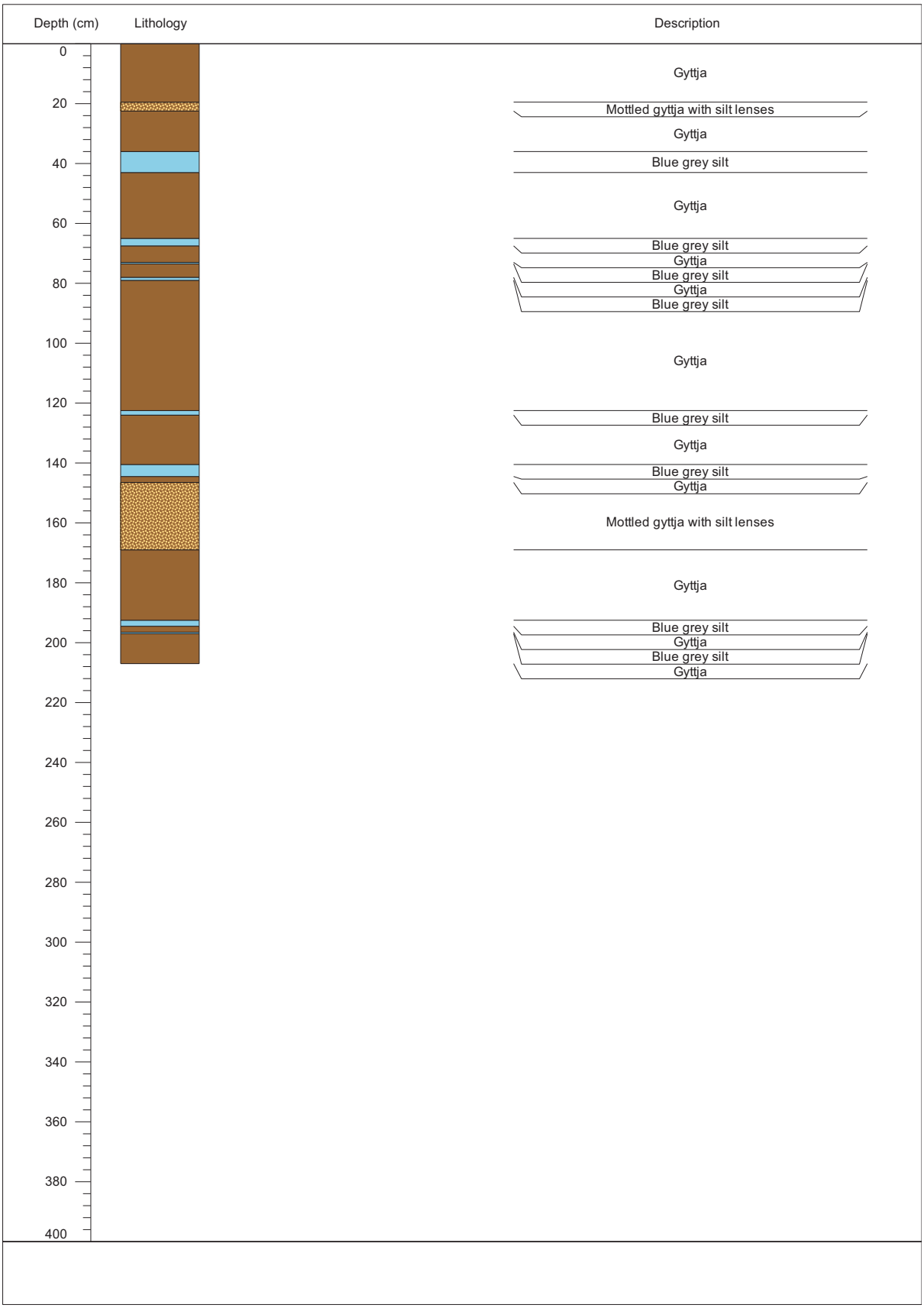
Depth (cm)
Lithology
Description
0
20
40
60
80
100
120
140
160
180
200
220
240
260
280
300
320
340
360
380
400
Gyttja
Mottled gyttja with silt lenses
Gyttja
Blue grey silt
Gyttja
Blue grey silt
Gyttja
Blue grey silt
Gyttja
Blue grey silt
Gyttja
Blue grey silt
Gyttja
Mottled gyttja with silt lenses
Gyttja
Blue grey silt
Gyttja
Blue grey silt
Gyttja

Appendix 2 - Description and idenitification of ostracods and molluscs

Ostracod classification

Family: Cytheridae (Baird, 1850)

Genus: *Gomphocythere* (Barclay, 1968)

Species: *Gomphocythere duffi* (Barclay, 1968)

First classified as *Limnocythere duffi* by Hornibrook (1955), and reclassified into the genus *Gomphocythere* by Barclay (1968) and an apparently rare species (Chapman, 1976). Sexes are markedly different; females tend to have a distinguishing bulge near the posterior end. Species named after Dr R. Duff, early Director of Canterbury Museum (Hornibrook, 1955).

Description: Large oval carapace with numerous pore canals, posterior and anterior margins rounded (Hornibrook, 1955). Elongate dorsal ridge extending longitudinally either side of straight dorsal margin. Prominent central muscle scars aligned in a vertical row of four, typical of family Cytheroidea (Holmes, 2001). Carapaces of females differ slightly; they are noticeably larger and have a distinguishing, reticulate tubercle at the postero-dorsal angle, for the retention of ripe ova (Barclay, 1968) and an indented medial strip along the location of the central muscle scar. Carapaces range from 690 - 950 μm in length, 270 - 320 μm in width and 420 - 510 μm in height.

Habitat: Species capable of moderate swimming (Chapman, 1963). Found in swamp, and lake environments. Ratio of male to female carapaces found typically 3:1 (Barclay, 1968), which is often encountered with the crustacean subphylum (Ian Henderson *pers. comm.*).

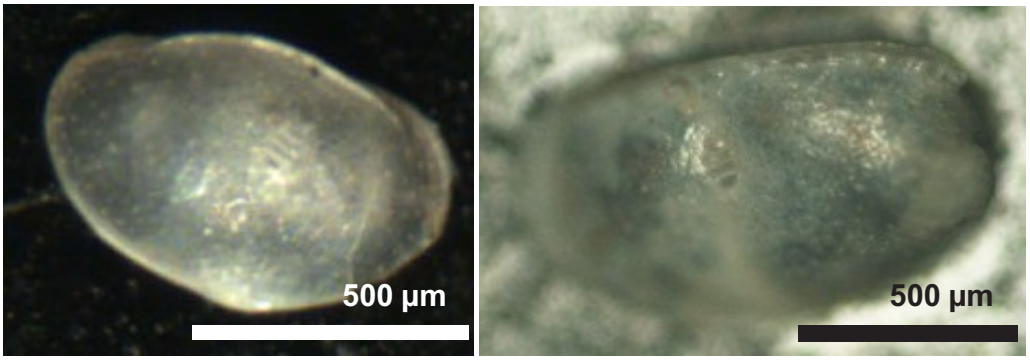

Left. Right valve of *G. duffi* (male) showing dorsal ridge and prominent central muscle scar. **Right.** Left valve of G. duffi (female) showing reticulate tubercle at posterior end.

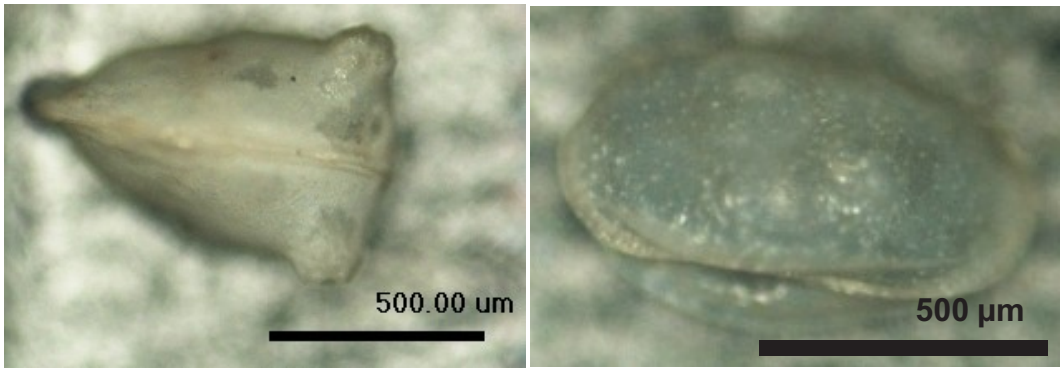

Left. Dorsal view of *G. duffi* (female), with pronounced bulge at posterior end. **Right.** Oblique dorsal view of *G. duffi* (male) showing elongate ridge

Family: Darwinulinidiae (Brady and Norman, 1889)

Genus: *Darwinula* (Brady and Robertson, 1885)

Species: *Penthesilenula kohanga* (Eager, 2005)

Genus first identified as *Darwinula* in Pyramid Valley Swamp by Hornibrook (1955) which was adapted by Chapman (1963), Barclay (1968) and Rossetti (1998) and later reclassified to *Penthesilenula* by Eager (2005), though some studies still use the original genus name. Species first classified by Rossetti (1998) as *Darwinula kohanga*, here the genus name follows that of Eager (2005). Species named after the Maori word meaning 'nest', referring to the brooding pouch in the carapace (Rosetti, 1998).

Description: Relatively glossy shell, large in comparison to other *Penthesilenula* species. Slender carapace with maximum width near rounded posterior end forming the brooding pouch, anterior end pointed. Dorsal margin gently sinuous (Rossetti *et al*., 1998). Faint central muscle scar resembles a circular rosette, typical of family Darwinuloidea (Holmes, 2001). Carapace ranging from 720 - 840 μm in length, 340 - 380 μm in width and 330 - 370 μm in height (Rossetti *et al*., 1998).

Habitat: Benthic genera that typically have limited movement, typically found in swamp, peat and lake environments (Chapman, 1963).

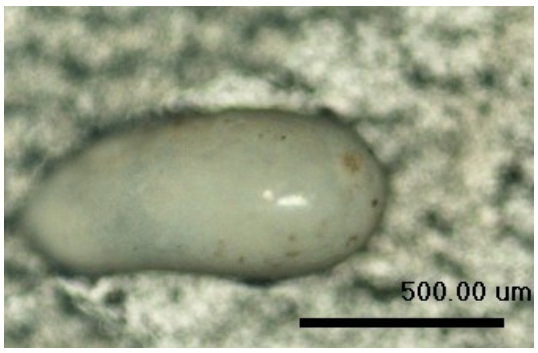

Dorsal view of *P. kohanga*, showing pointed anterior end (left) and rounded, enlarged dorsal end (right).

Mollusc classification

Family: Hydrobiidae

Genus: *Potamopyrgus* (Stimpson, 1865)

Species: *Potamopyrgus antipodarum* (Gray, 1943)

Common freshwater species endemic to New Zealand, previously called *Potamopyrgus jensinki* (Dieffenbach, 1843). Particularly invasive species, and has since become abundant in many countries (Zaranko *et al*., 1997; Levri *et al*., 2007).

Description: Ovate shell, rounded dextral whorls, ovate mouth and lengthened spire. Deep suture line is indicative of *Potamopyrgus* species (Margaret Morley *pers. comm.*). Shell ranging from 1 - 10 mm in length, and 0.4 - 3 mm in width.

Habitat: Found in all freshwater environments i.e. lakes, rivers, streams and swamps, also brackish environments, and tolerable to siltation and sediment disturbance. Benefits particularly from high nutrient flows which allow growth of green algae (Death *et al*., 2003). Prefers littoral zones in lakes or slow-moving streams, though also survives in fast-flowing streams or rivers by burrowing in the sediment substrate (Holomuzki and Biggs, 2000).

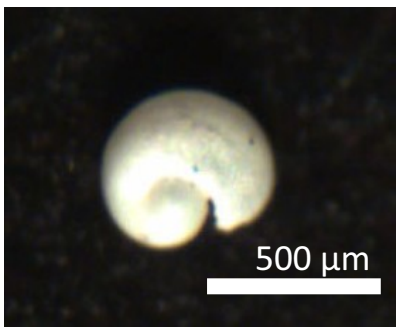

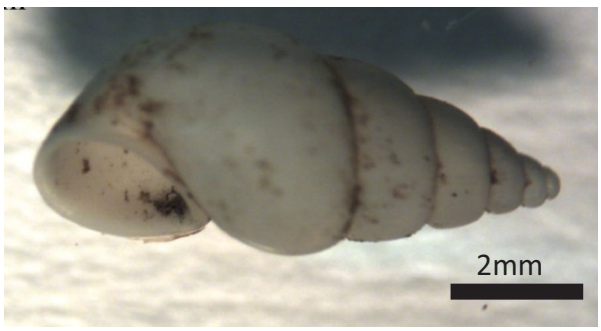

Left. Juvenille posterior view of *P. antipodarum*. **Right.** Dorsal view of *P. antipodarum*, showing rounded dextral whorls.

Family: Sphaeriidae

Genus: *Pisidium*

Species: *Pisidium novaezelandiae* (Prime, 1862)

Small freshwater bivalve mollusc, often known as fingernail clam, also known as *Sphaerium (Sphaerinova) novaezelandiae* (Deshayes, 1854) is an endemic species and most commonly found of the *Sphaeriidae* family. The Sphaeriidae, formerly *Corneocylas* (Winterbourn, 1973) family is, in general, poorly understood, and the three species within this family are difficult to distinguish on shell characteristics. Anatomical and molecular work will be necessary to establish the composition and relationships of the Sphaeriidae family (Bruce Marshall *pers. comm.*).

Description: Bivalve mollusc, medially located beak and ligament visible externally. Concentric orientated striae on shell. Shell ranging from 2 - 6 mm in length, and 2 - 5 mm in height.

Habitat: Benthic, prefer weedy environments and are often found burrowing in the sand of stream beds (Winterbourn, 1973). Found in all freshwater environments i.e. lakes, rivers, streams and swampy areas.

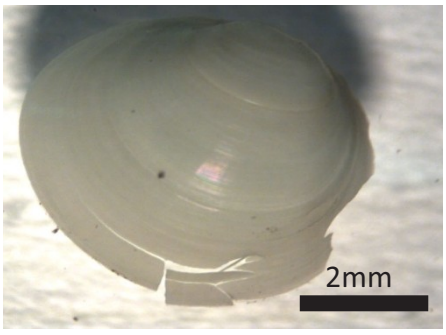

Dorsal view of *P. novaezelandiae*, showing concentric striae.

Appendix 3 - Major elemental glass chemistry data

Data recalculated to 100% on a volatile-free basis and shown as mean and standard deviation in wt%. Total iron expressed as FeO, water by difference from original analytical total

Tufa Trig Formation member 5

Sample ID	SiO_2	TiO_2	Al_2O_3	FeO	MnO	MgO	CaO	Na_2O	K_2O	Cl	TOTAL	H_2O
ID = 2822	60.29	0.73	16.90	5.82	0.05	3.86	6.77	3.73	1.79	0.07	100	1.48
ID = 2823	62.75	1.09	16.38	5.70	0.13	1.72	5.71	4.06	2.32	0.13	100	2.17
ID = 2824	64.49	1.14	14.09	6.48	0.00	2.51	4.63	3.76	2.78	0.12	100	1.83
ID = 2825	62.60	1.08	16.16	5.88	0.15	2.10	5.52	3.72	2.67	0.13	100	0.48
ID = 2826	63.84	0.95	15.32	5.99	0.07	1.56	5.13	4.08	2.94	0.13	100	1.64
ID = 2827	62.67	1.04	16.22	5.72	0.15	1.98	5.90	3.92	2.24	0.15	100	1.81
ID = 2828	64.04	1.21	15.66	5.73	0.11	1.55	5.20	3.95	2.40	0.15	100	1.96
ID = 2829	65.31	1.16	14.02	6.40	0.00	1.93	3.82	4.10	3.09	0.17	100	2.82
ID = 2830	60.90	0.71	18.68	4.55	0.15	1.82	7.15	4.03	1.84	0.15	100	1.60
ID = 2832	62.19	0.98	16.74	5.60	0.17	1.90	5.93	4.14	2.22	0.13	100	1.37
ID = 2833	63.40	0.92	15.03	5.91	0.12	3.13	5.36	3.65	2.33	0.13	100	1.41
ID = 2834	62.14	0.78	15.84	6.03	0.12	3.56	5.71	3.63	2.12	0.06	100	1.60
ID = 2835	60.07	0.71	19.18	4.77	0.05	1.86	7.56	4.02	1.64	0.14	100	1.91
ID = 2837	64.70	1.10	14.51	6.28	0.01	2.32	4.57	3.72	2.70	0.09	100	1.59
ID = 2838	62.17	0.94	17.07	5.52	0.08	1.68	6.34	4.08	2.02	0.10	100	0.99
ID = 2839	60.57	0.72	18.84	4.80	0.17	1.85	7.34	3.82	1.80	0.10	100	1.47

Tufa Trig Formation member 1

Sample ID	SiO_2	TiO_2	Al_2O_3	FeO	MnO	MgO	CaO	Na_2O	K_2O	Cl	TOTAL	H_2O
ID = 2841	60.66	0.94	15.89	6.41	0.08	3.37	7.17	3.47	1.87	0.15	100	1.69
ID = 2842	59.82	0.98	15.73	6.53	0.17	3.90	7.20	3.70	1.83	0.14	100	1.57
ID = 2845	59.47	0.92	14.48	6.76	0.15	5.24	7.94	3.28	1.60	0.14	100	1.40
ID = 2846	61.34	1.01	15.60	6.61	0.06	2.74	6.23	3.99	2.25	0.17	100	1.39
ID = 2847	60.48	0.95	15.65	6.46	0.12	3.26	7.19	3.78	1.90	0.21	100	1.52
ID = 2848	60.42	1.02	15.87	6.41	0.07	3.58	7.05	3.61	1.86	0.12	100	1.65
ID = 2849	60.56	0.95	16.10	6.38	0.05	3.15	7.20	3.57	1.89	0.15	100	1.62
ID = 2850	61.10	1.08	15.39	6.34	0.15	2.87	7.07	3.84	2.01	0.14	100	0.99
ID = 2851	58.70	0.92	14.98	7.12	0.05	6.23	6.76	3.42	1.68	0.14	100	0.32
ID = 2852	60.40	0.93	16.03	6.30	0.21	3.27	7.18	3.67	1.87	0.13	100	1.76
ID = 2853	60.33	0.89	15.55	6.73	0.00	3.36	7.21	3.78	1.92	0.23	100	2.26
ID = 2854	60.66	0.99	15.76	6.16	0.22	3.39	7.07	3.67	1.91	0.15	100	1.47
ID = 2855	60.58	1.12	15.85	6.42	0.11	3.33	6.86	3.66	1.93	0.13	100	1.67
ID = 2856	60.34	1.00	16.16	6.39	0.07	3.36	7.06	3.68	1.81	0.14	100	1.66

Taupo Pumice

Sample ID	SiO_2	TiO_2	Al_2O_3	FeO	MnO	MgO	CaO	Na_2O	K_2O	P_2O_5	SO_3	Cl
ID = 2858	75.05	0.31	13.03	2.09	0.03	0.19	1.53	4.52	2.95	0.00	0.00	0.30
ID = 2862	75.06	0.29	12.90	1.96	0.09	0.24	1.54	4.60	2.86	0.08	0.10	0.26
ID = 2866	74.99	0.30	12.76	1.75	0.17	0.21	1.50	4.80	2.87	0.14	0.00	0.25
ID = 2868	75.03	0.25	13.08	1.89	0.00	0.35	1.56	4.58	2.85	0.11	0.00	0.29
ID = 2871	75.09	0.39	12.90	2.08	0.07	0.21	1.49	4.53	2.86	0.00	0.12	0.26
ID = 2872	75.64	0.44	12.87	1.92	0.03	0.28	1.50	4.20	2.84	0.08	0.00	0.20
ID = 2874	75.18	0.32	12.75	1.91	0.10	0.27	1.48	4.60	3.01	0.00	0.00	0.23

Cr_2O_3	NiO	TOTAL	H_2O
0.00	0.01	100	2.78
0.01	0.00	100	1.77
0.00	0.26	100	2.19
0.00	0.00	100	3.37
0.00	0.00	100	2.60
0.00	0.00	100	3.57
0.02	0.12	100	1.47

Appendix 4 - Stable isotope data

From ostracod carapaces, *Gomphocythere duffi*.

Depth (cm)	Corrected depth (cm)	Inferred age (yrs B.P.)	$\delta^{13}C$ (‰)	$\delta^{18}O$(‰)
Lake water $\delta^{18}O$(‰): -5.91				
0	1	-59	-8.54	-5.18
9	6	-26	-9.36	-5.54
14	11	8	-8.48	-3.87
21	19	65	-9.99	-4.83
25	22	87	-10.48	-5.91
70	64.5	427	-8.95	-5.57
72	66.5	447	-9.44	-4.89
79	73.5	501	-9.61	-5.31
86	80.5	550	-9.37	-5.70
93	87.5	610	-9.70	-5.53
100	93	634	-8.07	-4.68
107	97.5	670	-8.19	-5.43
114	103.5	703	-7.95	-4.58
118	107.5	728	-6.89	-4.74
128	115	760	-7.65	-5.63
135	122	817	-8.53	-4.74
142	129	860	-6.53	-3.67
149	136	910	-8.67	-4.95
156	143	960	-9.42	-5.80
165	152	1004	-8.35	-4.71
172	159	1050	-7.69	-4.89
179	165	1088	-8.22	-5.05
186	172	1137	-6.87	-2.64
193	179	1180	-8.07	-4.50
200	182	1192	-8.40	-5.36
207	189	1240	-5.19	-5.19
221	203	1320	-5.01	-5.02
226	208	1355	-4.84	-5.27